THE EFFECT OF WHOLE FOODS ON THE GUT-ADIPOSE AXIS IN MODELS OF DIET-INDUCED OBESITY: THE CASE OF WHEAT GERM AND PINTO BEANS

By

BABAJIDE ABIDEMI OJO

Bachelor of Science in Biochemistry
Ekiti State University
Ado-Ekiti, Ekiti State, Nigeria
2011

Master of Science in Nutrition
Oklahoma State University
Stillwater, Oklahoma
2015

Submitted to the Faculty of the
Graduate College of the
Oklahoma State University
in partial fulfillment of
the requirements for
the Degree of
DOCTOR OF PHILOSOPHY
December, 2019

THE EFFECT OF WHOLE FOODS ON THE GUT-ADIPOSE AXIS IN MODELS OF DIET-INDUCED OBESITY: THE CASE OF WHEAT GERM AND PINTO BEANS

Dissertation Approved:

Committee Chair/Advisor Dr. Edralin A. Lucas

Committee Member Dr. Brenda Smith

Committee Member Dr. Stephen Clarke

Committee Member Dr. Winyoo Chowanadisai

Outside Committee Member Dr. Jerry W. Ritchey

ACKNOWLEDGEMENTS

I am forever indebted to Oklahoma State University (OSU), especially the graduate college, and the college of human sciences, and the nutritional science department for the opportunity to be part of this community and the conducive environment provided for learning and research. My appreciation goes to my advisor, Dr. Edralin Lucas, and other members of my committee for their guidance throughout the course of these studies, and for seldom pushing me beyond my comfort zone to become a better scientist. I appreciate the Oklahoma Agricultural Experiment Station, Northarvest Bean Growers Association, and Shawnee Milling Company for financial and material support for these studies. My appreciation also goes to staff of the nutritional science department, OSU Flow Cytometry Lab, OSU Food and Agricultural Processing Center (FAPC), UC Davis MMPC, and Second Genome Inc for their help in certain aspects of these studies.

I am grateful to my loving wife, Christianah Adebayo Jide-Ojo for her undying support during several late nights working in the lab. Special regards to my family, especially my Mom, Mrs. C.A. Ojo for making sure I have a solid educational background. I cannot but appreciate my wonderful Mom and Aunt, Mrs. Lucy Onisile, and my Cousin – Bola Fadipe, for their roles in stimulating my desire for a graduate degree at OSU. I appreciate my siblings, in-laws, extended family, and friends who have contributed to this journey.

Most importantly, I am grateful to the Most Holy Trinity and my Mother Mary for divine guidance in every thought and deed during my educational journey.

Name: BABAJIDE A. OJO
Date of Degree: DECEMBER, 2019
Title of Study: THE EFFECT OF WHOLE FOODS ON THE GUT-ADIPOSE AXIS IN MODELS OF DIET-INDUCED OBESITY: THE CASE OF WHEAT GERM AND PINTO BEANS
Major Field: Nutritional Sciences
Abstract:
The global alteration in food supply characterized by increased western-style diets (high in saturated fat and refined sugar) is a major driver of the obesity epidemic. Western diets disrupt the host-gut bacteria homeostasis, which elevates intestinal permeability to initiate obesity-related insulin resistance and adipose tissue inflammation. Dietary enrichment with fiber and more recently, tryptophan may mitigate these detrimental effects of obesity. Thus, the addition of whole foods to the western dietary pattern may be a convenient and cost-effective means to mitigate the damaging impact of obesity. The studies herewith were designed to understand the effect of two whole foods – wheat germ (WG) and pinto beans (PB) – on the gut bacteria and intestinal defenses against diet-induced obesity. In addition, the implication on glucose homeostasis and adipose tissue inflammation was examined. Results showed that WG only increased the abundance of taxa within the *Lactobacillaceae* family. PB had a robust effect on the gut bacteria, by increasing the abundance of *Lachnospiraceae*, and suppressing taxa within the Tenericutes and Proteobacteria phyla. Feeding a western-style diet consistently weakened signal transducer and activator of transcription (STAT)3 activation in the small intestine. However, both WG and PB reversed this effect potentially through different mechanisms involving interleukin (*Il)-22* and butyrate, respectively. Consequently, STAT3-induced antimicrobial peptide genes (Reg3β and Reg3γ) were significantly upregulated by WG and PB. In the adipose tissue, WG suppressed nuclear factor kappa-light-chain-enhancer of activated B cell (NFκB) activation by the western diet, and downregulated *Il-6* and lipopolysaccharide binding protein genes. PB suppressed the expression of tumor necrosis factor (*Tnf)-α* gene and the pro-inflammatory M1 macrophage marker, inducible nitric oxide synthase (*iNos)*, in the adipose tissue. Finally, both WG and PB improved glucose homeostasis in the animals fed a western diet. These studies show that the restoration of STAT3 activation in the small intestine is central to the gut-protective abilities of WG and PB albeit through separate mechanisms. Furthermore, these studies provide valuable foundational insights that should be considered for future studies that aim to identify the benefits of whole foods on gut and peripheral tissues using western diet-induced models of obesity.

TABLE OF CONTENTS

Chapter Page

Chapter Page

LIST OF TABLES

LIST OF FIGURES

Figure Page

CHAPTER II

CHAPTER III

CHAPTER IV

Figure Page

CHAPTER V

CHAPTER VI

CHAPTER I

INTRODUCTION

Background

The global rise in obesity across the last three decades has reached epidemic proportions, partly due to the drastic change in our food supply towards western-style diets (high fat, high sugar) (1). Data from the World Health Organization (WHO) estimates that about 30% of the world's population is either overweight or obese (2). It is also estimated that 13% of the world's obese population reside in the United States (2). Obesity is significantly associated with a variety of health complications, which includes insulin resistance (IR) that leads to type 2 diabetes (T2D), and increased risks of cardiovascular diseases and cancer (3). It is noteworthy that the precipitating factor for many of these complications is the state of low-grade chronic inflammation that accompanies the development of obesity (3). This is evident in increased circulation of pro-inflammatory cytokines such as tumor necrosis factor alpha (TNF-α), interleukin (IL)-1, and IL-6 in high fat (HF) diet-induced obese animals and in humans, which contributes to the development of T2D (4).

Recent studies have associated the onset of diet-induced obesity and its complications to disruption in gut homeostasis (5, 6). These changes include disruption of the commensal microbial populations (termed gut dysbiosis) and lamina propria lymphocytes which line our gastrointestinal tract to aid digestion, gut protection, and maintenance of gut

structure. Prominent among the gut microbes modified in HF diet-induced obesity and T2D include *Bifidobacteria, Akkermansia, Lactobacillus*, Bacteroides-related species and short chain fatty acid (SCFA)-producing genera such as *Roseburia* (7). In addition, immune cells vital for gut homeostasis including forkhead box (FOX)P3+ T-cells that are important in gut immunoregulation and Th17 cells, which are the most abundant T-cells in mucosal tissues (8), are also altered by HF diet (6). A vital function of the gut microbiota is the production of SCFAs from the fermentation of soluble dietary fiber and other non-digestible carbohydrates (9). Within the gut, SCFAs increase the expression of T-regulatory cells and promote the extra-thymic differentiation of T-cells into IL-10 producing T-cells, thus inducing gut tolerance to food and other antigens (9). This function is diminished in gut dysbiosis induced by a HF diet, which consequently results in increased intestinal permeability to endotoxin (5).

In order to combat systemic inflammation that may be initiated by the epithelial passage of both commensal and pathogenic microbes the mammalian gut develops a number of defense mechanisms. Among these are the antimicrobial peptides (AMPs) such as defensins, cryptidins, and the regenerating islet-derived protein (Reg)3 lectins, chiefly produced from the Paneth cells in the intestinal crypts (10). Interestingly, certain commensal bacteria show immunoprotective ability in the gut by metabolizing dietary factors which stimulate the release of AMPs. For example, gut bacteria-derived butyrate and tryptophan metabolites from *Lactobacillus* protect intestinal integrity by elevating the expression of IL-22 that is capable of activating the signal transducer and activator of transcription (STAT)3- regenerating islet-derived protein (Reg)3 pathway in intestinal epithelial cells (IECs) (11, 12). Consequently, an increase in gut Reg3 lectins prevent

bacterial translocation to peripheral tissues (13). Thus, it could be hypothesized that dietary approaches that enhance the production of AMPs in the gut may reduce the impact of HF diet-induced bacteremia/endotoxemia and suppress inflammation in peripheral tissues.

Strong scientific evidences accumulating in recent studies have shown that in HF diet-induced obesity, a reduction in specific gut bacteria and immune cells are observed in IR, a condition that precedes the development of T2D (5, 6, 14). Garidou et al. showed in a murine model of obesity that prior to the development of IR, HF feeding induces gut dysbiosis, suppresses antimicrobial peptide secretion (Reg3β and Reg3γ) and decreases ileal Th17 and FoxP3+ T-cells (6). Moreover, the early decrease in Th17 cells significantly correlated to a reduction in the bacterial family *Porphyromonadaceae*, whose members have been reported to trigger IL-17 production (6, 15). Furthermore, mice fed a HF diet experienced increased endotoxemia, which sets the tone for IR and inflammation in the liver and adipose tissue (5). These gut changes induced by the HF diet were observed as early as 10 days of HF feeding and continued until 30 days, preceding the onset of IR in mice (5, 6). Thus, these studies (5, 6, 14) infer that HF diet suppresses gut immune surveillance, which enhances translocation of bacteria and their products across the gut. These gut changes lead to the onset of IR in HF diet-induced obesity.

Prebiotics serve as food to the gut microbiome and may be a vital component in managing obesity related complications including IR and T2D (16). Dietary fiber and non-digestible carbohydrates such as inulin, oligofructose, resistant starch (RS) and glucooligosaccharide (GOS) have been reported for their gut modulatory and anti-

diabetic potential (17-19). Importantly, synbiotic (combination of prebiotic and probiotic) administration to mice fed a HF diet for 30 days prevented gut dysbiosis and the reduction in gut Th17 and FoxP3+ T-cells and consequently improved glucose tolerance (6). While most studies have concentrated on the impact of isolated fiber as a prebiotic, only few studies have shown that whole foods, such as maize, whole wheat, banana and mango may also show prebiotic properties (20-23). Therefore, investigating whole foods that modulate gut microbiota and immune cells may be an important approach in preventing the negative effects of HF diet.

Accumulating evidence shows that certain whole foods containing a variety of nutrients possess gut modulatory and prebiotic effects (20, 21). For example, wheat germ (WG) is a nutrient-dense component of the wheat grain that contains a modest 4% fiber, 23% protein, and several bioactive compounds with various health benefits (24). Apart from its fiber component, WG is a good source of the essential amino acid – tryptophan (300 mg / 100 g) (25), which could be available for the metabolic survival of certain commensal gut bacteria, including members of the *Lactobacillus* genera (26). Few studies have investigated the health benefits of WG. For example, fermented WG extracts showed anti-tumor properties (27). In addition, WG oil has been shown to have a strong anti-inflammatory and antioxidant effects in animal and in hypercholesterolaemic patients (28, 29). Furthermore, 6-month supplementation with 60 g WG modulated glucose homeostasis in T2D subjects (30). From a preventive standpoint, it is unclear if WG could influence the gut bacteria, SCFAs, and induce gut tolerance and protection required to prevent peripheral inflammation and obesity-induced insulin resistance.

Dry beans (*Phaseolus vulgaris*) on the other hand are high in fiber (15-45% wt/wt) depending on the variety, and may improve diet quality (31)[j]. Additionally, beans are nutrient dense foods that provide high quality protein, are low in fat, and contain many bioactive compounds such as vitamins, minerals, and polyphenols (32). The most commonly produced and consumed bean in the US is the pinto variety (*Phaseolus vulgaris L.*), which is approximately half of US dry bean production in 2009 (33). Pinto beans (PB) showed the potential to modulate the postprandial glucose response in T2D patients, and reduce risk factors of metabolic syndrome (34). Furthermore, PB influenced *in vitro* SCFA production and gut microbiota in individuals with pre-metabolic syndrome (35). Since our recent understanding of changes to the gut biology in obesity indicate that the disruption of the gut immune defense and gut microbiota precedes the onset of HF diet-induced T2D (5-7), no studies have been carried out on PB in preventing these early detrimental changes in the gut.

Due to the prevalence of diets rich in saturated fat and simple sugars in the current food supply, it is vital to identify dietary components that could mitigate the detrimental outcomes of the western-style diets. Hence, the incorporation of beneficial whole foods in the diet may potentially improve several facets of gut health when consuming either a normal diet or western-style diets. In turn, these gut modulatory effects of whole foods may be vital for the prevention of obesity-induced adipose tissue dysfunction and chronic inflammation that is typically associated with the induction of glucose intolerance in the long term.

Purpose: By using animal models of diet-induced obesity, the purpose of this project is to determine the gut-protective mechanisms of WG and PB when added to a western-style diet and the implication on glucose tolerance and the induction of proinflammatory cytokines in the adipose tissue.

Central Hypothesis: In animals fed a western diet, supplemental WG and PB will uniquely modulate gut bacterial diversity and composition, activate STAT3 signaling, and upregulate antimicrobial peptides (AMP) in the small intestine. These effects of WG and PB will contribute to the improvement of glucose homeostasis and suppression of proinflammatory markers in the visceral adipose tissue (VAT).

Specific Aim 1: To investigate the gut modulatory potential of WG on the gut microbiome, lamina propria lymphocytes, jejunal antimicrobial peptide expression and adipose tissue inflammation in C57BL6J mice fed a high fat, high sucrose (HFS) diet for 12 weeks

Sub-Aim 1.1: To evaluate the effects of WG supplementation on body composition, glucose homeostasis, and lipemia in C57BL/6J mice fed a HFS diet for 12 weeks.

Sub-Aim 1.2: To determine the effects of WG supplementation on the cecal microbial population, fecal SCFA, small intestinal CD4+ T cells, and systemic inflammation in C57BL/6J mice fed a HFS for 12 weeks.

Sub-Aim 1.3: To investigate the effect of supplemental WG on the STAT3-AMP pathway in the gut, and its potential to reduce inflammation and immune cell infiltration in the visceral adipose tissue of C57BL/6J mice fed a HFS for 12 weeks.

Working Hypothesis 1:

WG will prevent aspects of HFS-induced gut dysbiosis and induce AMP genes in the gut, indicating an enhanced capacity to mitigate HF-induced leaky gut. This effect of WG on the gut would be associated with reduced IR, immune cell infiltration and proinflammatory cytokines in the VAT.

Specific Aim 2: To determine the early protective effects of PB supplementation on the cecal microbiome, antigen presentation marker (major histocompatibility complex, MHC II), and antimicrobial peptide expression, and adipose tissue inflammation in C57BL6J mice fed a HFS diet for 30 days.

Sub-Aim 2.1: To evaluate the effects of PB supplementation on body composition and glucose homeostasis in C57BL/6J mice fed a HFS diet for 30 days.

Sub-Aim 2.2: To determine the effects of supplemental PB on cecal bacteria and fermentative capacity in C57BL/6J mice fed a HFS for 30 days.

Sub-Aim 2.3: To investigate the effect of PB supplementation on gut MHC II protein and Reg3 gene, and its potential to reduce immune cell infiltration and activation in the VAT of C57BL/6J mice fed a HFS for 30 days.

Working Hypothesis 2:

At the early onset of HFS-induced glucose intolerance, PB will beneficially modulate the gut bacteria, increase SCFAs, upregulate MHC II protein in the gut, and enhance Reg3 transcription. These PB effects in the gut of HFS-fed mice may explain its ability to prevent of glucose intolerance and reduced proinflammatory milieu in the visceral adipose tissue.

CHAPTER II

REVIEW OF LITERATURE

1.0 Obesity as a global health issue

Over the years, many countries have experienced a rising prevalence of overweight and obesity (36). Analysis of overweight and obesity prevalence in 188 countries between 1980 and 2013 revealed that none of the countries showed a decline in obesity in the past 33 years (2). During this period, the number of overweight and obese individuals rose from 857 million to 2.1 billion globally and 671 million of these individuals are classified as obese in 2013 (2). Additionally, more men were considered overweight and obese in developed countries, while a greater prevalence was observed in women than men in developing countries (Figure 1). The United States had the highest number of individuals classified as obese in 2013, accounting for 13% of obese people worldwide (2). To put this into more perspective, both China and India with a population of over 2.5 billion people (compared to the United States with population of about 300 million) account for 15% of the world's obese individuals (2).

The increase in overweight and obesity is a health concern for both developed and developing countries and has been characterized as a global pandemic (36, 37). Globally, obesity was estimated to account for 4% of disability-adjusted life years (DALYs) in

2010 (38). Furthermore, it accounts for 4% of years of life lost and 3.4 million deaths worldwide in the year 2010 (38). It is well known that overweight and obesity is a major risk factor for many chronic diseases such as diabetes, cancer and cardiovascular diseases (3, 38-40). All the problems associated with obesity makes it a global public health priority especially in the United States. Several explanations have been offered for the global rise in obesity, including caloric intake increase, diet compositional changes, lower levels of physical activity and recently, gut microbial changes (41-44). To alleviate the imminent health effects of rising overweight and obesity, it is vital to intervene against these determinants of obesity by active promotion of healthy food production and consumption, and encouraging physical activity.

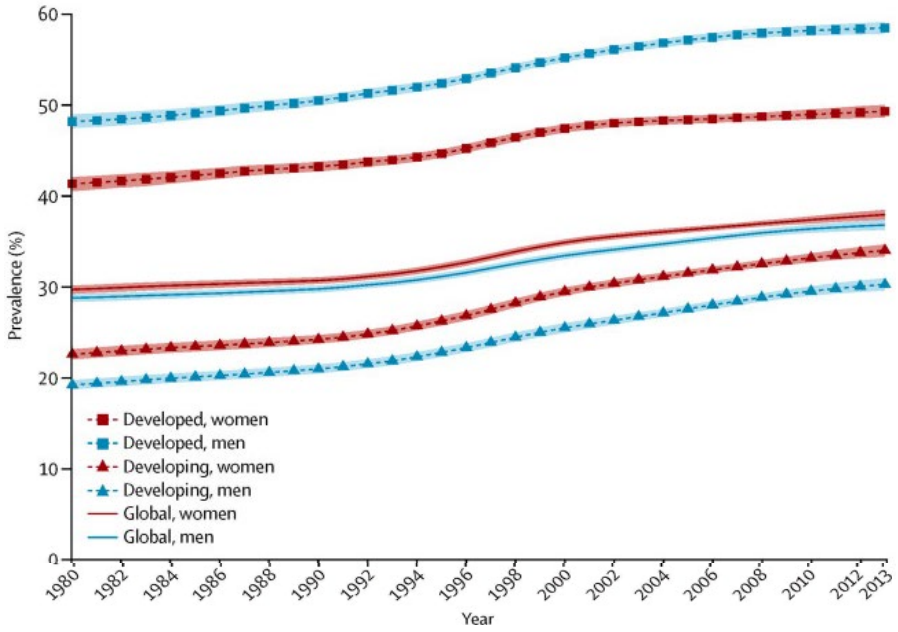

Figure 1: Age-standardized prevalence of overweight and obesity (BMI ≥ 25 kg/m^2) in developed and developing countries, ages ≥20 years, by gender, 1980–2013. BMI=body-mass index. Retrieved from Ng et al. (2)

2.0 Mechanisms linking obesity to type 2 diabetes (T2D)

One of the most devastating consequences of obesity is T2D, as over 80% of T2D patients are obese (45). In the year 2000, about 171 million people were estimated to live with T2D with the numbers projected to reach 366 million by 2030 (46). Furthermore, T2D prevalence is higher in men than in women, although more women have diabetes than men at the turn of the century (46). Moreover, the United States, India and China make up the top three countries with most people living with T2D in year 2000 and these positions are projected to be the same by 2030 (46).

Obesity is associated with insulin resistance (IR), a situation where insulin-responsive tissues become less sensitive to insulin action (47). However, at the early stages, most obese and insulin resistant people may not develop sustained hyperglycemia, due to the ability of the pancreatic beta cells to maintain normal glucose tolerance by elevating insulin release to compensate for reduced insulin efficiency (47). Over a period of time, pancreatic β-cells may lose their ability to continually compensate completely for the reduction in insulin sensitivity (also termed IR), which then leads to T2D characterized by hyperglycemia (48). Some factors in obesity that may result in the development of IR and T2D are further described below.

An important tissue contributing to the emergence of T2D in obesity is the adipose tissue. The adipose tissue contributes to the body's metabolism by the release of non-esterified fatty acid (NEFA), proinflammatory cytokines, and hormones such as adiponectin and leptin (49, 50). In obesity, the release of these products is significantly elevated. Increased NEFA levels are associated with IR in both obese and T2D subjects

(51). IR was observed within hours of acute elevation in human plasma NEFA (52). In contrast, an acute decrease in NEFA levels with acipimox (an antilipolytic agent) improved glucose uptake and glucose tolerance (53). Elevated intracellular NEFA may compete with glucose oxidation, resulting in the inhibition of the glycolytic enzymes hexokinase II and phosphofructokinase activity (54). Furthermore, increase intracellular NEFA results in an elevation of fatty acid metabolites such as ceramides, which leads to reduced activation of insulin receptor substrates (IRS) 1 and 2 (54). Consequently, activation of the PI(3)K pathway is impaired and other downstream events of insulin receptor signaling are reduced, leading to impaired insulin sensitivity (54).

Another factor that may contribute to the development of IR and T2D in obesity, especially intra-abdominal adiposity, is the macrophage-induced production of proinflammatory cytokines, primarily TNF-α, IL-6 and IL-1beta (4, 55, 56). In adipocytes, TNF-α affect the insulin signaling pathway via the inhibition of IRS-1 phosphorylation (56). Further, TNF-α and IL-6 may inhibit insulin action in the liver, thus increasing hepatic glucose output and further contributing to hyperglycemia (57). Moreover, elevation in TNF-α may stimulate hepatic production of free fatty acids in the liver (58), which may further contribute to IR as described above.

While it is believed that the adipose tissue is the major source of TNF-α in obese subjects, it may also be produced in other tissues such as the skeletal muscle (59). Gene expression and secretion of TNF-α was elevated in the skeletal muscle of IR and T2D patients (59, 60). Increased TNF-α gene expression correlated with reduced glucose uptake, thereby suggesting that TNF-α has a link to reduced insulin sensitivity in the skeletal muscle (59). Pro-inflammatory cytokines may also indirectly impact insulin

metabolism in pancreatic β-cells, as a combination of TNF-α, IL-1 and interferon (IFN)-γ, stimulated nitric oxide formation in human islets, resulting in an impairment of glucose-stimulated insulin secretion (61). Moreover, IL-1β induced pancreatic β-cell dysfunction via the expression of inducible nitric oxide synthase (iNOS) (62). Furthermore, exposure of rat pancreatic islets to TNF-α resulted in DNA double strand breaks and impaired insulin secretion (63). Together, these studies showed that elevation of free fatty acids and proinflammatory cytokines are directly or indirectly involved in the etiology of IR and T2D in obesity.

Interestingly, recent studies have accumulated evidence about the involvement of the gut, most importantly the gut bacteria and resident immune cells in the pathophysiology of obesity and T2D. This concept is further discussed in detail below.

3.0 The gut microbiome

The human gastrointestinal tract houses trillions of commensal bacteria, which acts as a bioreactor that is powered by dietary macronutrients to generate bioactive compounds (64). About 500 times more genes are encoded by the microbial genome compared to the human genome (65-67). The gut microbiome and signals originating from these microorganisms modulate host metabolism in various ways, and a distortion in the gut microbial composition and metabolites, contribute to many human diseases (64).

In humans, microbial density increases as we move down the gastrointestinal tract, which is predominantly colonized by anaerobic bacteria (67). Five phyla dominate the gut microbial community: Firmicutes, Bacteroidetes, Proteobacteria, Verrucomicrobia

and Actinobacteria (64). The Firmicutes are the most dominant phylum, and it includes key members of the genera *Lactobacillus, Ruminococcus, Clostridium,* and butyrate producers such as *Roseburia, Fecalibacterium* and *Eubacterium*. The phylum Bacteroidetes includes the *Bacteroides, Xylanibacter* and *Prevotella* which are all efficient dietary fiber-degrading genera. *Desulfovibrio* and *Escherichia* are key genera in the phylum Proteobacteria. At the moment, the only genus identified in the Verrucomicrobia phylum is the mucus-degrading *Akkermansia*. Lastly, the Actinobacteria phylum consist of a major genus called *Bifidobacterium*, and many taxa within this genus are used in probiotic supplements (64).

Environmental and genetic factors vastly influence the gut microbial composition starting in early life (68). For example, the phylum Bacteroidetes seem to be influenced by environmental factors, while the abundance of the family Christensenellaceae is influenced by host genetics (69). Furthermore, babies born via vaginal delivery have a different gut microbial community compared to cesarean delivery (70). The direct contact with the intestinal and maternal vaginal flora during vaginal delivery is important in establishing the biodiversity of the infant gut microbial community (70). This direct contact is absent in cesarean delivery, leading to intestinal colonization of the infant with more of environmental and non-maternally derived bacteria (71). During infancy, the gradual development of an adult-like anaerobic population of the gut microbiome is largely dependent on diet (64, 67). Diet quality and quantity, such as fiber, fat and carbohydrate content modulate gut microbial stability (72, 73). Moreover, antibiotic usage may induce loss of gut microbial stability, and the restoration of the core gut microbes may delay for a long time, or not recover at all (74, 75). It is worthy to note that

gut microbial community perturbations may occur dramatically within a few days by factors such as diet, infection or a change of environment (76-78). Together, these reports show that an established gut microbiota is an integral part of the host and disruptions may impact host metabolism and overall health.

4.0 Gut Microbiota-derived Signaling Molecules in Health and Disease

The homeostatic relationship between the gut microbiota and the gut mucosal immune system is important in the maintenance of the host's overall health (64). Health maintenance or disease manifestation is modulated by several signaling molecules, which can either be bacterial metabolites or structural components of bacteria. Some of these gut signaling molecules which have been implicated in the pathophysiology of obesity and IR are discussed below.

4.1 *The Interplay between Gut Bacteria and Immune Cells*

Certain pattern-recognition receptors (PRRs) such as nucleotide-binding oligomerization domain (NOD)-like receptors (NLRs) and toll-like receptors (TLRs), are embedded on intestinal epithelial cells (IECs) and immune cells (79). These PRRs recognize microbe-associated molecular patterns (MAMPs) on both normal gut flora and pathogens such as bacterial flagellin, lipopolysaccharide (LPS, an endotoxin in gram negative bacteria), peptidoglycan and other bacterial structural components (79). The PRRs' recognition prevents MAMPs from translocating across the gut epithelial barrier (64). The localization of MAMPs to the gut is also dependent on mucins and epithelial tight junction proteins, including zonula occludens 1 (ZO-1) and occludin (7). Diet may significantly impact the intestinal tight junctions and the protective mucus layer, as a

reduction in the thickness of the colonic mucus layer was observed in mice fed a HF diet (80). Moreover, tight junction proteins were reduced in mice fed a HF diet (7), which may promote the passage of bacteria and MAMPs across the intestinal epithelium.

The translocation of MAMPs across the gut epithelial barrier may be the most significant factor linking HF diet-induced obesity to systemic IR (64). Although translocation of MAMPs and other bacterial products are generally prevented in eubiosis, very low amounts of MAMPs, especially LPS, may be packaged with chylomicrons and delivered to the systemic circulation (81, 82). Increased LPS concentrations was observed in the blood (termed endotoxemia) of HF fed mice (5), and postprandial levels in humans were elevated after a high fat meal but not after smoking (83). Upon reaching peripheral tissues, LPS may induce IR via TLR4/CD14 signaling (5). Furthermore, LPS and other bacterial products in the plasma may activate TLRs on adipocytes leading to macrophage recruitment in a CCL2 dependent manner (84). TLR activation and monocyte recruitment to the white adipose tissue may then contribute to the pathophysiology of obesity-related IR, by increasing the release of free fatty acids and production of pro-inflammatory molecules (as discussed in section 2.0).

Under gut homeostatic conditions, IECs produce antimicrobial peptides (AMPs) and mucins, which control their interaction with the gut microbiota (85, 86)). Also, upon the identification of MAMPs by innate lymphoid cells 3 (ILC3), IL-22 is delivered to IECs which results in the production of antimicrobial peptides (α-defensins, REG3β and REG3γ), that kill or inhibit bacteria around the IEC's surface (85). The production of AMPs is impaired in HF diet-induced obesity (6, 87). When compared to mice fed a chow diet, mice fed a HF diet had reduced numbers of Paneth cells, which are specialized

IECs responsible for producing AMPs (87). Furthermore, as early as 30 days after HF feeding, mice became IR and have a significant reduction in REG3β and REG3γ gene expression in the ileum (6). In contrast, a symbiotic administration (probiotic and prebiotic) improved the gene expression of the AMPs to the level of control (6). This shows that HF diet reduced homeostatic gut immune surveillance by AMPs, thus exposing the IECs to direct bacterial interaction which may stimulate gut inflammation.

Under eubiosis, there exists a healthy balance of the commensal gut bacteria and inflammation is often directed towards gut tolerance (86). In this healthy gut state, recognition of MAMPs induces the IEC to produce mucins, AMPs and anti-inflammatory cytokines, such as IL-33, transforming growth factor β (TGF-β), and IL-25 (86). This in turn, stimulates the development of tolerogenic dendritic cells and macrophages (86). The tolerogenic macrophage secretes the anti-inflammatory cytokine, IL-10, which inhibits further activation, differentiation and proliferation of immune cells (86)[j]. Tolerogenic dendritic cells on the other hand, stimulates T-regulatory cells (T-reg cells) expressing the transcription factor FoxP3, to also secrete IL-10 via a TGF-β and retinoic acid – dependent mechanism (86). Furthermore, the induced T-reg cells secrete TGF-β which promotes the production of immunoglobulin A (IgA) from IgA^+ plasma cells (86). This ensures the abundance of IgA in the lumen, which further limits the interaction of the microbiota with the IEC (just like AMPs and mucins). Interestingly, HF feeding has been shown to reduce IL-10 levels and FoxP3+ T-cells in the gut (6, 88). Rats fed a 45% HF diet had a significant reduction of the IL-10 gene in the ileum as early as 1 week from the commencement of HF feeding (88). Moreover, mice became insulin resistant and a reduction of FoxP3-expressing T-cells was observed as early as 10 days of HF feeding,

which became statistically significant after 30 days of HF feeding (6). These studies suggest that HF feeding disrupts eubiosis and immune gut tolerance mechanisms.

TH17 cells, on the other hand, are vital in the containment and elimination of pathogenic bacteria, fungi and other MAMPs in the gut (8). This important function of TH17 cells make them one of the most abundant T-helper cell, together with T-reg cells, in the intestinal lamina propria (8). Upon pathogen recognition, dendritic cells deliver the cytokines, TGF-β and IL-6 to naïve T-cells, which stimulate the expression of the transcription factor retinoic acid orphan receptor (ROR)γt, and their subsequent differentiation to TH17 cells (89). The effector function of TH17 cells is the production of a subset of cytokines, including IL-17A, IL-17F, IL-22, and IL-26 (86, 89). IL-17A and IL-17F are vital cytokines for neutrophilia, since they stimulate IECs to produce CXC chemokines, which promote the recruitment of neutrophils for pathogen elimination (86, 90). Furthermore, IL-22 produced from TH17 cells promote epithelial proliferation and barrier maintenance, and the production of antimicrobial peptides, including REG3β, REG3γ and lipocalin-2, thereby restricting pathogens to the gut lumen (89, 90). The gut protective effect of TH17 cells during pathogen invasion was shown in IL-17RA$^{-/-}$ mice, where the absence of IL-17 signaling in *Salmonella typhimurium* –induced diarrhea led to a defect in neutrophil recruitment and promoted bacteremia (91). Furthermore, recent evidence showed that mice fed a HF diet for 30 days had a dysbiotic microbial signature and developed IR coupled with a significantly reduced TH17 cells and antimicrobial peptides (6). Thus, it was postulated that a reduction in TH17 cells with HF feeding suppresses the effector functions of these cells in orchestrating gut mucosal protection – a situation which encouraged endotoxemia-induced IR (6).

Despite the gut protective ability of TH17 cells, these cells may exist in a dichotomy of help and harm. Due to their high degree of plasticity, delivery of the cytokines IL-23 or IL-12 from dendritic cells or macrophages lead to the transition of TH17 cells to the IFNγ-producing TH1 cells, which are pro-inflammatory (86). Therefore, since T-regs are vital in inducing tolerance, a balance between TH17 cells and T-reg cells may be central in the maintenance of eubiosis (8).

4.2 *Short Chain Fatty Acids (SCFAs)*

Prebiotics are substrates that can be selectively utilized by the gut microbiota and confer a health benefit to the host (92). These complex carbohydrates also known as fiber, (including inulin, oligofructose, resistant starch, pectin, β-glucan etc) are selectively fermented into SCFAs in the distal GI tract (93). Acetate, butyrate and propionate are the main products of dietary fiber fermentation. Depending on the microbiota composition, fiber intake and intestinal transit time, SCFAs concentrations may reach 20-140 mM, and they may be absorbed and contribute 6-10% of the total daily energy requirement (94, 95). SCFAs serve as vital energy sources for both the commensal gut bacteria and intestinal epithelial cells of the host (96). Thus, dietary fiber can be beneficial to both the host and gut microbiota's health in many ways, which includes modulation of major shifts in the gut microbiota composition and gut mucosal immunomodulation towards an anti-inflammatory phenotype (93).

The anti-inflammatory effects of fiber are mainly due to gut microbial-dependent SCFAs production. For example, butyrate has been widely studied for its gut immunomodulatory functions (97-102). Butyrate serves as the main source of energy for

colonic epithelial cells and augments intestinal barrier function by upregulating tight junction proteins (97, 98). Also, butyrate may reduce colon cancer by inhibiting the activity of histone deacetylases (HDACs) (99). Furthermore, the administration of a diet rich in soluble fiber, resistant starch and inulin in an inflammatory bowel disease (IBD) model, resulted in high butyrate concentrations which was associated with elevated T-reg cells and reduced IFN-γ production (100). Moreover, butyrate administration in ulcerative colitis patients reduced NF-kB signaling pathways, by upregulating peroxisome proliferator activated receptor (PPAR)γ, which contributes to the reduction of intestinal inflammation (101, 102).

Due to the increasing evidence of the benefits of SCFAs to the host, its mechanism of action is becoming clearer (103). Three G protein-coupled receptors (GPRs) have been identified as vital in SCFAs signaling. These SCFAs receptors are GPR41 (Ffar1), GPR43 (Ffar2) and GPR10A (Hcar2), and are expressed by numerous cell types including IECs and immune cells (93). The adipose tissue expresses GPR41 and it is also expressed on peripheral blood mononuclear cells (PBMC) at low levels (93). On the other hand, GPR43 is expressed on immune cells, particularly high on neutrophils and eosinophils (103). This is evident in a colitis model, which showed that SCFAs induced the expansion and suppressive function of FoxP3+ T-reg cells in a GPR43-dependent manner (104). Indeed, mice lacking the GPR43 gene showed an increased susceptibility to inflammatory bowel disease (IBD), and were incapable to resolve inflammation due to the lack of SCFAs signaling on their immune cells (103). Furthermore, activation of GPR41 by SCFAs prevented colitis by inducing the differentiation of T-reg cells and IL10-producing T-cells (105). Since, SCFAs (especially

acetate) may be absorbed and reach high concentrations in the blood, systemic anti-inflammatory effects may also be observed (93). Therefore, SCFAs induction of gut tolerance may be vital to maintain eubiosis, by preventing the disruption in the communication between the gut microbiome and immune cells, which is significantly associated with the onset of metabolic disease.

5.0 The Gut-Adipose Axis in Obesity

The intestinal epithelium is a vital physiological barrier that prevents the passage gut bacteria and endotoxins into the circulation (106, 107). The regulation of this barrier is impaired in diet-induced obesity leading to increased adherence of bacteria and subsequent translocation mainly via paracellular channels (7, 108, 109). Similarly, LPS from gram negative bacteria may get into the systemic circulation mainly via passive transcellular diffusion (110). Primarily, LPS exits the gut through the lymphatic system more than through portal gateways (111). The entry of LPS into systemic circulation is via the thoracic duct (at the subclavian vein) (112). Thereafter, circulating LPS may bind to LPS-binding protein (LBP) to induce inflammation and impair insulin sensitivity in peripheral tissues such as the skeletal muscle, adipose tissue, or liver (113-115). Consequently, circulating LBP has been suggested as a marker for IR in obesity (116). Furthermore, LPS could be attached to lipoproteins and delivered to the adipose tissue where they contribute to chronic inflammation and adipose tissue dysfunction (81, 82).

In ideal situations, translocated bacteria are normally phagocytosed and processed by antigen presenting cells for effective elimination of such bacteria (108, 112, 117, 118). This process is impaired at the early stages of diet-induced obesity, as only a 10-day

feeding of a HF diet adequately suppressed MHC II signals in the distal ileum (6). The failure of gut restriction or elimination of bacteria encourages translocation into the mesenteric fat surrounding the gut and they may also reach mesenteric lymph nodes (108, 112, 117-119). This was evident in the study using GFP-labelled *E. coli* which showed that after only one week of HF feeding, live bacteria were observed in the white adipose tissue of mice fed a HF diet before the induction of pro-inflammatory markers such as TNF-α and IFN-γ (108). By the 4th week of HF feeding, observed adipose bacteria were 2-folds higher than week 1, which consequently corresponded to the elevated TNF-α and IFN-γ genes in the adipose tissue (108). Importantly, these changes occurred before the onset of HF diet-induced diabetes in the animals (5-7, 108). This is not surprising since the white adipose tissue contributes significantly to the chronic inflammatory state in obesity, which enables the impairment of insulin sensitivity (5, 120, 121).

In support of this, adipocytes express several PRRs such as TLR4, which is activated by LPS to generate proinflammatory factors such as IL-6, IL-1β, TNF-α and chemokines such as monocyte chemoattractant protein (MCP)-1 (122, 123). Furthermore, the abundance of immune cells such as macrophages in obese visceral adipose tissue may further enhance the pro-inflammatory state, since LPS-activated macrophages generate M1-like macrophages characterized by nitric oxide production and other mediators for microbicidal activity (124, 125). In agreement with the notion that gut-derived signals mediate adipose inflammation and obesity-induced diabetes, studies in germ-free (GF) mice showed that in comparison to conventionally raised mice, GF mice were resistant to obesity, were more glucose tolerant, and had less adipose inflammation (126-128). These studies suggest that mechanisms that improve intestinal homeostasis may aid the

restriction of bacteria and LPS to the gut, and be beneficial to prevent obesity-induced adipose inflammation and subsequent IR.

6.0 The Role of Signal Transducer and Activator of Transcription (STAT)3 in Gut Homeostasis

STAT proteins are cytoplasmic transcription factors that play a central role in signaling from the cell membrane to the nucleus (129). There exists seven members of the STAT family (129). Of these, STAT3 stands out as key in several vital cell types in the body. The importance of STAT3 is evident in the fact that whole body STAT3-KO mice did not survive past the embryogenesis stage (130).

STAT3 is a key player in intestinal health, but its impact in intestinal epithelial cells (IEC) have been mostly studied using $STAT3^{IEC\text{-}KO}$ mice (131-133). For example, restoration of intestinal homeostasis in DSS-induced colitis models required STAT3 activation (131, 134). STAT3 is activated by several signals, including the binding of IL6, IL-22, and IL-11 to their receptors, which results in the phosphorylation and nuclear translocation of STAT3 (131, 133). This leads to the transcription of STAT3 responsive genes involved in antimicrobial defense response and wound healing, such as Reg3β, Reg3γ, birc5 and pla2g5 genes (131). Among STAT3-inducing cytokines, IL-22 seems to be more important since IL-22 KO mice did not show any STAT3 phosphorylation in the IECs (131). Indeed, both IL-22 KO and $STAT3^{IEC\text{-}KO}$ mice showed a similar phenotype (131). This demonstrates that IL-22 signaling in the IECs is central to STAT3 activation and intestinal defense and healing to achieve homeostasis.

More recently, studies show that the SCFA, butyrate, contributes to intestinal homeostasis via the activation of the STAT3 pathway in intestinal epithelial cells (12, 135). Gut microbiota-derived or orally administered butyrate activated STAT3 in a GPR43-dependent manner, to induce the expression of Reg3γ and defensins in IECs (12). At the moment, it is unclear if the effect of butyrate on epithelial cell STAT3 could occur independent of IL-22. However, *in vitro* evidence suggest that butyrate plays a supportive role in IL22 signaling in human Caco2 cells, by upregulating the pivotal chain of the heterodimeric IL22 receptor- IL22R1 (135).

Apart from bacterial-derived butyrate, more evidence shows that the gut microbiome is involved in STAT3 activation in IECs to promote intestinal health (11, 136). Indeed, *Lactobacillus*-related bacteria may convert tryptophan into indole 3 acetic acid (I3A), which is capable of inducing IL-22 expression in innate lymphoid cells via the aryl hydrocarbon receptor (136). Consequently, STAT3 is activated leading to the expression of the Reg3 antimicrobial proteins (11, 136). Collectively, these studies imply that dietary sources of fiber and tryptophan may be vital in producing butyrate and I3A respectively, which could activate STAT3 in IECs for antimicrobial defense or wound healing. Consequently, HF diet-induced gut translocation into the blood or tissues such as the adipose and liver may be suppressed corresponding to the amelioration of inflammation and IR.

7.0 The Nutritional and Health Potential of Wheat Germ

Wheat germ (WG) is about 3.8% of the wheat grain and comprises of the scutellum and the embryonic axis (24). WG is a rich source of oil used in the production of certain

vitamins such as alpha-tocopherol (24). Due to its rich unsaturated oil content, WG is separated during the wheat milling process to prevent oxidative rancidity which is a significant commercial factor (137). Worldwide, WG is underutilized despite being a nutrient-dense component of the wheat grain. It is a significant source of concentrated nutrients such as phytosterols, tocopherols, policosanols, carotenoids and thiamin (24). The reports on its fiber content are somewhat inconsistent, as it has been reported to contain up to 4.5% fiber (24) or 13% fiber (**Table 1**) (138). In addition, WG is a rich

Table 1: Nutrient content of Wheat Germ

Nutrient	**Per 100 g Wheat Germ (crude)**
Total kcal	360
Carbohydrate (g)	51.8
Fiber (g)	13.2
Fat (g)	9.72
Protein (g)	23.15
Leucine (mg)	1571
Lysine (mg)	1468
Tryptophan (mg)	317
Calcium (mg)	39
Phosphorus (mg)	842
Potassium (mg)	892

USDA FoodData Central for Standard Reference Release 28 (138)

source of high quality protein (23% protein) (24). For example, a digestibility study using the digestible indispensable amino acid score (DIAAS) showed that WG is a good source

of the essential amino acid – tryptophan (300 mg / 100 g, **Table 1**) (25, 138). This suggests that apart from its fiber component, its tryptophan content could also be available for the metabolic survival of certain beneficial gut bacteria (26). Despite its reported nutrient richness, only few studies have investigated the potential health benefits of WG. For example, fermented WG extracts showed anti-tumour properties, including the induction of apoptosis and anti-proliferative effects in HT-29 colon cancer cells (27, 139). In addition, WG oil reduced chronic inflammation and oxidative stress in rats (28, 140), and exerted anti-oxidant effects in hypercholesterolaemic patients (29). Furthermore, 6-month supplementation with 60 g WG modulated glucose homeostasis in T2D subjects (30). More recently, a randomized crossover trial showed that daily intake of WG bread (6g) may promote a healthy gut bacteria and gut health, due to an increase in *Bifidobacterium spp.* as measured by quantitative polymerase chain reaction (141). Despite the reported health benefits, the potential mechanisms of WG action in promoting gut health *in vivo,* and how it may avert the gut and systemic implications of obesity is still largely unknown.

8.0 The Nutritional and Health Potential of Dried Beans

In developing countries, beans serve as an economical source of nutrients in the diet (32). However, consumption of dried bean has declined over the years due to the adoption of more western-style diets (32). Specifically, between 1960 and 1990, bean intake decreased by 24% and 40% in Mexico and India, respectively (142). In North America, dried beans are vastly underutilized (31). An NHANES data (1999-2002) reported that less than 8% of Americans consume beans on any given day with pinto variety being the most consumed (31). Furthermore, there is considerable variability in

consumption among ethnic groups, as the Hispanics represent 25% of those who consume any variety of dried beans daily (31).

Beans are protein-rich foods uniquely known for their low fat and high carbohydrate content. Interestingly, only about 3% of kilocalories in beans come from fat, which is mostly unsaturated fat (32). Apart from its high protein and low fat content, what makes beans considerably important especially for those on a plant-based diet is its content of the indispensable amino acid lysine. Indeed, a 60-kg individual may obtain 25% of the total lysine requirement by consuming one-half cup of beans (32). In addition, the NHANES 1999-2002 data showed that bean consumers are likely to consume more magnesium, folate, iron and zinc than non-consumers (31). Importantly, beans are also a good source of potassium, as one-half cup of cooked beans provides up to 436 mg potassium **(Table 2)** (138), similar to that provided by one serving of cow's milk (32).Additionally, beans have some antioxidant ability due to its content of polyphenols, such as flavonoids, phenolic acids and tannins (32, 143).

In comparison with other legumes and grains, beans are particularly rich in resistant starch (RS), which is the portion of starch that escapes digestion in the small intestine (144, 145). For example, the RS content of cooked beans may range from 1.7 – 4.2 g/100g, while that of oatmeal is 0.2 g/100g (32). Moreover, beans also have a high fiber content compared with other plant foods. Specifically, one-half cup of cooked pinto beans may provide about 9 g of total fiber **(Table 2)** compared to a maximum of about 4 g provided by one-half cup of whole grains (32). Interestingly, beans are also one of the best sources of soluble fiber (146). Its content of soluble fiber makes beans a suitable dietary component since it may promote gut bacterial fermentation to produce SCFAs.

The high content of RS and fiber in dried beans may be beneficial in maintaining gastrointestinal health, by sustaining the microbiome and promoting microbial fermentation. Pinto beans increased *in vitro* SCFAs production, especially

Table 2: Nutrient Content of Pinto Beans

Nutrient	Per 100 g cooked pinto beans
Total kcal	143
Carbohydrate (g)	26.22
Fiber (g)	9
Sugar (g)	0.34
Starch (g)	15.12
Fat (g)	0.65
Protein (g)	9
Leucine (mg)	664
Lysine (mg)	571
Tryptophan (mg)	98
Calcium (mg)	46
Phosphorus (mg)	147
Potassium (mg)	436

USDA FoodData Central for Standard Reference Release 28 (138)

propionate in human with pre-metabolic syndrome (35). Moreover, supplementation with red kidney beans resulted in high butyrate production in rats (147). Due to the ability of these SCFAs, especially butyrate, to induce growth arrest and apoptosis *in vitro*, it has been suggested that beans possess anti-cancer properties (34, 148).

Dried bean may be beneficial in glycemic control and management of diabetes due to their low glycemic index (GI). The replacement of carbohydrate-rich foods with beans reduced postprandial glucose levels in both nondiabetic and diabetic individuals (149, 150). Diabetic subjects who increased their intake of legumes with low GI (i.e. cooked beans, chickpeas or lentils), to 1 cup/day, had a decrease in glycated hemoglobin (HbA_{1c}) levels compared to those supplemented with wheat fiber (151). Also, a prospective epidemiological study, the Shanghai Women's Health Study, showed that there is decreased risk of developing diabetes with bean intake (152).

Furthermore, dried bean consumption may also modulate other diseases other than diabetes. For example, half cup of pinto bean consumption for 8 weeks resulted in a decrease in serum total cholesterol and LDL-cholesterol in moderately insulin resistant subjects (153). Also, a significant reduction in serum cholesterol upon pinto bean intake has been shown in both normolipidemic and hyperlipidemic men (154, 155). In separate studies, bean intake was shown to reduce acute inflammation which may lead to the progression of diseases (156, 157). Hull extracts of four different bean variety inhibits cyclooxygenase (COX)1, COX2 and lipooxygenease (157). In vitro, hydrolates of pinto bean cultivars showed an inhibition of inflammation via the modulation of NF-kB (156). These studies show the antioxidant and anti-inflammatory potential of bean consumption and its ability to markers of cardiovascular disease risk.

In conclusion, dried beans are a protein-rich, low-fat food with some micronutrients. Beans are also rich in RS and fiber that may explain some of their health benefits. While beans are an important part of the diet in developing countries, it is severely underutilized in North America. Thus, in an era where western diets are

prevalent and more people tend to turn to supplement intake, it is vital for nutrition and health professionals to encourage more whole food intake. This could be achieved in part, by understanding how whole foods may avert some of the HF diet-induced maladies. To this end, this project aims to determine the gut-protective mechanisms of WG and PB when added to a western-style diet and the implication on IR and the induction of proinflammatory cytokines in the adipose tissue.

CHAPTER III

Wheat Germ Supplementation Alleviates Insulin Resistance in an Animal Model Of Diet-Induced Obesity

Abstract

Obesity is strongly associated with insulin resistance (IR), along with mitochondrial dysfunction to metabolically active tissues and increased production of reactive oxygen species (ROS). Foods rich in antioxidants such as wheat germ (WG), protect tissues from damage due to ROS and modulate some negative effects of obesity. This study examined the effects of WG supplementation on markers of IR, mitochondrial substrate metabolism and innate antioxidant markers in two metabolically active tissues (i.e. liver and heart) of C57BL/6 mice fed a high fat-high sucrose diet (HFS) diet. Six-week-old male C57BL/6 mice were randomized into four dietary treatment groups (n=12 mice/group): control (C, 10% fat kcal), control+10% WG (C+WG), HFS (60% fat kcal), or HFS+10% WG (HFS+WG). After 12 weeks of treatment, HFS+WG mice had significantly less visceral fat (-16%, P=0.006) compared to the HFS group. WG significantly reduced serum insulin (P=0.009), the insulinotropic hormone, gastric inhibitory peptide (GIP, P = 0.0003), and the surrogate measure of insulin resistance, HOMA-IR (P=0.006). HFS diet significantly elevated (45%, P=0.02) cardiac complex 2 mitochondrial oxygen consumption, suggesting increased metabolic stress, while WG stabilized this effect to the level of control. Consequently, genes which mediate antioxidant defense and mitochondrial biogenesis (*Sod2* and *Pgc1a,* respectively) were significantly reduced (P<0.05) in the heart of the HFS group while WG supplementation tended to upregulate both genes. WG significantly increased hepatic gene expression of *Sod2* (P=0.048) but not *Pgc1a*. Together, these results showed that WG supplementation in HFS diet, reduced insulin resistance and improved cardiac mitochondrial metabolic functions.

*This chapter has been published in Br J Nutr. 2017 Aug;118(4):241-249.

Introduction

Consumption of diets high in simple sugar and saturated fat (i.e. the Western diet) is linked to the development of obesity, insulin resistance (IR), and cardiovascular diseases [1]. Increased intake of highly energy-dense diets causes lipid accumulation in non-adipose tissue such as the liver, heart, and skeletal muscle that leads to metabolic disturbances [2-5]. Fat accumulation in the heart results in lipid-induced IR in cardiac myocytes and cardiovascular dysfunction [6, 7], and fat in the liver can lead to peripheral IR [8, 9]. With the mitochondria being a major cellular site involved in lipid metabolism and the main source of reactive oxygen species (ROS), mitochondrial dysfunction plays a major role in fat deposition and increased oxidative stress which may result to impaired hepatic and cardiac function in high fat (HFS) diet-induced obesity and IR [10]. Therefore, approaches that reduce detrimental effects on mitochondrial function and ROS generation in these metabolically active tissues may help delay the development of IR.

Although medical advancements in recent years have increased the opportunities for the pharmacological management of IR and type 2 diabetes (T2D), these drugs may have potential side effects. Several drugs, including diabetic treatment and anti-inflammatory drugs, may undermine mitochondrial function and induce mitochondrial toxicity [11, 12]. Therefore, alternative approaches such as identification of dietary components that prevent or delay IR and hyperglycemia, may consequently modulate mitochondrial function and associated metabolic stress.

Wheat germ (WG) is an understudied portion of the wheat grain that contains several bioactive compounds, including large amounts of tocopherols, carotenoids, flavonoids and phytosterols, each of which possesses antioxidant properties [13].

Traditionally, WG has been mostly ignored as a byproduct of wheat milling. When utilized, it has been most frequently used to produce wheat germ oil or to add bulk to livestock feed [13]. However, extracts from fermented WG has been studied for their anti-tumor properties [14]. Additionally, WG oil showed a dose-dependent inhibitory potential towards acute and chronic inflammation in rats [15]. In their report, Allesandri and colleagues concluded that WG oil supplementation, due to its n-3 fatty acid content, exerted anti-atherosclerotic effects by reducing oxidative stress and platelet CD40 ligand expression in hypercholesterolemic patients [16]. Furthermore, six-month supplementation with high dose WG (30 g, twice daily), reduced fasting blood glucose and glycosylated hemoglobin in T2D subjects [17]. Despite the reported health potential of WG and its bioactive components, its impact on mitochondrial function and antioxidant potential in metabolically active tissues such as the liver and heart is unknown. Therefore, using a model of HFS diet- induced obesity, this study evaluated the effects of WG supplementation on markers of IR, mitochondrial oxidative capacity, and innate antioxidant markers in the liver and heart of C57BL/6 mice fed a HFS diet for 12 weeks. We hypothesized that WG supplementation, due to its many bioactive compounds, will delay the development of IR, preserve mitochondrial oxidative capacity, and maintain the antioxidant ability of the liver and heart, in mice fed a HFS diet.

Methods

Study design

Forty-eight, six-week-old male C57BL/6 (Charles River Laboratory) mice were housed at the Oklahoma State University (OSU, Stillwater, OK, USA) Laboratory

Animal Research facility in a temperature and humidity-controlled environment, maintained on a 12 hr light:dark cycle. Mice were acclimated to standard rodent diet (AIN-93M, Harlan-Teklad Diets, Envigo, WI, USA) for 1 week. Following acclimation, mice were randomly assigned to four dietary treatment groups (n=12 mice/group): control (C, 10% fat; AIN-93M), control + 10% wheat germ (C+WG), high fat-high sucrose (HFS; 60% fat), and HFS + 10% wheat germ (HFS+WG) for 12 weeks. The level of fat in the diet was based on our previous study [18] while the 10% wheat germ dose was based on similar studies that investigated other components of the wheat grain in animals [19] and WG supplementation in humans [16, 17]. The 10% WG dose used in this study is equivalent to approximately 50 g WG when calculated on a dry human diet (w/w) basis, which is within the range of what has been used in other human studies [16, 17].

WG from Oklahoma red winter wheat were obtained from Shawnee Milling Co (Shawnee, OK, USA), analyzed for its nutrient composition by NP Analytical Laboratories, (St Louis, MO, USA), and added to the control or HFS diets (10%, wt/wt). The WG diets were adjusted to have the same macronutrient composition, Ca and P to the control or HFS diets. Summary of diet compositions are presented in **Supplementary Table 1**. Individual body weights were measured weekly and food intake was recorded 3 times/week. Deionized water and food were provided *ad libitum*. The Institutional Animal Care and Use Committee at OSU approved all animal handling and procedures and were strictly followed.

Glucose Tolerance Test (GTT)

After 11 weeks of dietary treatment, mice were fasted for 6 hours before undergoing an intraperitoneal GTT. Blood glucose was measured from tail blood (baseline) followed by injection of a 20% glucose solution (2 g /kg body weight). Blood glucose was measured again at 15, 30, 60, and 120 minutes post-glucose injection using an AlphaTrak glucometer (Abbott Laboratories, IL, USA).

Necropsy and Tissue Processing

At the end of the 12 week dietary treatment, mice were feed-deprived for 3 hours and anesthetized with a cocktail of ketamine/xylazine (80 and 8 mg/kg, respectively). Body composition was assessed using a whole-body densitometer (PixiMus, GE Lunar, Madison, WI, USA). Serum was processed from blood collected from the carotid artery and stored at -80^{0}C for later analyses. Abdominal fat, heart, and liver were collected, weighed, snap-frozen in liquid nitrogen, and stored at -80^{0}C for further analyses. A portion of fresh liver and heart was isolated for mitochondrial function analyses (as detailed below).

Serum Measurements

Serum lipids, inflammatory markers, and diabetes markers were determined as described previously [20]. Briefly, serum concentrations of triglycerides (TGs), non-esterified fatty acids (NEFA), total cholesterol (TC), and HDL cholesterol were measured using a BioLis 24i automated analyzer (Carolina Chemistry, NC, USA). Diabetic markers were assessed with the Bio-Plex mouse diabetic markers kit (product # 171F7001M; gastric inhibitory peptide [GIP], glucagon-like peptide 1 [GLP1], insulin, leptin,

plasminogen activator inhibitor 1 [PAI-1], and resistin) using the Bio-Plex MAGPIX Multiplex reader (Bio-Rad Laboratories Inc, CA, USA) according to the manufacturer's instructions. IR was estimated utilizing the homeostatic model assessment of insulin resistance (HOMA-IR) as described previously [21]: HOMA-IR = (fasting insulin (μU/mL) x fasting glucose (mg/dL)/405.

Mitochondrial Respirometry

Liver and heart samples (60 mg) were homogenized on ice at low speed (Qiagen homogenizer) in 0.5 mL of mitochondrial isolation buffer (210 mM mannitol, 70 mM sucrose, 5 Mm HEPES, 1 mM EGTA and 0.5% (w/v) fatty acid-free BSA, pH 7.2), followed by a series of centrifugation steps as described earlier [22]. Isolated mitochondrial pellets were suspended in mitochondrial assay solution (1X MAS, 70 mM sucrose, 220 mM mannitol, 5 mM $MgCl_2$, 2 mM HEPES, 10 mM KH_2PO_4, 1 mM EGTA, 0.2% (w/v) fatty acid-free BSA) and protein concentration was determined using Pierce BCA protein assay kit (ThermoScientific, Rockford, IL). Mitochondrial pellet was re-suspended in 200 μg/mL mitochondrial assay solution for further analyses. Mitochondrial respiration was measured as oxygen consumption rates (OCR) using the Seahorse XF 96 flux analyzer (Seahorse Bioscience, Billerica, MA, USA) following the manufacturer's instructions. Briefly, isolated mitochondria from the liver and heart samples were seeded in triplicates into a 96-well microplate at 4 ug/well and 1 ug/well, respectively. For the coupling assay, final concentrations of compounds after port injections were 4 mM ADP (port A), 1.5 μM oligomycin (port B), 4 μM FCCP (port C) and 4 μM antimycin A (port D). Final concentrations of compounds for the electron flow assay were 2 μM rotenone

(port A), 10 mM succinate (port B), 4 μM antimycin A (port C) and 10 mM/100 μM ascorbate/TMP (port D). From these reactions, basal respiration, proton leak, maximal respiratory capacity, complex 1, 2, 4, and 5 OCR were calculated using the adjusted method from previous study [23] and as illustrated in **Supplementary Figure 1**. Results are reported as pmol O_2 min^{-1} μg^{-1} protein.

Gene Expression Analyses

Total RNA was isolated from frozen liver and heart samples using Trizol reagent (Thermo Fisher Scientific, Middletown, VA) following the manufacturer's protocol. RNA concentration and quality were assessed using a Nanodrop spectrophotometer (Thermo Fisher Scientific, Middletown, VA) and agarose gel electrophoresis [18]. Real time polymerase chain reaction was carried out as previously described [20]. In the liver and heart samples, relative abundance of genes involved in mitochondrial biogenesis (peroxisome proliferator-activated receptor γ coactivator [Pgc] 1-α, and Pgc-1β) and innate antioxidant defense (*Sod1, Sod2, Sod3*) were assessed using SYBR green chemistry on an ABI 7900HT system (Applied Biosystems, Grand Island, NY, USA). Relative quantitation for each gene was determined using the $2^{-\Delta\Delta CT}$ method [24] with cyclophilin B as the invariant control. Oligonucleotide primer sequences used in these experiments are listed in **Supplemental Table 2**. The results are presented relative to the control group.

Statistical Analyses

To calculate power, or the probability of detecting a specified difference, a two-tailed significance level of 0.05 was used. All data are reported as means SE. Differences between treatments groups were determined using two-way ANOVA with factors of high fat/high sucrose (HFS) and wheat germ (WG), followed by Tukey adjustment. For the weekly body weights and GTT data, repeated measures ANOVA were also conducted. All statistical analyses were carried out using SAS 9.4 software (SAS Institute, NC, USA). A P-value < 0.05 was considered statistically significant.

Results

Body Weights, Food Intake and Body Composition

Mice had similar body weights at the start of dietary treatment through the third week of feeding (Fig. 1a). Starting at the fourth week of dietary treatment, significant differences in weekly body weights were observed until the end of the twelve week study (P< 0.0001, Fig. 1a). A statistically significant main effect of HFS (P< 0.0001) and WG (P=0.008) on weekly body weight was observed. HFS diets increased body weight compared to those receiving the control diets starting at week five of treatment (P< 0.0001, Fig. 1a). At the end of the 12-week treatment, mice fed the control diet had the lowest body weight and the rest of the groups were statistically similar.

There was a significant main effect of HFS (P=0.003) on food intake (calories consumed/day) but not WG (Fig. 1b). As expected, HFS diet decreased relative amount of lean mass and increased relative amount of fat mass in comparison to the control diets (P< 0.0001, Fig 1c). The addition of WG also tended to decrease relative lean mass

(P=0.056) and increase relative fat mass (P=0.057). Similarly, HFS decreased relative liver weight and increased relative visceral fat mass (P< 0.0001) and the addition of WG has no effect on liver weight (Fig. 1c). Compared to control, the HFS diet significantly increased relative visceral fat mass by 32% (P<0.0001). However, WG supplementation in the HFS diet resulted in a 16% reduction (P=0.006) in relative visceral fat mass compared to HFS (Fig. 1c).

Glucose and Insulin Metabolism

Data from the glucose tolerance test showed that after 11 weeks of dietary treatment, mice that received the HFS diet had approximately 23% higher blood glucose (P<0.0001, Fig. 2a) compare to control prior to glucose injection (baseline, 0 min). Mice that received WG in combination with the control or HFS diet had similar baseline glucose to both the control and HFS diets. Following glucose injection, there is a significant interaction effect of HFS and WG (P = 0.037) as well as main effect of HFS (P<0.00010) but not WG (P=0.340, Fig. 2a). Both HFS and HFS+WG group had significantly higher (P< 0.05) blood glucose after 15, 30, 60 and 120 min of glucose injection, compared to both control diets. (Fig. 2a). The 19% decrease in blood glucose at the 120 min time point in HFS+WG compared to HFS was not statistically significant (P=0.256; Fig. 2a). In addition, HFS feeding significantly elevated (P< 0.0010) glucose total area under the curve (tAUC) by 48% compared control (Fig. 2b). The addition of WG to both the control and HFS diets had no effect on tAUC. Despite an 8% decrease in tAUC in the HFS+WG group compared to HFS, this did not reach significant levels (P=0.242).

Addition of WG to both the control and HFS diets resulted in approximately 50% reduction in fasting insulin (P=0.0009; Fig. 2c). Furthermore, WG also decreased serum concentration of the insulinotropic hormone, GIP (P=0.0003, Fig. 2d), and a trend to decrease the other insulinotropic hormone, GLP-1 (-27%, P=0.088, Fig. 2e). Finally, WG but not the HFS diet, significantly reduce (-46%, P=0.006, Fig. 2f) the surrogate measure of insulin resistance, HOMA-IR.

Serum Lipids

Analysis of serum triglycerides showed a significant main effect of HFS (P=0.002) and a trend in the HFS and WG interaction (P=0.063, Fig. 3a). WG significantly increased (P=0.010) serum NEFA in C diet group, but not in the groups consuming the HFS diet (Fig. 3b). Both the HFS (P<0.0001) and WG (P<0.005) treatments increased serum cholesterol (Fig. 3c). Finally, HDL was elevated in the HFS group compared to control (P<0.0001) while the addition of WG had no effect (Fig. 3d).

Hepatic and Cardiac Mitochondrial Respirometry

Mitochondrial function may be assessed by measuring its OCR to various challenges [25]. Mitochondrial respirometry data showed that neither HFS nor WG had an effect on hepatic mitochondrial OCR during basal respiration, maximum respiration, at each complexes of the electron transport chain, and proton leak (Fig. 4a). However, in the mitochondria from the myocardium, complex 1 OCR was significantly reduced by both HFS (P=0.011) and WG (P=0.021; Fig. 4b). In complex 2, the HFS diet significantly elevated OCR by 45% (P=0.024) compared to control, but OCR was normalized to the

level of control in the HFS+WG group (Fig. 4b). Despite the increase in complex 2 OCR by HFS diet, complex 5 OCR was significantly reduced by the HFS diet compared to control (23% decrease; P=0.002, Fig. 4b). The addition of WG to the HFS diet had no statistically significant effect on complex 5 OCR (Fig. 4b). Complex 4 OCR tended (P=0.060) to be decreased by the addition of WG.

Mitochondrial Biogenesis and Gene Expression of Innate Antioxidants

Similar to the results of hepatic mitochondrial OCR, hepatic gene expression of mitochondrial biogenesis and antioxidants were not significantly affected by dietary treatments, with the exception of WG effects on hepatic *Sod2* (Fig. 5a). A 38% increase (P=0.048) in hepatic gene expression of Sod2 was observed with the addition of WG to both the C and HFS diets. In the heart, the HFS diet significantly suppressed the expression of *Pgc1α* by 49% (P=0.0034) compared to control. WG decreased *Pgc1α* when added to the C diet, but increased in the HFS+WG group to the level of both the C and HFS groups (Fig. 5b). *Pgc1β* was not significantly modulated by the dietary treatments (Fig. 5b). Furthermore, expression of the mitochondrial isoform of the innate antioxidant gene, *Sod2*, was significantly lowered (-45%; P=0.02) by HFS feeding compared to control (Fig. 5b). In contrast to the HFS group, HFS+WG diet showed a trend (P=0.11) to counteract the HFS-induced decrease in *Sod2* expression (Fig. 5b). Finally, neither the cytoplasmic *Sod1* nor the extracellular *Sod3* was impacted by dietary treatments (Fig. 5b).

Discussion

We evaluated the effects of WG supplementation on markers of IR, mitochondrial oxidative capacity, and antioxidant markers in the liver and heart of mice fed a high fat-high sucrose diet. The liver and the heart are metabolically active tissues and increased intake of highly energy-dense diets causes lipid accumulation and oxidative stress in these tissues that leads to metabolic disturbances. In this study, WG supplementation reduced IR and stabilized complex 2 mitochondrial metabolism in the heart but not the liver. This study also demonstrates the potential of WG in modulating mitochondrial biogenesis and antioxidant markers.

Few studies have investigated the impact of WG in reducing components of T2D, which is characterized by insulin resistance and prolonged hyperglycemia [17, 26]. In diabetic patients, daily intake of WG (60 g) reduced fasting blood glucose and glycosylated hemoglobin levels [17]. Furthermore, WG possess α-glucosidase inhibitory properties that may be vital in preventing post-prandial hyperglycemia, a key factor in managing T2D [26]. The present study shows from a preventive standpoint that WG supplementation may afford protection against the hyperinsulinemic response and insulin resistance associated with high fat feeding. This effect may be aided by the reduction in visceral fat seen in this study, since accumulation of such fat may predict the development of insulin resistance [27]. It should also be noted that WG supplementation lowered serum GIP in both control and HFS mice, accompanied by a reduction in serum insulin and the insulin resistance index, HOMA-IR. Interestingly, reports have shown that ablation of the GIP signaling pathway with a GIP antagonist reverses insulin resistance in mice [28, 29]. This suggests that WG supplementation in this study may have modulated

insulin metabolism via reduction in the production or signaling of GIP, although this effect needs to be further explored.

HFS diet-induced damage to organs such as the liver and the heart can be due to ROS overproduction by the mitochondrial respiratory chain [30]. ROS overproduction results from the hyperpolarization of the mitochondrial membrane potential, leading to accumulation of electrons which consequently drives the reduction of O_2 to the superoxide radical [30]. High fat feeding in this study significantly elevated complex 2 OCR in the cardiac mitochondria compared to control, without increasing complex 5 OCR. WG supplementation normalized the complex 2 OCR to the level of the control. Turner et al [31] previously reported similar findings in the skeletal muscle of HFS-fed mice, where excess lipid availability increased the protein expression of mitochondrial complexes, including complex 2. It is noteworthy that HFS feeding in this study significantly elevated serum triglycerides compared to control. Therefore, our findings suggest that electrons generated in the cardiac mitochondria of the HFS group were not efficiently passed down the subsequent mitochondrial complexes for ATP generation which may potentiate increased ROS production. Subsequently, WG supplementation in the HFS diet showed the ability to counteract the HFS-induced cardiac mitochondrial inefficiency and dysfunction.

Correspondingly, our results indicate that the ability of the heart muscle to cope with the potential ROS generation was impaired as the HFS-fed mice had a significant decrease in cardiac *Sod2* gene compared to control. This is in agreement with the study of Sreekumar et al [32] where HFS feeding reduced free radical scavenging enzymes, including Sod1 and Sod2, in rat skeletal muscle. Sod2 is particularly important in

preventing mitochondrial oxidative injury as Sod2-deficient mice experienced perinatal mortality due to cardiomyopathy and fatty liver [33, 34]. WG supplementation in the HFS diet showed an antioxidant potential to upregulate hepatic and cardiac *Sod2* transcript. This effect may be due to the richness of WG in tocopherols and bioactive compounds such as carotenoids and flavonoids [13]. Although cardiac *Sod2* upregulation by WG in the HFS diet is still statistically similar to HFS, it is probable that the 12-week supplementation in this study was insufficient, as a 36-week supplementation period with antioxidants in HFS diet was reported to upregulate *Sod1* and *Sod2* transcript in rat skeletal muscle [32]. Furthermore, it is interesting to note that our data on *Sod2* transcript follows a similar pattern to *Pgc1α* gene expression in the heart of mice fed a HFS diet. HFS feeding significantly reduced *Pgc1α* compared to control while WG supplementation showed a potential for upregulation compared to HFS diet. Apart from its mediation of mitochondrial biogenesis, Lu et al [35] demonstrated that *Pgc1α* plays a vital role in regulating the expression of mitochondrial antioxidants including *Sod2*, in the hearts of mice. Therefore, our results suggests that HFS feeding reduces the ability of the heart to cope with ROS generation by suppressing *Pgc1α* and *Sod2* gene expression, but WG supplementation showed the potential to counter this effect.

Furthermore, WG supplementation in HFS-fed mice increased serum total cholesterol. This finding is in contrast to a previous report in humans [36]. Apart from the physiological differences in mice versus humans, a factor in modulating cholesterol action of WG may be its phytosterol content. Phytosterol-rich wheat germ significantly reduced plasma cholesterol compared to phytosterol-depleted wheat germ in normolipidemic volunteers [37]. This effect of phytosterols on cholesterol metabolism was

also found to be dose-dependent [38]. Since we did not assess the phytosterol content of the WG used in this study, it is possible that the phytosterol content of the WG was insufficient to modulate cholesterol metabolism. Limitations of our study include the use of single dose of WG and we did not assess the individual bioactive components present in the WG used in this study. Therefore, future studies should address these limitations as well as explore different sources of WG (i.e. from different wheat varieties), its dose-dependent effects on markers of IR and mitochondrial function, and including other mechanistic pathways it modulates. Furthermore, studies focused on the effects of WG on lipid metabolism should consider analyzing the phytosterol content.

In conclusion, this study showed that WG supplementation in HFS-fed C57BL/6 mice reduced IR and improved cardiac, but not liver mitochondrial function. WG also showed a potential to improve the HFS diet-induced reduction in *Sod2* and *Pgc1a* gene expression in the hearts of mice. The bioactive components in WG may be vital in mitigating some of the detrimental effects of HFS diet-induced obesity and IR.

References

1. Cordain L, Eaton SB, Sebastian A *et al.* (2005) Origins and evolution of the Western diet: health implications for the 21st century. *Am J Clin Nutr* **81**, 341-354.
2. Samuel VT, Shulman GI (2012) Mechanisms for insulin resistance: common threads and missing links. *Cell* **148**, 852-871.
3. Anderson EJ, Lustig ME, Boyle KE *et al.* (2009) Mitochondrial H 2 O 2 emission and cellular redox state link excess fat intake to insulin resistance in both rodents and humans. *J Clin Invest* **119**, 573-581.
4. Bonnard C, Durand A, Peyrol S *et al.* (2008) Mitochondrial dysfunction results from oxidative stress in the skeletal muscle of diet-induced insulin-resistant mice. *J Clin Invest* **118**, 789-800.
5. Rector RS, Thyfault JP, Uptergrove GM *et al.* (2010) Mitochondrial dysfunction precedes insulin resistance and hepatic steatosis and contributes to the natural history of non-alcoholic fatty liver disease in an obese rodent model. *J Hepatol* **52**, 727-736.
6. Dirkx E, van Eys GJ, Schwenk RW *et al.* (2014) Protein kinase-D1 overexpression prevents lipid-induced cardiac insulin resistance. *J Mol Cell Cardiol* **76**, 208-217.
7. Kok BP, Brindley DN (2012) Myocardial fatty acid metabolism and lipotoxicity in the setting of insulin resistance. *Heart Fail Clin* **8**, 643-661.
8. Hwang J-H, Stein DT, Barzilai N *et al.* (2007) Increased intrahepatic triglyceride is associated with peripheral insulin resistance: in vivo MR imaging and spectroscopy studies. *Am J Physiol Endocrinol Metab* **293**, E1663-E1669.
9. An J, Muoio DM, Shiota M *et al.* (2004) Hepatic expression of malonyl-CoA decarboxylase reverses muscle, liver and whole-animal insulin resistance. *Nat Med* **10**, 268-274.
10. Heilbronn L, Smith S, Ravussin E (2004) Failure of fat cell proliferation, mitochondrial function and fat oxidation results in ectopic fat storage, insulin resistance and type II diabetes mellitus. *Int J Obes* **28**, S12-S21.
11. Chan K, Truong D, Shangari N *et al.* (2005) Drug-induced mitochondrial toxicity. *Expert Opin Drug Metab Toxicol* **1**, 655-669.
12. Dykens JA, Will Y (2007) The significance of mitochondrial toxicity testing in drug development. *Drug Discov today* **12**, 777-785.
13. Brandolini A, Hidalgo A (2012) Wheat germ: not only a by-product. *International J Food Sci Nutr* **63**, 71-74.
14. Boros LG, Nichelatti M, Shoenfeld Y (2005) Fermented wheat germ extract (Avemar) in the treatment of cancer and autoimmune diseases. *Ann N. Y. Acad Sci* **1051**, 529-542.

15. Mohamed DA, Ismael AI, Ibrahim AR (2005) Studying the anti-inflammatory and biochemical effects of wheat germ oil. *Deut Lebensm Rundsch* **101**, 66-72.
16. Alessandri C, Pignatelli P, Loffredo L *et al.* (2006) Alpha-linolenic acid–rich wheat germ oil decreases oxidative stress and CD40 ligand in patients with mild hypercholesterolemia. *Arterioscler, Thromb, Vasc Biol* **26**, 2577-2578.
17. Haripriya S, Premakumari S (2010) Beta sistosterol of wheat germ reduces blood glucose in humans. *J Life Sci* **2**, 87-92.
18. Lucas EA, Li W, Peterson SK *et al.* (2011) Mango modulates body fat and plasma glucose and lipids in mice fed a high-fat diet. *Brit J Nutr* **106**, 1495-1505.
19. Neyrinck AM, Possemiers S, Druart C *et al.* (2011) Prebiotic effects of wheat arabinoxylan related to the increase in bifidobacteria, Roseburia and Bacteroides/Prevotella in diet-induced obese mice. *PLoS One* **6**, e20944.
20. Ojo B, El-Rassi GD, Payton ME *et al.* (2016) Mango supplementation modulates gut microbial dysbiosis and short-chain fatty acid production independent of body weight reduction in C57BL/6 mice fed a high-fat diet. *J Nutr* **146**, 1483-1491.
21. Berglund ED, Li CY, Poffenberger G *et al.* (2008) Glucose metabolism in vivo in four commonly used inbred mouse strains. *Diabetes* **57**, 1790-1799.
22. Bharadwaj MS, Tyrrell DJ, Lyles MF *et al.* (2015) Preparation and respirometric assessment of mitochondria isolated from skeletal muscle tissue obtained by percutaneous needle biopsy. *JoVE* e52350-e52350.
23. Lay S, Sanislav O, Annesley SJ *et al.* (2016) Mitochondrial stress tests using Seahorse respirometry on intact dictyostelium discoideum cells. *Chemotaxis: Methods Protoc*, 41-61.
24. Schmittgen TD, Livak KJ (2008) Analyzing real-time PCR data by the comparative CT method. *Nat Protoc* **3**, 1101-1108.
25. Montgomery MK, Turner N (2015) Mitochondrial dysfunction and insulin resistance: an update. *Endocr Connect* **4**, R1-R15.
26. Liu L, Deseo MA, Morris C *et al.* (2011) Investigation of α-glucosidase inhibitory activity of wheat bran and germ. *Food Chem* **126**, 553-561.
27. Miyazaki Y, Glass L, Triplitt C *et al.* (2002) Abdominal fat distribution and peripheral and hepatic insulin resistance in type 2 diabetes mellitus. *Am J Physiol Endocrinol Metab* **283**, E1135-E1143.
28. McClean PL, Irwin N, Cassidy RS *et al.* (2007) GIP receptor antagonism reverses obesity, insulin resistance, and associated metabolic disturbances induced in mice by prolonged consumption of high-fat diet. *Am J Physiol Endocrinol Metab* **293**, E1746-E1755.
29. Gault VA, Irwin N, Green BD *et al.* (2005) Chemical ablation of gastric inhibitory polypeptide receptor action by daily (Pro3) GIP administration improves glucose tolerance and ameliorates insulin resistance and abnormalities of islet structure in obesity-related diabetes. *Diabetes* **54**, 2436-2446.

30. Rolo AP, Palmeira CM (2006) Diabetes and mitochondrial function: role of hyperglycemia and oxidative stress. *Toxicol Appl Pharmacol* **212**, 167-178.
31. Turner N, Bruce CR, Beale SM *et al.* (2007) Excess lipid availability increases mitochondrial fatty acid oxidative capacity in muscle evidence against a role for reduced fatty acid oxidation in lipid-induced insulin resistance in rodents. *Diabetes* **56**, 2085-2092.
32. Sreekumar R, Unnikrishnan J, Fu A *et al.* (2002) Impact of high-fat diet and antioxidant supplement on mitochondrial functions and gene transcripts in rat muscle. *Toxicol Appl Pharmacol* **282**, E1055-E1061.
33. Li Y, Huang T-T, Carlson EJ *et al.* (1995) Dilated cardiomyopathy and neonatal lethality in mutant mice lacking manganese superoxide dismutase. *Nat Genet* **11**, 376-381.
34. Lebovitz RM, Zhang H, Vogel H *et al.* (1996) Neurodegeneration, myocardial injury, and perinatal death in mitochondrial superoxide dismutase-deficient mice. *Proc Natl Acad Sci* **93**, 9782-9787.
35. Lu Z, Xu X, Hu X *et al.* (2010) PGC-1α regulates expression of myocardial mitochondrial antioxidants and myocardial oxidative stress after chronic systolic overload. *Antioxid Redox Signal* **13**, 1011-1022.
36. Cara L, Armand M, Borel P *et al.* (1992) Long-term wheat germ intake beneficially affects plasma lipids and lipoproteins in hypercholesterolemic human subjects. *J Nutr* **122**, 317-326.
37. Ostlund RE, Racette SB, Stenson WF (2003) Inhibition of cholesterol absorption by phytosterol-replete wheat germ compared with phytosterol-depleted wheat germ. *Am J Clin Nutr* **77**, 1385-1389.
38. Racette SB, Lin X, Lefevre M *et al.* (2010) Dose effects of dietary phytosterols on cholesterol metabolism: a controlled feeding study. *Am J Clin Nutr* **91**, 32-38.

Figures

Figure 1: (a) Weekly body weights, **(b)** Food intake, and **(c)** Body composition and liver weight of C57BL/6 mice fed either a control (C) or high fat-high sucrose (HFS) diet supplemented with 10% wheat germ for 12 weeks. Data = mean ± SE, n=12/group. *P* values for significant main effects are shown in each panel. **Fig 1(a):** Symbols indicate significant differences between groups ($P<0.05$, two-way repeated measures ANOVA). *C is different from HFS and HFS + WG; # C + WG is different from HFS and HFS + WG; † C is different from HFS + WG. **Fig (c):** When the interaction HFS × WG was significant ($P<0.05$, two-way ANOVA), different letters indicate differences between groups as determined by the post-hoc testing. Dietary treatments: control (C), control + 10% wheat germ (C+WG), high fat-high sucrose (HFS), and high fat-high sucrose + 10% wheat germ (HFS+WG).

Figure 2: (a) Glucose tolerance test (GTT), **(b)** GTT total area under the curve (tAUC), **(c)** serum insulin concentration, **(d)** serum GIP concentration, **(e)** serum GLP-1 concentration and **(f)** HOMA-IR in C57BL/6 mice fed either a control (C) or high fat-high sucrose (HFS) diet supplemented with 10% wheat germ (WG) for 12 weeks**.** Data = mean ± SE, Figures **(a)-(b)** is n=10-12/group while Figure **(c)-(f)** is n=9/group. *P* values for significant main effects are shown in each panel. **Fig 2 (a):** When the interaction HFS × WG was significant ($P<0.05$, two-way repeated measures ANOVA), symbols indicate differences between groups at a given time point as determined by the post-hoc testing. Δ C is different from HFS, * C is different from HFS and HFS + WG; # C + WG is different from HFS and HFS + WG; † C + WG is different from HFS.
Dietary treatments: control (C), control + 10% wheat germ (C+WG), high fat-high sucrose (HFS), and high fat-high sucrose + 10% wheat germ (HFS+WG). GIP = Gastric inhibitory peptide, GLP1 = glucagon-like peptide 1, HOMA-IR = homeostatic model assessment of insulin resistance.

Figure 3: Serum concentrations of **(a)** Triglyceride, **(b)** NEFA, **(c)** Total cholesterol, and **(d)** HDL-cholesterol of C57BL/6 mice fed either a control (C) or high fat-high sucrose (HFS) diet supplemented with 10% wheat germ (WG) for 12 weeks. Data = mean ± SE, n=12/group.
P values for significant main effects are shown in each panel. When the interaction HFS × WG was significant ($P<0.05$, two-way ANOVA), different letters indicate differences between groups as determined by the post-hoc testing. Dietary treatments: control (C), control + 10% wheat germ (C+WG), high fat-high sucrose (HFS), and high fat-high sucrose + 10% wheat germ (HFS+WG). NEFA= Non-esterified fatty acid, HDL= high density lipoprotein

Figure 4: Mitochondrial oxygen consumption rates (OCR) in the **(a)** liver and **(b)** heart of C57BL/6 mice fed either a control (C) or high fat-high sucrose (HFS) diet supplemented with 10% wheat germ (WG). Mitochondrial OCR was measured in both liver and heart samples using the Seahorse XF^e 96 Extracellular Flux Analyzer (see methods). Data = mean ± SE, n=5/group.
P values for significant main effects are shown in each panel. When the interaction HFS × WG was significant ($P<0.05$, two-way ANOVA), different letters indicate differences between groups as determined by the post-hoc testing. Dietary treatments: control (C), control + 10% wheat germ (C+WG), high fat-high sucrose (HFS), and high fat-high sucrose + 10% wheat germ (HFS+WG).

Figure 5: Relative gene expression of mitochondrial biogenesis (*Pgc1α, Pgc1β*) and antioxidant markers (*Sod1, Sod2, Sod3*) in the **(a)** liver and **(b)** heart of C57BL/6 mice fed either a control (C) or high fat-high sucrose (HFS) diet supplemented with 10% wheat germ (WG) for 12 weeks. Data = mean ± SE, n=6/group. *P* values for significant main effects are shown in each panel. When the interaction HFS × WG was significant ($P<0.05$, two-way ANOVA), different letters indicate differences between groups as determined by the post-hoc testing. Dietary treatments: control (C), control + 10% wheat germ (C+WG), high fat-high sucrose (HFS), and high fat-high sucrose + 10% wheat germ (HFS+WG). Pgc1α= Peroxisome proliferator-activated receptor gamma coactivator 1-alpha; Pgc1β= Peroxisome proliferator-activated receptor gamma coactivator 1-beta; Sod1=Superoxide dismutase 1; Sod2=Superoxide dismutase 2; Sod3=Superoxide dismutase 3.

Figure 1

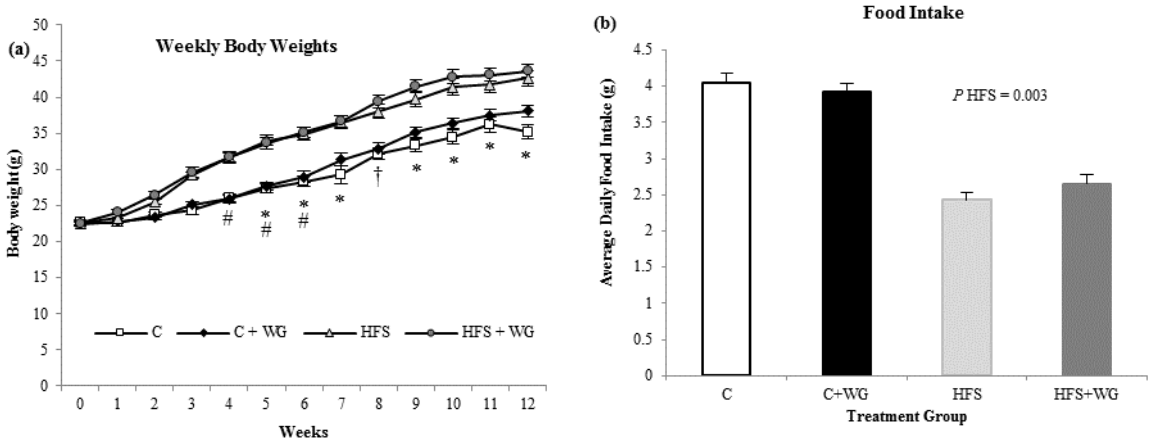
(a)
Weekly Body Weights
Body weight (g)
Weeks
C
C + WG
HFS
HFS + WG
(b)
Food Intake
Average Daily Food Intake (g)
P HFS = 0.003
C
C+WG
HFS
HFS+WG
Treatment Group

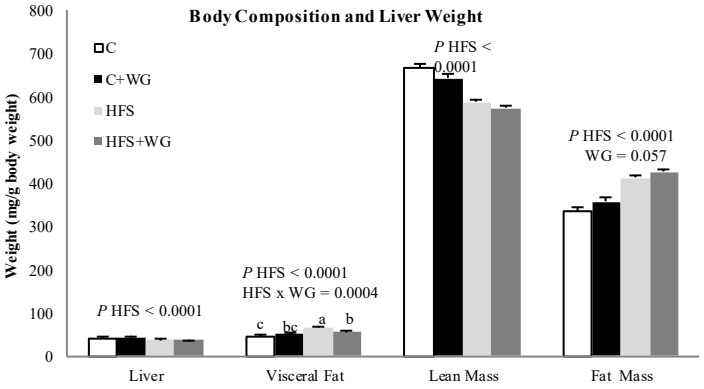
Body Composition and Liver Weight
Weight (mg/g body weight)
C
C+WG
HFS
HFS+WG
P HFS < 0.0001
P HFS < 0.0001
HFS x WG = 0.0004
P HFS < 0.0001
WG = 0.057
Liver
Visceral Fat
Lean Mass
Fat Mass

Figure 2

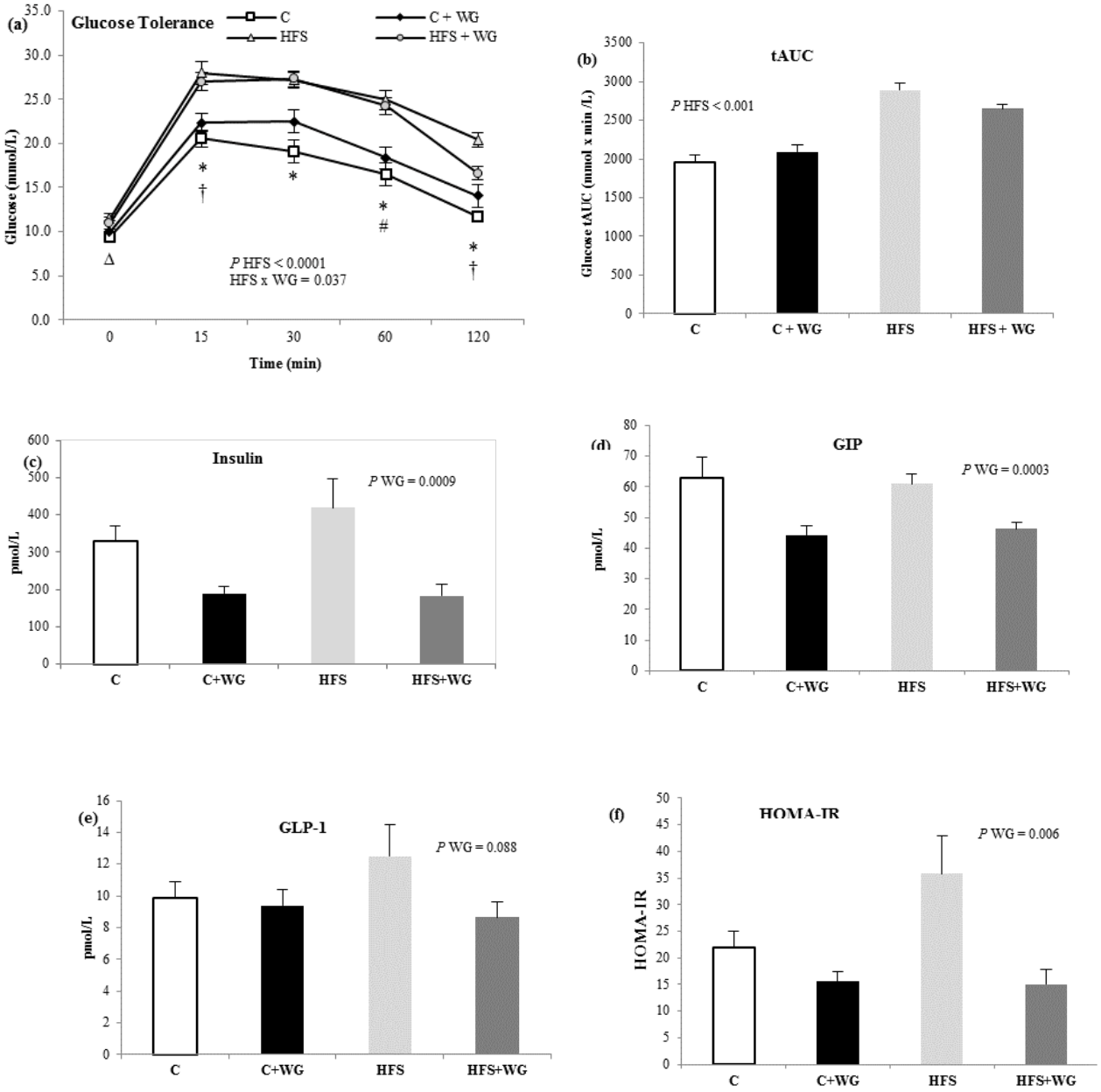
(a)
Glucose Tolerance
C
HFS
C + WG
HFS + WG
Glucose (mmol/L)
Time (min)
P HFS < 0.0001
HFS x WG = 0.037
(b)
tAUC
P HFS < 0.001
Glucose tAUC (mmol x min /L)
C
C + WG
HFS
HFS + WG
(c)
Insulin
P WG = 0.0009
pmol/L
C
C+WG
HFS
HFS+WG
(d)
GIP
P WG = 0.0003
pmol/L
C
C+WG
HFS
HFS+WG
(e)
GLP-1
P WG = 0.088
pmol/L
C
C+WG
HFS
HFS+WG
(f)
HOMA-IR
P WG = 0.006
HOMA-IR
C
C+WG
HFS
HFS+WG

Figure 3

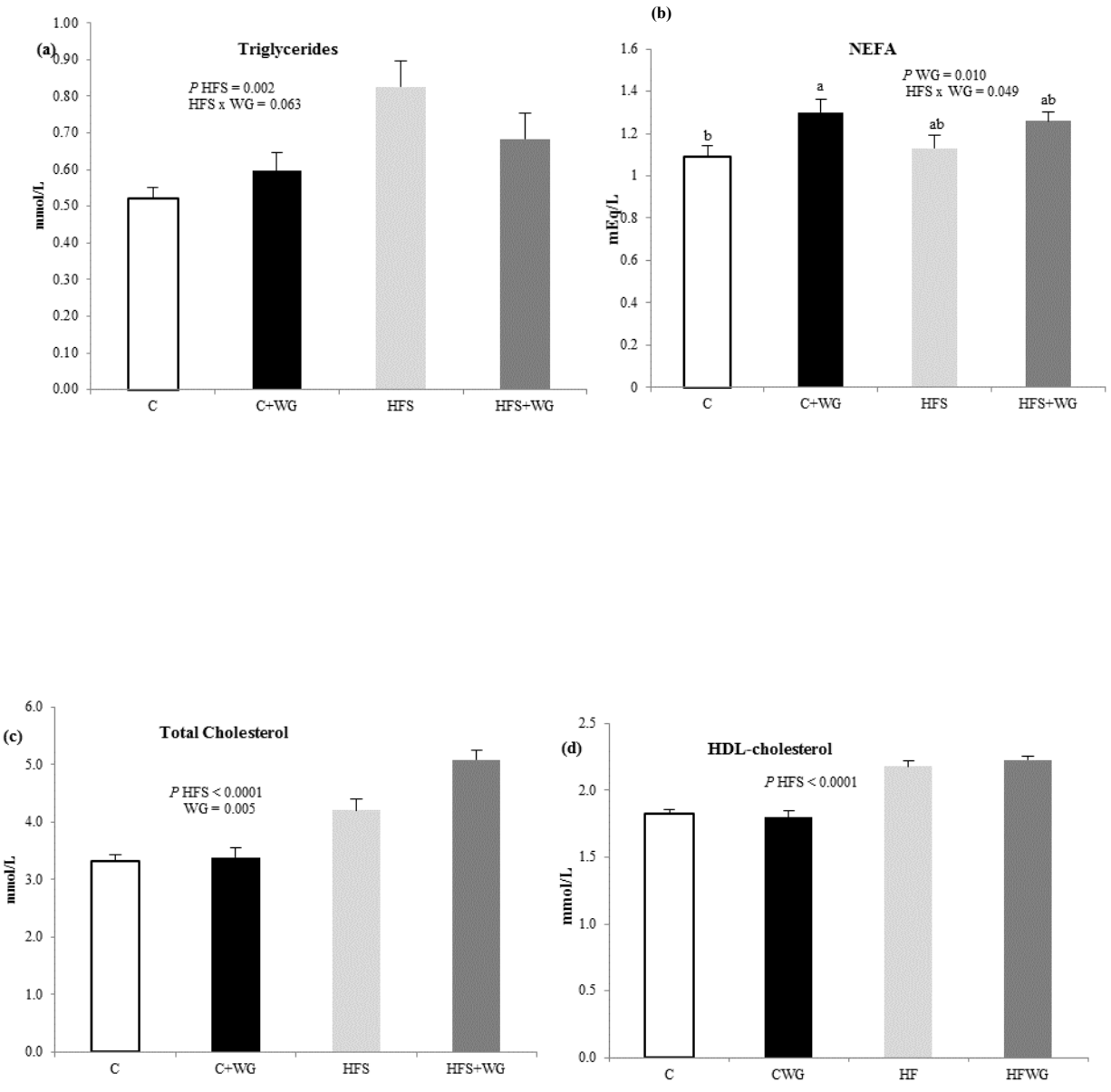
(a)
Triglycerides
P HFS = 0.002
HFS x WG = 0.063
mmol/L
1.00
0.90
0.80
0.70
0.60
0.50
0.40
0.30
0.20
0.10
0.00
C
C+WG
HFS
HFS+WG
(b)
NEFA
P WG = 0.010
HFS x WG = 0.049
mEq/L
1.6
1.4
1.2
1
0.8
0.6
0.4
0.2
0
a
b
ab
ab
C
C+WG
HFS
HFS+WG
(c)
Total Cholesterol
P HFS < 0.0001
WG = 0.005
mmol/L
6.0
5.0
4.0
3.0
2.0
1.0
0.0
C
C+WG
HFS
HFS+WG
(d)
HDL-cholesterol
P HFS < 0.0001
mmol/L
2.5
2.0
1.5
1.0
0.5
0.0
C
CWG
HF
HFWG

Figure 4

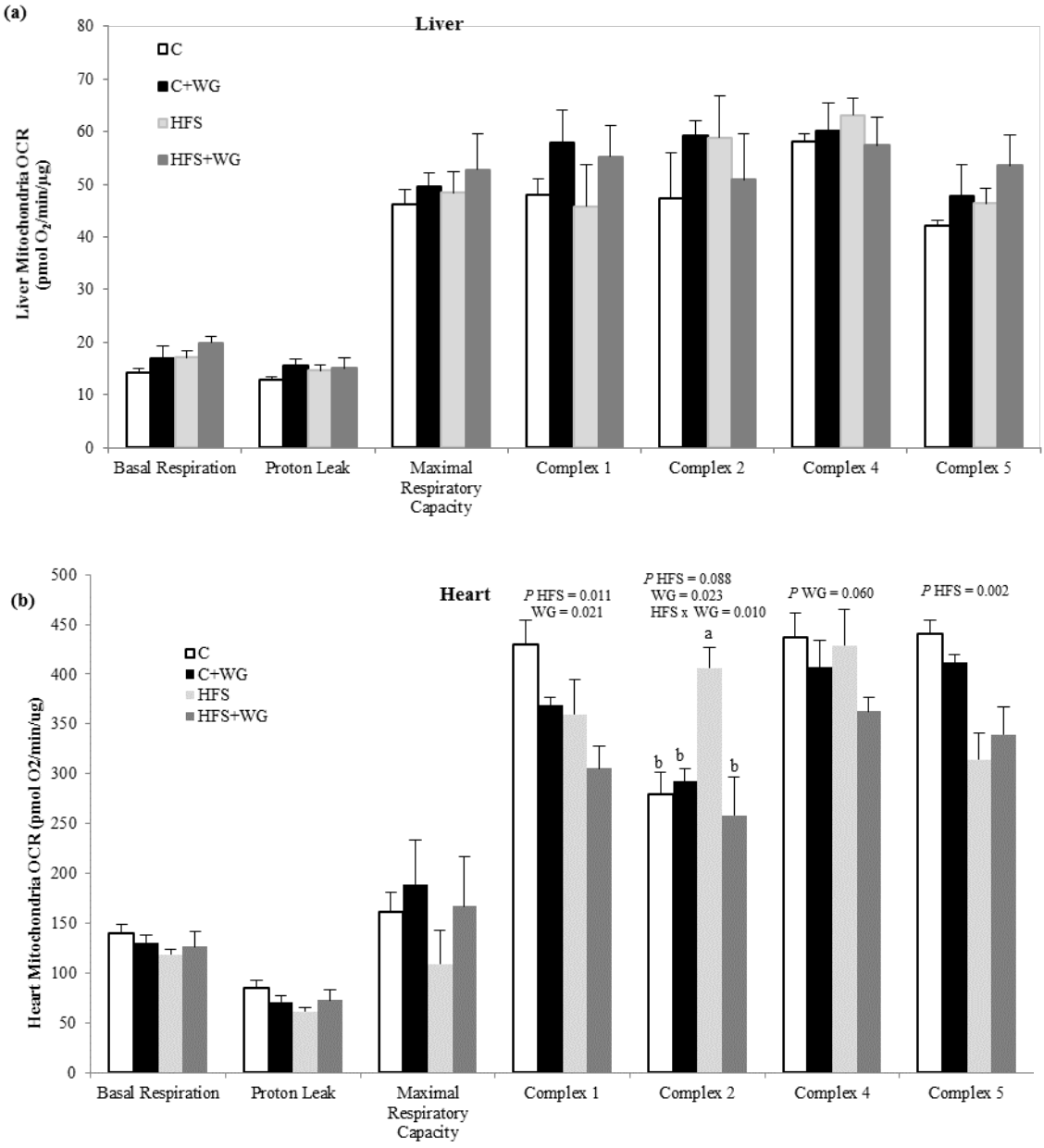
(a)
Liver
C
C+WG
HFS
HFS+WG
Liver Mitochondria OCR (pmol O2/min/µg)
80
70
60
50
40
30
20
10
0
Basal Respiration
Proton Leak
Maximal Respiratory Capacity
Complex 1
Complex 2
Complex 4
Complex 5
(b)
Heart
P HFS = 0.011
WG = 0.021
P HFS = 0.088
WG = 0.023
HFS x WG = 0.010
P WG = 0.060
P HFS = 0.002
C
C+WG
HFS
HFS+WG
Heart Mitochondria OCR (pmol O2/min/ug)
500
450
400
350
300
250
200
150
100
50
0
a
b
b
b
Basal Respiration
Proton Leak
Maximal Respiratory Capacity
Complex 1
Complex 2
Complex 4
Complex 5

Figure 5

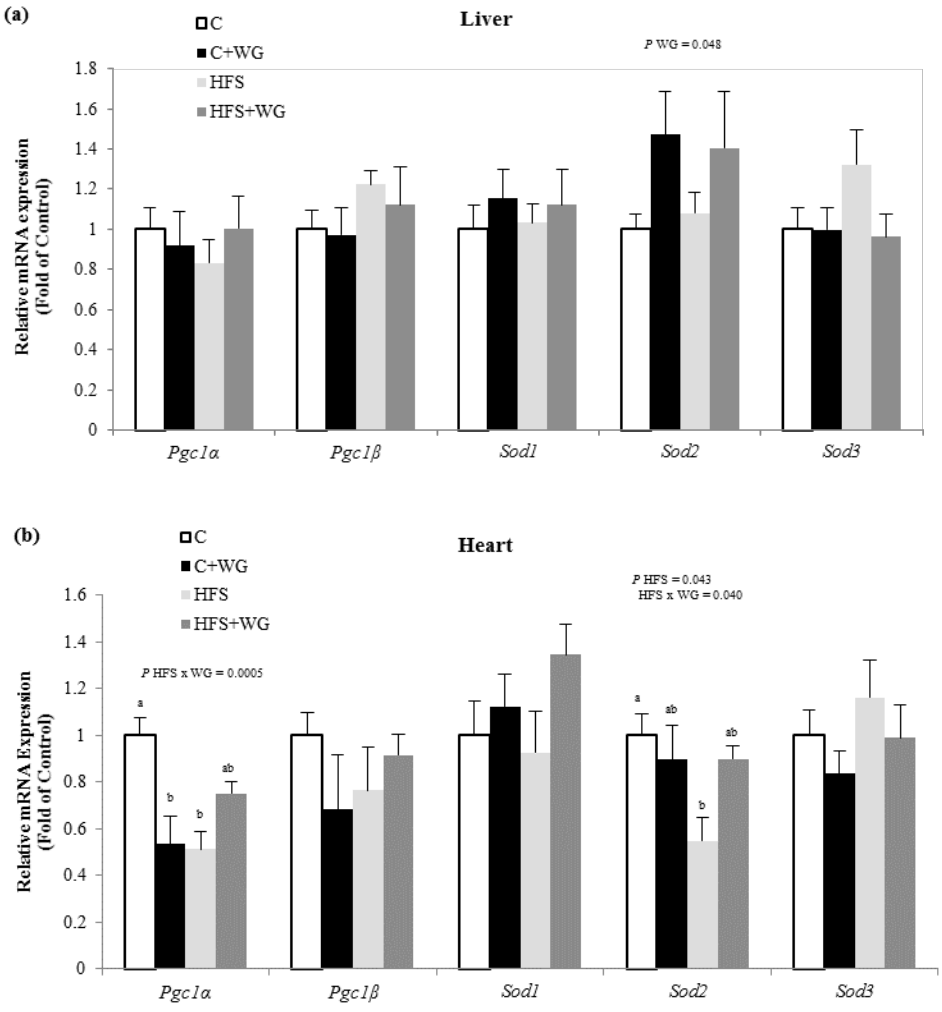
(a)
Liver
C
C+WG
HFS
HFS+WG
P WG = 0.048
Relative mRNA expression (Fold of Control)
1.8
1.6
1.4
1.2
1
0.8
0.6
0.4
0.2
0
Pgc1α
Pgc1β
Sod1
Sod2
Sod3
(b)
Heart
C
C+WG
HFS
HFS+WG
P HFS = 0.043
HFS x WG = 0.040
P HFS x WG = 0.0005
Relative mRNA Expression (Fold of Control)
1.6
1.4
1.2
1
0.8
0.6
0.4
0.2
0
a
b
b
ab
a
ab
b
ab
Pgc1α
Pgc1β
Sod1
Sod2
Sod3

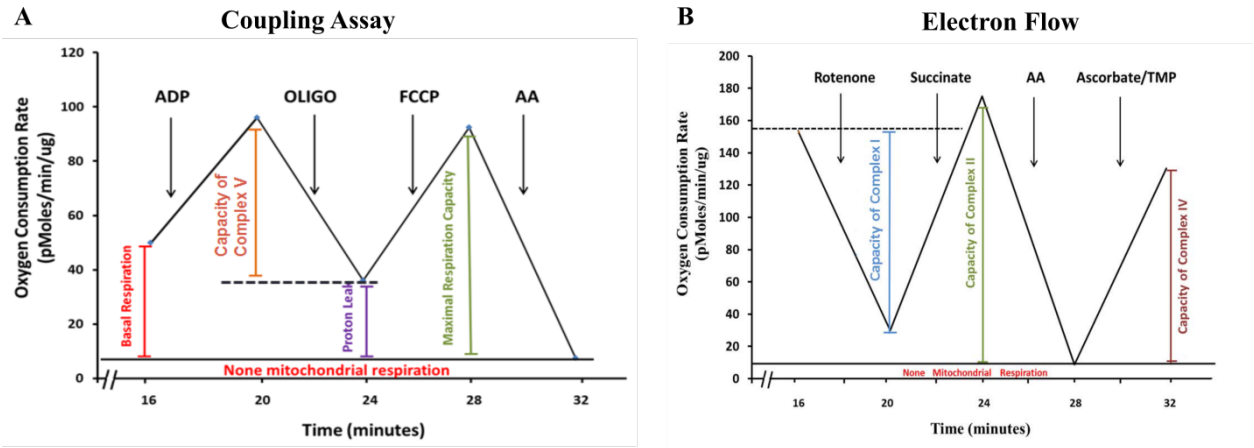

Supplementary Figure 1: Template for Seahorse XF^{e} 96 mitochondria respirometry analysis

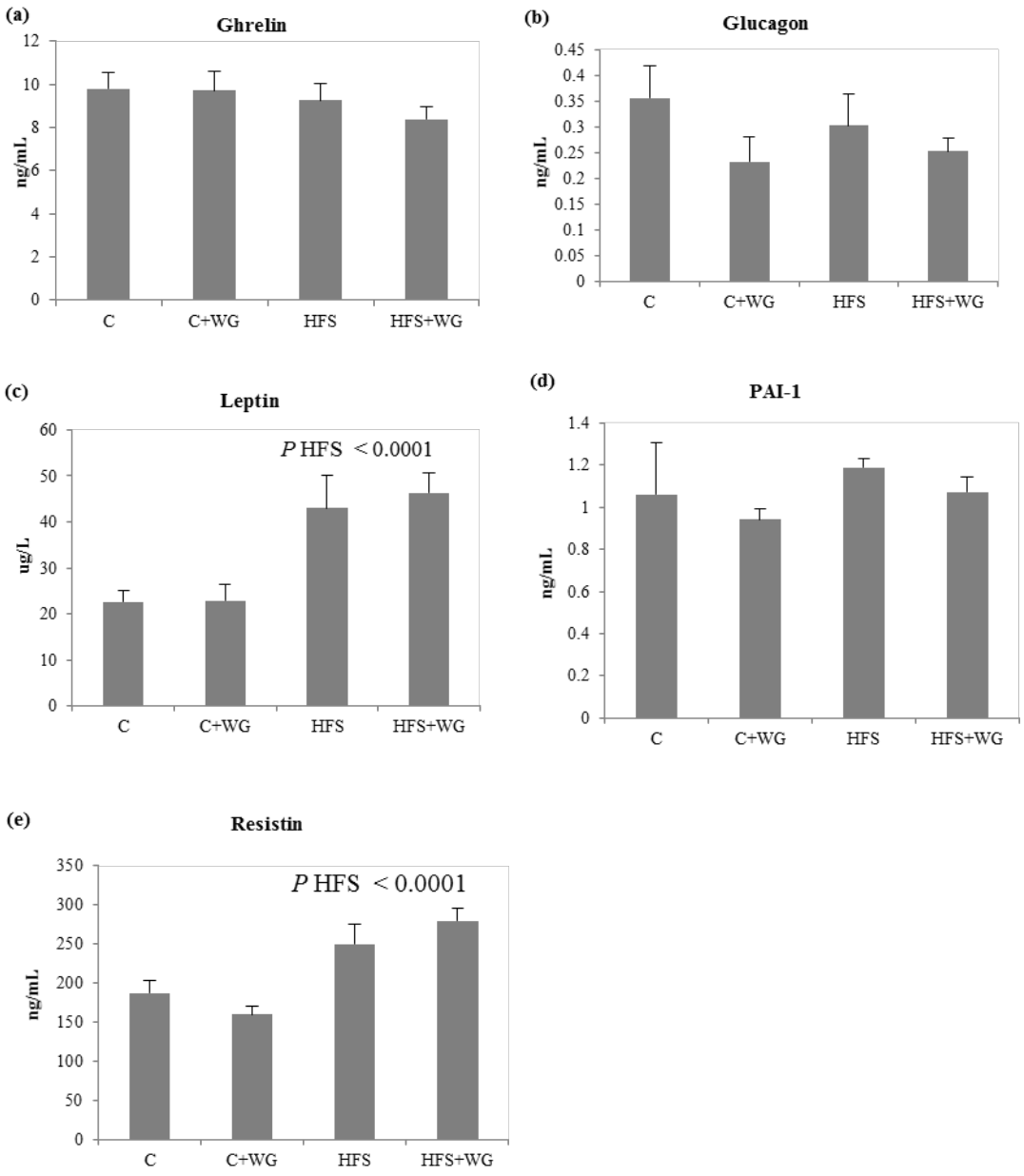

Supplementary Figure 2: Serum concentrations of **(a)** Ghrelin, **(b)** Glucagon, **(c)** Leptin, **(d)** PAI-1 and **(e)** Resistin in C57BL/6 mice fed either a control (C) or high fat-high sucrose (HFS) diet supplemented with 10% wheat germ (WG) for 12 weeks. Results were obtained using the Bio-Plex MAGPIX Multiplex Reader and as part of the Bio-Rad kit (product # 171F7001M; Bio-Rad Laboratories, CA, USA) described in the methods section. Data = mean ± SE, n=9/group.

P values for significant main effects are shown in each panel. When the interaction HFS × WG was significant ($P<0.05$, two-way ANOVA), different letters indicate differences between groups as determined by the post-hoc testing. Dietary treatments: control (C), control + 10% wheat germ (C+WG), high fat-high sucrose (HFS), and high fat-high sucrose + 10% wheat germ (HFS+WG); PAI-1=plasminogen activator inhibitor 1.

Tables

Supplementary Table 1: Diet Composition (g/kg)

	C	C+WG	HFS	HFS+WG
Wheat Germ (WG)[1]	--	100	--	100
Carbohydrates				
Total	722.1	724.77	372.26	374.93
Cornstarch	466	412.9	0	0
Sucrose	100	100	270	270
Dextrinized Cornstarch	155	155	100	46.9
WG[1]	--	53.1	--	53.1
Protein				
Total	140	140	180	180
Casein	140	116.6	180	156.6
WG[1]	--	23.4	--	23.4
Fat				
Total	40	40	350	350
Soybean Oil	40	33.35	40	33.35
Lard	0	0	310	310
WG[1]	--	6.65	--	6.65
Fiber				
Total	50	50	50	50
Cellulose	50	45.84	50	45.84
WG[1]	--	4.16	--	4.16
Vitamin Mix[2]	10	10	10	10
Mineral Mix[3]				
Total	35	35	35	35
Calcium	25.9	25.7	25.9	25.7
Calcium from WG[1]	--	0.06	--	0.06
Sodium Phosphate	5.6	3.8	4.8	3.02
Potassium Phosphate	2.4	1.65	2.06	1.3
Phosphorous from WG[1]	--	0.8	--	0.8
Sucrose	1.1	3.76	2.3	4.92
Kcal/g	3.8	3.8	5.4	5.4

[1]Wheat germ composition (Shawnee Mills, OK, USA) was analyzed by NP Analytical Laboratory (St. Louis, MO, USA): carbohydrates, 53.1%; protein, 23.4%; fat, 6.65%; fiber, 4.16%; calcium, 0.06%; and phosphorus, 0.08%.
[2]Harlan-Teklad Laboratories (TD 94047, WI, USA).
[3]Complete mineral mix (TD94049, Harlan-Teklad Laboratories) was used for the control diet (C) and a calcium and phosphorus deficient mineral mix (TD 98057, Harlan-Teklad Laboratories) was used for the C+WG and the HFS diets.
C=Control; C+WG= Control + 10% Wheat Germ; HFS=High Fat-High Sugar; HFS+WG=High Fat-High Sugar + 10% Wheat Germ

Supplementary Table 2: Oligonucleotide Primers for qRT-PCR

Target gene	Primer Sequence
Pgc1α	F 5' AAC-CAC-ACC-CAC-AGG-ATC-AGA 3'
	R 5' TCT-TCG-CTT-TAT-TGC-TCC-ATG-A 3'
Pgc1β	F 5' GAG-GGC-TCC-GGC-ACT-TC 3'
	R 5' CGT-ACT-TGC-TTT-TCC-CAG-ATG-A 3'
Sod1	F 5' GCC-CGG-CGG-ATG-AAG-A 3'
	R 5' CGT-CCT-TTC-CAG-CAG-TCA-CA 3'
Sod2	F 5' CTC-TGG-CCA-AGG-GGA-GAT-GTT 3'
	R 5' GTC-CCC-CAC-CAT-TGA-ACT-TC 3'
Sod3	F 5' CAG-ACA-AAG-GAG-CGC-AAG-AAG 3'
	R 5' TGA-GGC-TTA-AGT-GGT-CTT-GCA 3'

CHAPTER IV

Wheat Germ Supplementation Increases *Lactobacillaceae* and Promotes Gut and Systemic Anti-inflammatory Milieu in C57BL/6 Mice Fed a High Fat High Sucrose Diet

Abstract

A link between high fat diet consumption and obesity-related diseases is the disruption of the normal gut bacterial population which promotes local and systemic inflammation. Wheat germ (WG) is rich in bioactive components with antioxidant and anti-inflammatory properties, but its gut modulatory potential is unknown. This study investigated the effects of WG supplementation in modulating changes to the normal gut bacterial population and inflammatory markers in the gut and in the blood of mice fed a high fat high sucrose (HFS) diet. Six-wk-old male C57BL/6 mice were randomly assigned to four groups (n=12/group), and fed a control (C, 10% kcal fat, 10% kcal sucrose) or HFS (60% kcal fat, 20% kcal sucrose) diet with or without 10% WG (wt/wt) for 12 wk. Cecal bacteria was assessed via 16 S rDNA sequencing while fecal short chain fatty acids were measured by gas chromatography. Small intestinal CD4+ lymphocytes were evaluated using flow cytometry. Gut antimicrobial peptide genes and inflammatory markers were also assessed by qPCR. Data was analyzed by 2-way ANOVA using factors of HFS and WG. A four-fold increase ($p=0.007$) was observed in the abundance of the beneficial bacterial family, *Lactobacillaceae*, in HFS+WG group compared to HFS-fed group. WG supplementation in the control diet raised propionic and butyric acid concentrations compared to other groups ($P_{HFS \times WG} \leq 0.01$). Furthermore, T-regulatory cells ($CD4^+FOXP3^+$) in the small intestine were significantly higher (≥168%, $P_{WG}=0.005$) in both WG-supplemented groups compared to their respective unsupplemented groups, indicating an anti-inflammatory gut environment with WG feeding. Similarly, WG feeding increased ($P_{WG} = 0.038$) the anti-inflammatory cytokine gene, *Il-10*, in the ileum. Moreover, the anti-microbial peptide genes (*Reg3β* and *Reg3γ*) were upregulated in the ileum by at least 95% ($P_{HFS \times WG} \leq 0.02$) in the HFS+WG group compared to other groups. Pro-inflammatory cytokines, TNFα, IL1β, IL6 and IFNγ were significantly lower (P_{WG} <0.01) in the serum of WG-supplemented mice. WG showed strong gut modulatory and anti-inflammatory properties which may be vital in preventing HFS diet-induced morbidities. Indeed, WG may pose a significant economic value to wheat growers if its anti-inflammatory and gut modulatory potential can be harnessed.

*This chapter has been published in J Nutr. 2019 Jul 1;149(7):1107-1115.

Introduction

Obesity is an inflammatory disease which may be induced by various factors including excessive caloric intake predominantly from diets high in fat (HF). The inflammatory consequence of HF diets originates in part, from the disruption of gut eubiosis, involving detrimental changes in the gut microbiome and gut protective factors including mucin, antimicrobial peptides and immune cells (1, 2). Prominent reductions in core gut microbes observed in HF diet-induced morbidities include *Akkermansia, Bifidobacteria, Roseburia and Lactobacillus,* and few taxa within these genera are used in probiotics (1, 3-5). Moreover, high fat diets may decrease the gut protective mucin layer and reduce luminal concentrations of antimicrobial peptides, which in turn increase the chances of direct contact of the gut epithelium with resident bacteria and other microbe associated molecular patterns (MAMPs) (2, 6, 7). In addition, immune cells vital for gut homeostasis, including FOXP3+ T-regulatory cells important in gut immunoregulation, and Th17 cells essential in enteric pathogen elimination, are also altered in the ileum by HF diets (7, 8). Consequently, an increase in bacteremia or metabolic endotoxemia may follow HF feeding leading to the proinflammatory gut and systemic environment observed in HF diet-induced obesity and comorbidities (9, 10).

Prebiotics are mainly complex carbohydrates that are selectively utilized by host microbes and confer a health benefit (11). As such, several studies have shown the potential of fiber in ameliorating the consequences of HF-induced gut dysbiosis leading to morbidities (12-14). These complex carbohydrates serve as substrates to the gut microbiome, and thereby selectively stimulate the growth and activity of specific core or more dominant gut bacteria (15). Furthermore, the gut microbial fermentation of fiber

into short chain fatty acids (SCFAs) play a key role in the gut protective properties of dietary fiber.

SCFAs are vital energy sources of the hosts' intestinal epithelial cells (16). Specifically, butyrate may augment intestinal barrier function by upregulating tight junction proteins, making the gut impenetrable to resident bacteria and their MAMPs (17, 18). Moreover, SCFAs modulate a shift in gut mucosal immunity towards an anti-inflammatory phenotype. This is evident by the SCFA-induced differentiation and expansion of gut T-cells into both FOXP3+IL10- T_{reg} cells and FOXP3+IL10+ T_{reg} cells, indicating an increase in gut tolerance (19, 20). Thus, prebiotics may prevent HF diet-induced modifications to the gut microbiota, promote SCFA production and enhance gut homeostasis. While most studies have concentrated on the impact of isolated fiber as a prebiotic, only few studies have shown that whole foods, such as maize, whole wheat, bananas and mangoes, may also show prebiotic properties (21-24). Therefore, investigating whole foods that modulate the gut microbiota and immune cells may be an important approach in preventing the detrimental effects of western diets.

Wheat germ (WG) is a less appreciated by-product of the wheat milling process, with potential health benefits (25). WG, which represents about 2.5% (w/w) of the total wheat seed, is rich in various bioactive compounds, including carotenoids, tocopherols, flavonoids, policosanols, phytosterols and polyunsaturated fatty acids which have potent antioxidant and anti-inflammatory properties (25). In animal models, WG was shown to possess anti-tumor properties and the ability to combat acute and chronic inflammation (26, 27). In humans, the addition of WG or its oil to the diet showed anti-atherosclerotic effects in hypercholesterolemic patients, reduced postprandial triglyceride and cholesterol

in healthy subjects (28-30). Moreover, we previously reported that the addition of WG to a diet high in fat and sucrose (HFS) reduced insulin resistance (IR) and showed cardioprotective potential (31). Fiber derived from wheat bran have been reported to show prebiotic and antidiabetic properties (32, 33). However, WG also contains about 4% fiber, but its availability for microbial fermentation and gut modulation is still unknown despite its reported health potential (25, 30, 31). This is important since dietary approaches that reduce gut dysbiosis may alleviate the onset of diet-induced inflammation and IR (10). Hence, the present study evaluated the effects of WG supplementation in preventing changes in the abundance and fermentative activity of the gut bacterial population, together with WG's effect on inflammatory markers in the gut and in the blood of C57BL/6 mice fed a control and HFS diet.

Methods

Study Design and Diets. 6-wk old, male C57BL/6 mice (n = 48) were obtained from Charles River Laboratory and housed in wire-bottom cages (4 mice/cage) at the Oklahoma State University Laboratory Animal Research facility under humidity and temperature-controlled conditions, maintained on a 12 h light–12 h dark cycle. After a week acclimation to the standard rodent diet, AIN-93M (34), mice were randomly assigned to one of four dietary treatment groups (n=12/group): control (C, 10% kcal fat, 10% kcal sucrose; AIN-93M), C + 10% WG (C+WG), HFS (60% kcal fat, 20% kcal sucrose), and HFS + 10% WG (HFS+WG) for 12 weeks.

Wheat germ from Oklahoma red winter wheat were obtained from Shawnee Milling Co. (Shawnee, OK), analyzed for its nutrient composition (NP Analytical Laboratories, St Louis, MO) and incorporated into one of the control and one of the HFS diets (10%, w/w). The WG-supplemented diets were adjusted to have the same macronutrient composition, total fiber, calcium and phosphorus as the control or HFS diets. Food and water was provided *ad libitum* for 12-wk. Specific details of the diet compositions and metabolic characterization for this study have been reported previously (31). All procedures strictly followed guidelines set forth by the Oklahoma State University Animal Care and Use Committee.

Tissue Sampling and Processing. Fecal samples were collected per cage during the last week of dietary treatment and frozen at -80ºC until analyses. After 12-wk of dietary treatment, mice were fasted for 3 hours, anesthetized, and body composition were assessed using a whole-body PixiMus densitometer (GE Lunar, Madison, WI). Serum was processed from blood obtained via the carotid artery. Cecal contents were flushed into sterile tubes, centrifuged, and the precipitate was snap-frozen and stored at -80ºC until analyses. In preparation for isolating gut lamina propria lymphocytes, the Peyer's patches were excised and the small intestine (duodenum, jejenum and ileum) was flushed with RPMI medium supplemented with 2% fetal bovine serum (FBS). Flushed small intestinal specimens were opened longitudinally, cut into small pieces, and placed in complete medium (RPMI + 2% FBS + 1mM DTT) until processing. Furthermore, mucosal samples were carefully removed from sections of the distal ileum and stored in RNA*later* (ThermoFisher) for gene expression analyses.

Gut Microbiota. Cecal bacterial analyses was carried out as described previously (24). Briefly, nucleic acid isolation was performed on frozen cecal samples (n = 6 or 9 mice/group, equal representation per cage) with the MoBio PowerMag® Microbiome kit (Carlsbad, CA) according to manufacturer's guidelines and optimized for high-throughput processing. All samples were quantified via the Qubit® Quant-iT dsDNA High Sensitivity Kit (Invitrogen, Life Technologies, Grand Island, NY). Samples were PCR-amplified to enrich the 16S v4 rDNA region using two differently bar coded V4 fusion primers (*515f*: GTGYCAGCMGCCGCGGTAA; *806r*: GGACTACNVGGGTWTCTAAT). Enriched 16S v4 samples were pooled, amplified, barcoded and sequenced on a Miseq instrument (Illumina) for 2 x 250 cycles using custom primers for pair-end sequencing (Second Genome Inc, San Francisco, CA). For Operational Taxonomic Unit (OTU) determination, sequenced pair-end reads were merged and dereplicated with USEARCH, followed by clustering of unique sequences at 97% similarity by UPARSE to enable the determination of representative consensus sequences per *de novo* OTU (35). To generate an abundance table for *de novo* OTUs, all non-strain sequences that passed the quality filtering were mapped to the representative consensus sequences. Representative OTU sequences were assigned taxonomic classification using Mothur's Bayesian classifier (36) trained against the Greengenes reference database (37) of 16S rRNA gene sequences with 80% classification confidence.

Short Chain Fatty Acids. Fecal samples collected per cage at the end of the study were processed in duplicates for SCFA analyses. Acetic, propionic, n-butyric and iso-butyric

acids were determined from fecal samples via gas chromatography, while fecal lactate was quantified following Taylor's method as previously described (24, 38).

Flow Cytometry (FCM). Single-cell suspensions of lamina propria lymphocytes were prepared from the small intestine (SI) of mice (duodenum, jejenum and ileum) and analyzed as described previously with few modifications (39) . Flushed and excised SI was incubated with HBSS with 2mM EDTA at room temperature to remove epithelial cells, followed by a 3X incubation with 0.20 mg/mL collagenase Type VIII (Sigma-Aldrich, St. Louis, MO). Cell suspensions were filtered through a 70 um sterile filter and separated on 40% and 80% Percoll gradients. Cells at the interface were collected and washed in complete media thrice. Cells were then fixed (10 million cells/ml) using the mouse Foxp3 fixation buffer (BD Biosciences) and washed once. Viable cells ($1x10^6$) were permeabilized (Mouse FoxP3 permeabilization buffer, BD Biosciences), and stained with mouse antibodies specific for T-helper cells (CD4), Foxp3, IL-17a, using the mouse Th17/Treg phenotyping kit and their respective single stains and isotype controls (BD Biosciences, San Jose, CA) following manufacturer instructions. FCM analyses were carried out at the flow cytometry laboratory, Center for Veterinary Health Sciences, Oklahoma State University, (Stillwater, OK), using BD FACSAria III (BD Biosciences, San Jose, CA). 10^5 events were acquired and data were analyzed with the BD FACSDiva Software (version 8.0.1).

Gene Expression Analyses. Total RNA was isolated from distal ileum mucosal samples using Trizol reagent (Ambion, Carlsbad, CA) following the manufacturer's protocol. The

Nanodrop spectrophotometer (Thermo Fisher Scientific) and agarose gel electrophoresis were used to evaluate RNA concentration and quality, respectively. Relative abundance of genes encoding antimicrobial peptides (*Reg3b* and *Reg3g*), mucin (*Muc2*), inflammatory markers (*Il6* and *Il-10*) and transcription activator (*Stat3*) were evaluated using SYBR green chemistry on an ABI 7900HT system (Applied Biosystems, Grand Island, NY, USA) as previously described (24). The primer sequences used in this study are presented in **Supplemental Table 1**.

Serum Inflammatory Cytokines. Systemic inflammatory signature was determined by the evaluation of cytokines (IL-10, IL-17, IL-1b, IL-6, IFN-y and TNF-a) in the serum using the Bio-Plex Pro Mouse Cytokine Th17 Panel A 6plex kit (Product #: M6000007NY, Bio-Rad, Hercules, CA). Concentrations of these analytes were measured using the Bio-Plex MAGPIX Multiplex Reader and the Bio-Plex Manager 6.1 (Bio-Rad, Hercules, CA) following manufacturer's instructions.

Statistical Analyses: For the cecal microbiota data, differential abundance of OTUs was tested using a negative binomial noise model for the over-dispersion and Poisson process intrinsic to the data, as implemented in the DESeq2 package and described for microbiome applications (40, 41). DESeq was run under default settings and the Benjamini-Hochberg procedure was used to correct p-values, thereby controlling for false discovery rates (42). Differences between two groups were determined with a Kruskal-Wallis rank sum test followed by *post-hoc* analysis using Dunn's test. OTUs with the adjusted P value < 0.05 and more than one log 2-fold change were reported for the

bacterial genus data. For all other data, two-way ANOVA (factors of HFS and WG) and least square means were calculated using the mixed model procedure and Fisher's least significant difference was used in comparing groups. Analyses were conducted using SAS 9.4 software (SAS Institute, NC, USA). Data presented are means ± SEM and a *P*-value < 0.05 was considered statistically significant. In any case where the *P*-value for interaction ($P_{HFS \times WG}$) was not significant, significant main effect *P*-values (P_{HFS}, P_{WG}) were given.

Results

In our previous report focused on the metabolic response of these animals (31), WG had no significant effect on body weight or food intake in this study. In addition, HFS-fed mice had a 32% increase in visceral fat compared to control (P <.0001), while the HFS+WG group had a 16% reduction in visceral fat compared to the HFS group (P=0.006). In the serum, a significant main effect of WG was observed in reducing fasting insulin (P_{WG} = 0.0009) and gastric inhibitory peptide (P_{WG} = 0.0003). Moreover, WG showed a significant main effect of decreasing (P_{WG} = 0.006) the surrogate measure of insulin resistance - homeostatic model of insulin resistance (HOMA-IR), in the WG-supplemented groups (31).

WG supplementation increases Lactobacillaceae in the cecal microbiota of HFS-fed mice. Principal coordinate analysis of OTUs revealed that the experimental groups separated along axis 1 according to C or HFS dietary treatment (**Figure 1A**; Permanova, p=0.001). While the C and C+WG largely clustered similarly, HFS samples separated according to WG treatment along axis 2 (**Figure 1A**). Phylum level changes showed a

95% reduction in the abundance of Actinobacteria ($P = 0.04$) in the HFS group compared to control (**Figure 1B**, **Supplemental Table 2**). Accordingly, 2 OTUs each belonging to the genera *Bifidobacterium* and *Adlercreutzia* were ≤16 fold lower ($P \leq 0.04$) in the HFS group compared to control (**Supplemental Figure 1A**). The highest effect of HFS feeding was observed in the Deferribacteres phylum, which increased by over 2130 folds ($P = 0.01$) in HFS compared to control (**Figure 1B**, **Supplemental Table 2**). Consequently, 3 OTUs belonging to the *Mucispirillum* genus (species *schaedleri*) were ≥78 fold higher ($P \leq 0.0002$) in the HFS compared to control (**Supplemental Figure 1A**).

The most significant impact of WG supplementation was observed within the Firmicutes phylum. A mild increase was seen in Firmicutes (32%, $P = 0.10$) with HFS-feeding compared to control (**Figure 1B**, **Supplemental Table 2**). Further analysis revealed that HFS feeding resulted in a non-significant decrease (-70%, $P = 0.32$) in the family *Lactobacillaceae*, a prominent member of the Firmicutes phylum, compared to control (**Figure 1C**, **Supplemental Table 3**). However, WG supplementation in the HFS diet resulted in a 4 fold increase ($P = 0.007$) in *Lactobacillaceae* compared to HFS only (**Figure 1C**, **Supplemental Table 3**). Subsequently, four OTUs belonging to the genus *Lactobacillus* were at least 4 fold greater ($P \leq 0.03$) in the HFS+WG group compared to HFS (**Supplemental Figure 1B**). Generally, WG supplementation in the control diet had no statistically significant effect on the cecal microbiota compared to the control diet (**Figure 1B**, **C, Supplemental Table 2, 3**).

WG supplementation elevates fecal SCFA in mice fed a control but not HFS diet. After 90 days of dietary treatment, a main effect of HFS ($P_{HFS} \leq 0.02$) was observed at decreasing acetic acid, i-butyric acid, and lactic acid content of mice fecal samples (**Figure 2 A, C, E**). However, WG increased fecal propionic acid in the control diet group (140%, $P_{HFS\,x\,WG} = 0.003$) but not in the HFS-fed group (**Figure 2B**). Similarly, WG supplementation in the control diet resulted in a 4-fold increase ($P_{HFS\,x\,WG} = 0.01$) in n-butyric acid compared to other groups (**Figure 2D**). Compared to HFS group, the small numerical increase in n-butyric acid and lactic acid in the HFS+WG group were not statistically significant.

WG supplementation modulates CD4+ T-cells in the small intestine of mice fed a control and HFS diet. Analyses of small intestinal lymphocytes (**Figure 3**) showed the impact of WG feeding on vital CD4+ T-cell subsets. WG supplementation showed significant main effects in elevating FoxP3-expressing CD4+ T cells (T_{reg} cells) by at least 168% higher in WG-supplemented groups compared to unsupplemented diets ($P_{WG} = 0.005$, **Figure 3A**). Furthermore, WG supplementation increased IL17a+ T-cells by at least 19% compared to unsupplemented groups ($P_{WG} = 0.03$, **Figure 3B**). Finally, the ratio of T_{reg} to Th_{17} cells tended to increase (≥73%, $P_{WG} = 0.06$) in both WG supplemented groups (**Figure 3C**).

WG supplementation increases anti-microbial peptide genes in the ileum of HFS diet- fed mice. As presented in **Figure 4**, the *Il6* and *Muc2* gene were not impacted by dietary treatments (**Figure 4A, C**, P>0.05). However, *Il-10* gene was elevated in the ileum of mice with WG supplementation (**Figure 4B**, P_{WG} = 0.038). The anti-microbial peptide gene, *Reg3β*, was at least 95% higher ($P_{HFS\ x\ WG}$ = 0.02) in the HFS+WG group than other groups (**Figure 4D**). Similarly, another anti-microbial peptide gene, *Reg3γ*, was upregulated in the HFS+WG group (≥135%, $P_{HFS\ x\ WG}$ = 0.008), compared to other groups (**Figure 4E)**. Finally, *Stat3* gene was significantly downregulated by HFS feeding compared to control (-27%, *P* = 0.03; **Figure 4F**), while WG increased it to the level of control, but still not significantly different from the HFS group (*P*=0.17).

WG supplementation reduces pro-inflammatory cytokines in the serum of mice fed a C or HFS diet. Data presented in **Figure 5** showed the impact of WG on serum inflammatory cytokines. We observed significant main effects of WG supplementation in reducing IL1b (≥ -19%, P_{WG} = 0.002), IL6 (≥ -31%, P_{WG} = 0.007), IFNy (≥ -15%, P_{WG} = 0.012), and TNFα (≥ -14%, P_{WG} = 0.002), after 12 wk of dietary treatment (**Figure 5A**, **B**, **E** and **F,** respectively).

Discussion

This study evaluated the effect of WG supplementation in modulating the gut microbiota, local and systemic inflammatory markers in mice fed a control or HFS diet for 12 wk. Findings from our study revealed that WG increased the abundance of cecal *Lactobacillaceae* in mice fed a HFS diet. Additionally, WG increased gut bacterial

fermentation as evident in increased fecal propionic and butyric acids. Furthermore, WG showed the potential to induce gut anti-inflammatory environment by elevating small intestinal T-regulatory cells and anti-microbial peptides, and a less inflammatory signature in the serum.

High fat (HF) feeding has been shown to significantly change the proportions of certain dominant gut bacteria, that lead to obesity and comorbidities such as insulin resistance (10). Some of these HF-induced changes may include a global increase in Firmicutes, accompanied by taxa specific decreases in other phyla such as Actinobacteria and Verrucomicrobia (4). Our HFS model in this study showed a similar pattern. Although our western diet model mildly raised total Firmicutes levels, several beneficial OTU-level taxa within this phyla, including *Lactobacillus* and *Roseburia*, were several folds lower than in control-fed mice. On the other hand, WG addition to the HFS diet increased OTUs belonging to *Lactobacillus* when compared to the HFS group. This might not be surprising as the soluble dietary fiber of several varieties of the parent plant, wheat, has been shown to allow selective *in vitro* proliferation of *Lactobacillus* strains (43, 44). This suggests that WG (with 4% fiber in this study) has a gut prebiotic potential, especially in a gut milieu unsettled by HFS feeding.

The impact of WG on the gut microbiome was also reflected in its potential to increase bacterial fermentation, as evident in increased propionic and butyric acids especially in mice fed a control diet. Apart from serving as a growth substrate for gut epithelial cells, these SCFAs may also impact gut homeostasis by modulating T-cell proliferation towards an anti-inflammatory phenotype (19). In this study, WG in both C and HFS diets increased both CD4 T-cell subsets vital for gut homeostasis. Garidou et al,

previously reported a significant reduction of gut surveillance by HF diet, involving a reduction in both IL17 T-cells and FOXP3 T cells in the ileum (7). Consequently, a gradual increase in endotoxemia may ensue, resulting in systemic inflammation and the onset of IR (7, 10). This may be expected since IL17 T-cells and FOXP3 T-cells are vital in enteric pathogen elimination and gut immunoregulation respectively (2, 8). However, these detrimental effects of HF on gut CD4+ T-cells were reversed when mice were fed a combination of pre- and pro-biotics known as a synbiotic (7). Interestingly, WG supplementation in this study increased both small intestinal FOXP3+ and IL17a+ T cells, with an overall potential to maintain the gut environment in an anti-inflammatory manner, by an increase in the Treg/Th17 ratio and the *Il10* gene. It is noteworthy that WG in this study also reduced serum pro-inflammatory markers. Thus, the previously reported ability of WG to reduce IR in this same set of mice may have been aided by its potential to improve gut immunosurveillance, thus reducing the occurrence and impact of bacteremia or metabolic endotoxemia in eliciting systemic inflammation associated with IR (10, 31).

Furthermore, WG showed the ability to upregulate antimicrobial peptides genes (*Reg3β* and *Reg3γ*) in the ileum, with the HFS+WG group showing the highest fold increase. This is consistent with the effect of certain prebiotics in HF feeding (4, 7). In the present study, this finding may have two possible implications. First, Huang et al. (45) recently demonstrated that gut restricted REG3γ overexpression in mice significantly increased the proportion of *Lactobacilli* in both the ileum and colon. The REG3γ-associated *Lactobacillus* further promoted an anti-inflammatory milieu within the gut lamina propria in a STAT3-dependent manner (45). Therefore, it is probable that the

elevation of the *Reg3* lectin genes by WG in this study enabled the growth of *Lactobacillus*-related bacteria, as seen especially in the HFS+WG group. Secondly, it is feasible that the upregulation of antimicrobial genes by WG, especially in the HFS group, is due to an increased need to ward off certain bacteria that may have gained more access within the gut mucosal tissue. In this study, we observed that compared to control, HFS feeding significantly elevated OTUs belonging to *Mucispirillum schaedleri* (phylum Deferribacteres), while WG supplementation could not mitigate this HFS-induced effect. While little is known about the role of this taxon at the moment, it is however, reported that *Mucispirillum schaedleri* dwells within the gut mucosal layer in rodents (46). Moreover, probiotic administration significantly reduced *Mucispirillum* genus in a model of DSS-induced colitis, suggesting that this genus might play a detrimental role in the gut (47). Therefore, a copious increase of this bacteria in the mucosal layer as seen in our HFS group, may require adequate response of antimicrobial peptides, as seen in the WG supplemented group, to curtail possible implications of excessive mucosal habituation of bacteria. This effect of WG is vital, since elevated Reg3-lectins in the gut confines bacteria to mucosal surfaces and diminishes bacterial translocation which may induce detrimental systemic implications (48).

A limitation in this study is our inability to measure fecal SCFAs in individual mouse, as opposed to samples collected per cage. The mice used in this study were group-housed from the commencement of the study and hence, we were wary of disrupting the design for individual mouse fecal collection, since perturbations in mouse immediate environment may significantly alter the composition of the gut microbiome (49). Also, questions remain if a lower fat content as opposed to the 60% fat in this study

will lead to a better outcome with WG supplementation, especially with the SCFA and gut immune cell results. Hence, future studies which investigate the effect of WG in a model more suited to a western type diet are warranted. Nevertheless, this study provides evidence of the prebiotic potential of WG in mice fed both normal and caloric-dense diets.

In conclusion, WG supplementation selectively increased gut *Lactobacillaceae*, impacted SCFA levels, elevated anti-microbial peptides in the ileum, and showed the potential to modulate intestinal CD4+ T cells towards an anti-inflammatory phenotype. Furthermore, WG reduced pro-inflammatory cytokines in the serum which may have implications for its effect on modulating insulin resistance (31). Indeed, WG may be of significant health and economic value to wheat consuming and growing communities if its anti-inflammatory and gut modulatory potential is further investigated and exploited.

Acknowledgement

We appreciate Shawnee Milling Co. (Shawnee, OK) for providing the wheat germ used in this study. Also, we are very grateful to the following people for their technical assistance during the course of this work: Angie Lathrop, Robert M. Kerr Food and Agricultural Products Center, Oklahoma State University; Marie Montelongo, Flow cytometry lab, Centre for Veterinary Health Sciences, Oklahoma State University; and Luisa Chan, Second Genome Inc, San Francisco, CA.

References

1. Cani PD, Bibiloni R, Knauf C, Waget A, Neyrinck AM, Delzenne NM, Burcelin R. Changes in gut microbiota control metabolic endotoxemia-induced inflammation in high-fat diet–induced obesity and diabetes in mice. Diabetes 2008;57(6):1470-81.
2. Winer DA, Luck H, Tsai S, Winer S. The intestinal immune system in obesity and insulin resistance. Cell Metab 2016;23(3):413-26.
3. Everard A, Belzer C, Geurts L, Ouwerkerk JP, Druart C, Bindels LB, Guiot Y, Derrien M, Muccioli GG, Delzenne NM. Cross-talk between Akkermansia muciniphila and intestinal epithelium controls diet-induced obesity. Proc Natl Acad Sci USA 2013;110(22):9066-71.
4. Everard A, Lazarevic V, Gaïa N, Johansson M, Ståhlman M, Backhed F, Delzenne NM, Schrenzel J, Francois P, Cani PD. Microbiome of prebiotic-treated mice reveals novel targets involved in host response during obesity. ISME J 2014;8(10):2116.
5. Neyrinck AM, Possemiers S, Druart C, Van de Wiele T, De Backer F, Cani PD, Larondelle Y, Delzenne NM. Prebiotic effects of wheat arabinoxylan related to the increase in bifidobacteria, Roseburia and Bacteroides/Prevotella in diet-induced obese mice. PloS one 2011;6(6):e20944.
6. Schroeder BO, Bäckhed F. Signals from the gut microbiota to distant organs in physiology and disease. Nat Med 2016;22(10):1079.
7. Garidou L, Pomié C, Klopp P, Waget A, Charpentier J, Aloulou M, Giry A, Serino M, Stenman L, Lahtinen S. The gut microbiota regulates intestinal CD4 T cells expressing RORγt and controls metabolic disease. Cell Metab 2015;22(1):100-12.
8. Littman DR, Rudensky AY. Th17 and regulatory T cells in mediating and restraining inflammation. Cell 2010;140(6):845-58.
9. Erridge C, Attina T, Spickett CM, Webb DJ. A high-fat meal induces low-grade endotoxemia: evidence of a novel mechanism of postprandial inflammation–. Am J Clin Nutr 2007;86(5):1286-92.
10. Cani PD, Amar J, Iglesias MA, Poggi M, Knauf C, Bastelica D, Neyrinck AM, Fava F, Tuohy KM, Chabo C. Metabolic endotoxemia initiates obesity and insulin resistance. Diabetes 2007;56(7):1761-72.
11. Gibson GR, Hutkins R, Sanders ME, Prescott SL, Reimer RA, Salminen SJ, Scott K, Stanton C, Swanson KS, Cani PD. Expert consensus document: The International Scientific Association for Probiotics and Prebiotics (ISAPP) consensus statement on the definition and scope of prebiotics. Nat Rev Gastroenterol Hepatol 2017;14(8):491.

12. Dehghan P, Gargari BP, Jafar-Abadi MA. Oligofructose-enriched inulin improves some inflammatory markers and metabolic endotoxemia in women with type 2 diabetes mellitus: a randomized controlled clinical trial. Nutr J 2014;30(4):418-23.
13. Monsan P, Valet P, Remaud-Simeon M, Saulnier-Blache J-S, Burcelin R. Use of prebiotics, preferably glucooligosaccharide, for the prevention of the onset of type II diabetes. Google Patents, 2009.
14. Fuentes-Zaragoza E, Riquelme-Navarrete M, Sánchez-Zapata E, Pérez-Álvarez J. Resistant starch as functional ingredient: A review. Food Res Int 2010;43(4):931-42.
15. Slavin J. Fiber and prebiotics: mechanisms and health benefits. Nutrients 2013;5(4):1417-35.
16. Rooks MG, Garrett WS. Gut microbiota, metabolites and host immunity. Nat Rev Immunol 2016;16(6):341.
17. Wang H-B, Wang P-Y, Wang X, Wan Y-L, Liu Y-C. Butyrate enhances intestinal epithelial barrier function via up-regulation of tight junction protein Claudin-1 transcription. Dig Dis Sci 2012;57(12):3126-35.
18. Gibson PR, Rosella O, Wilson AJ, Mariadason JM, Rickard K, Byron K, Barkla DH. Colonic epithelial cell activation and the paradoxical effects of butyrate. Carcinogenesis 1999;20(4):539-44.
19. Smith PM, Howitt MR, Panikov N, Michaud M, Gallini CA, Bohlooly-y M, Glickman JN, Garrett WS. The microbial metabolites, short-chain fatty acids, regulate colonic Treg cell homeostasis. Science 2013:1237242.
20. Singh N, Gurav A, Sivaprakasam S, Brady E, Padia R, Shi H, Thangaraju M, Prasad PD, Manicassamy S, Munn DH. Activation of Gpr109a, receptor for niacin and the commensal metabolite butyrate, suppresses colonic inflammation and carcinogenesis. Immunity 2014;40(1):128-39.
21. Carvalho-Wells AL, Helmolz K, Nodet C, Molzer C, Leonard C, McKevith B, Thielecke F, Jackson KG, Tuohy KM. Determination of the in vivo prebiotic potential of a maize-based whole grain breakfast cereal: a human feeding study. Brit J Nutr 2010;104(9):1353-6.
22. Costabile A, Klinder A, Fava F, Napolitano A, Fogliano V, Leonard C, Gibson GR, Tuohy KM. Whole-grain wheat breakfast cereal has a prebiotic effect on the human gut microbiota: a double-blind, placebo-controlled, crossover study. Brit J Nutr 2008;99(1):110-20.
23. Mitsou E, Kougia E, Nomikos T, Yannakoulia M, Mountzouris K, Kyriacou A. Effect of banana consumption on faecal microbiota: a randomised, controlled trial. Anaerobe 2011;17(6):384-7.
24. Ojo B, El-Rassi GD, Payton ME, Perkins-Veazie P, Clarke S, Smith BJ, Lucas EA. Mango Supplementation Modulates Gut Microbial Dysbiosis and Short-Chain Fatty Acid Production Independent of Body Weight Reduction in C57BL/6 Mice Fed a High-Fat Diet–3. J Nutr 2016;146(8):1483-91.
25. Brandolini A, Hidalgo A. Wheat germ: not only a by-product. Int J Food Sci Nutr 2012;63(sup1):71-4.

26. Boros LG, Nichelatti M, Shoenfeld Y. Fermented wheat germ extract (Avemar) in the treatment of cancer and autoimmune diseases. Ann N Y Acad Sci 2005;1051(1):529-42.
27. Iyer A, Brown L. Fermented wheat germ extract (Avemar) in the treatment of cardiac remodeling and metabolic symptoms in rats. Evid Based Complement Alternat Med 2011;2011.
28. Alessandri C, Pignatelli P, Loffredo L, Lenti L, Del Ben M, Carnevale R, Perrone A, Ferro D, Angelico F, Violi F. Alpha-linolenic acid–rich wheat germ oil decreases oxidative stress and CD40 ligand in patients with mild hypercholesterolemia. Arterioscler Thromb Vasc Biol 2006;26(11):2577-8.
29. Haripriya S, Premakumari S. Beta sistosterol of wheat germ reduces blood glucose in humans. J Life Sci 2010;2(2):87-92.
30. Cara L, Dubois C, Borel P, Armand M, Senft M, Portugal H, Pauli A, Bernard P, Lairon D. Effects of oat bran, rice bran, wheat fiber, and wheat germ on postprandial lipemia in healthy adults. Am J Clin Nutr 1992;55(1):81-8.
31. Ojo B, Simenson AJ, O'Hara C, Wu L, Gou X, Peterson SK, Lin D, Smith BJ, Lucas EA. Wheat germ supplementation alleviates insulin resistance and cardiac mitochondrial dysfunction in an animal model of diet-induced obesity. Brit J Nutr 2017;118(4):241-9.
32. Glei M, Hofmann T, Küster K, Hollmann J, Lindhauer MG, Pool-Zobel BL. Both wheat (Triticum aestivum) bran arabinoxylans and gut flora-mediated fermentation products protect human colon cells from genotoxic activities of 4-hydroxynonenal and hydrogen peroxide. J Agric Food Chem 2006;54(6):2088-95.
33. Neyrinck AM, Van Hee VF, Piront N, De Backer F, Toussaint O, Cani PD, Delzenne NM. Wheat-derived arabinoxylan oligosaccharides with prebiotic effect increase satietogenic gut peptides and reduce metabolic endotoxemia in diet-induced obese mice. Nutr Diabetes 2012;2(1):e28.
34. Reeves PG, Nielsen FH, Fahey Jr GC. AIN-93 purified diets for laboratory rodents: final report of the American Institute of Nutrition ad hoc writing committee on the reformulation of the AIN-76A rodent diet. Oxford University Press, 1993.
35. Edgar RC. UPARSE: highly accurate OTU sequences from microbial amplicon reads. Nat Methods 2013;10(10):996.
36. Schloss PD, Westcott SL, Ryabin T, Hall JR, Hartmann M, Hollister EB, Lesniewski RA, Oakley BB, Parks DH, Robinson CJ. Introducing mothur: open-source, platform-independent, community-supported software for describing and comparing microbial communities. Appl Environ Microbiol 2009;75(23):7537-41.
37. DeSantis TZ, Hugenholtz P, Larsen N, Rojas M, Brodie EL, Keller K, Huber T, Dalevi D, Hu P, Andersen GL. Greengenes, a chimera-checked 16S rRNA gene database and workbench compatible with ARB. Appl Environ Microbiol 2006;72(7):5069-72.
38. Taylor KA. A simple colorimetric assay for muramic acid and lactic acid. Appl Biochem Biotechnol 1996;56(1):49-58.

39. Niess JH, Leithäuser F, Adler G, Reimann J. Commensal gut flora drives the expansion of proinflammatory CD4 T cells in the colonic lamina propria under normal and inflammatory conditions. J Immunol 2008;180(1):559-68.
40. Love MI, Huber W, Anders S. Moderated estimation of fold change and dispersion for RNA-seq data with DESeq2. Genome Biol 2014;15(12):550.
41. McMurdie PJ, Holmes S. phyloseq: an R package for reproducible interactive analysis and graphics of microbiome census data. PloS one 2013;8(4):e61217.
42. Benjamini Y, Hochberg Y. Controlling the false discovery rate: a practical and powerful approach to multiple testing. J R Stat Soc Series B Stat Methodol 1995:289-300.
43. Napolitano A, Costabile A, Martin-Pelaez S, Vitaglione P, Klinder A, Gibson GR, Fogliano V. Potential prebiotic activity of oligosaccharides obtained by enzymatic conversion of durum wheat insoluble dietary fibre into soluble dietary fibre. Nutr Metab Cardiovasc 2009;19(4):283-90.
44. Marotti I, Bregola V, Aloisio I, Di Gioia D, Bosi S, Di Silvestro R, Quinn R, Dinelli G. Prebiotic effect of soluble fibres from modern and old durum-type wheat varieties on Lactobacillus and Bifidobacterium strains. J Sci Food Agric 2012;92(10):2133-40.
45. Huang Y, Qi H, Zhang Z, Wang E, Yun H, Yan H, Su X, Liu Y, Tang Z, Gao Y. Gut REG3γ-Associated Lactobacillus Induces Anti-inflammatory Macrophages to Maintain Adipose Tissue Homeostasis. Front Immunol 2017;8:1063.
46. Berry D, Pfann C, Steinberger M, Hanson B, Herp S, Brugiroux S, Gomes Neto JC, Boekschoten M, Schwab C, Urich T. Insights into the ecology and evolution of the mucus-dwelling gut bacterium Mucispirillum schaedleri. 2017.
47. Song H, Wang W, Shen B, Jia H, Hou Z, Chen P, Sun Y. Pretreatment of Probiotic Bifico Ameliorates Colitis-Associated Cancer in Mice: Transcriptome and Gut Flora Profiling. Cancer Sci 2017.
48. Wang L, Fouts DE, Stärkel P, Hartmann P, Chen P, Llorente C, DePew J, Moncera K, Ho SB, Brenner DA. Intestinal REG3 lectins protect against alcoholic steatohepatitis by reducing mucosa-associated microbiota and preventing bacterial translocation. Cell host & microbe 2016;19(2):227-39.
49. Hildebrand F, Nguyen TLA, Brinkman B, Yunta RG, Cauwe B, Vandenabeele P, Liston A, Raes J. Inflammation-associated enterotypes, host genotype, cage and inter-individual effects drive gut microbiota variation in common laboratory mice. Genome Biol 2013;14(1):R4.

Figures

FIGURE 1: Effect of WG supplementation on the gut microbiome in C57BL/6 mice fed a C or HFS diet for 12 wk.

DNA was isolated from individual cecal samples and subjected to 16S rDNA sequencing (*n*= 6-9 mice/group). Principal Coordinate Analysis of gut bacteria based on the Bray-Curtis distance of OTUs in microbiome samples (A). Relative abundance of the gut bacterial phyla (B). Mean percent relative abundance of the most abundant taxa at the family level (C). The statistically significant changes in specific phyla and family are presented in Supplemental Table 2. n=6-9 mice/group C, control; C+WG, control + 10% wheat germ; HFS, high fat and sucrose; HFS+WG, high fat and sucrose + 10% wheat germ

FIGURE 2: Fecal short chain fatty acids in C57BL/6 mice fed a C or HFS diet supplemented with 10% WG for 12 wk.

As described in the methods section, fecal samples were collected per cage and each sample was processed in duplicates for the SCFA analyses (*n*=3/group). Data are means±SEM. Differences between groups as indicated with letters when the HFS x WG interaction was significant ($P < 0.05$, 2-way ANOVA). Labelled means without a common letter are significantly different from each other ($P<0.05$). C, control; C+WG, control + 10% wheat germ; HFS, high fat and sucrose; HFS+WG, high fat and sucrose + 10% wheat germ

FIGURE 3: Small intestinal CD4+ T cells in C57BL/6 mice fed a C or HFS diet supplemented with 10% WG for 12 wk.

Lymphocytes were processed from 2 pooled small intestines and 10^6 cells were stained and analyzed by flow cytometry for CD4+FOXP3+ cells (A), CD4+IL17a+ cells (B) and T_{reg}/Th_{17} ratio (C). Gating strategy for CD4+ T-cells and subsets shown in (D). Data are means±SEM (*n*=6 / group). Main effects were considered statistically significant when $P < 0.05$ (2-way ANOVA). C, control; C+WG, control + 10% wheat germ; HFS, high fat and sucrose; HFS+WG, high fat and sucrose + 10% wheat germ

FIGURE 4: Relative gene expression of interleukin (*Il*)*6* (A), *Il10* (B), *Muc2* (C), *Reg3β* (D), *Reg3γ* (E), and *Stat3* (F) in the ileum LP of C57BL/6 mice fed a C or HFS diet supplemented with 10% WG for 12 wk.

Data are means±SEM (*n*=6 mice/group). Only significant *P* values are shown in each panel. Differences between groups were indicated with letters when the HFS x WG interaction was significant ($P < 0.05$, 2-way ANOVA). Labeled means without a common letter are significantly different from each other ($P<0.05$). C, control; C+WG, control + 10% wheat germ; HFS, high fat and sucrose; HFS+WG, high fat and sucrose + 10% wheat germ**;** LP, lamina propria; *Muc2,* Mucin 2; *Reg3β*, regenerating islet-derived protein 3-beta; *Reg3γ*, regenerating islet-derived protein 3-gamma; *Stat3*, signal transducer and activator of transcription 3

FIGURE 5: Serum concentrations of inflammatory cytokines in C57BL/6 mice fed a C or HFS diet supplemented with 10% WG for 12 wk.

Interleukin (IL) 1β (A), IL6 (B), IL10 (C), IL17a (D), IFNγ (E) and TNF alpha (F) in C57BL/6 mice fed a C or HFS diet supplemented with 10% WG for 12 wk (n=9 mice/group). Data are means±SEM (*n*=9 mice/group). Main effects were considered statistically significant when $P < 0.05$ (2-way ANOVA). C, control; C+WG, control + 10% wheat germ; HFS, high fat and sucrose; HFS+WG, high fat and sucrose + 10% wheat germ; IFNγ, Interferon gamma.

Figure 1

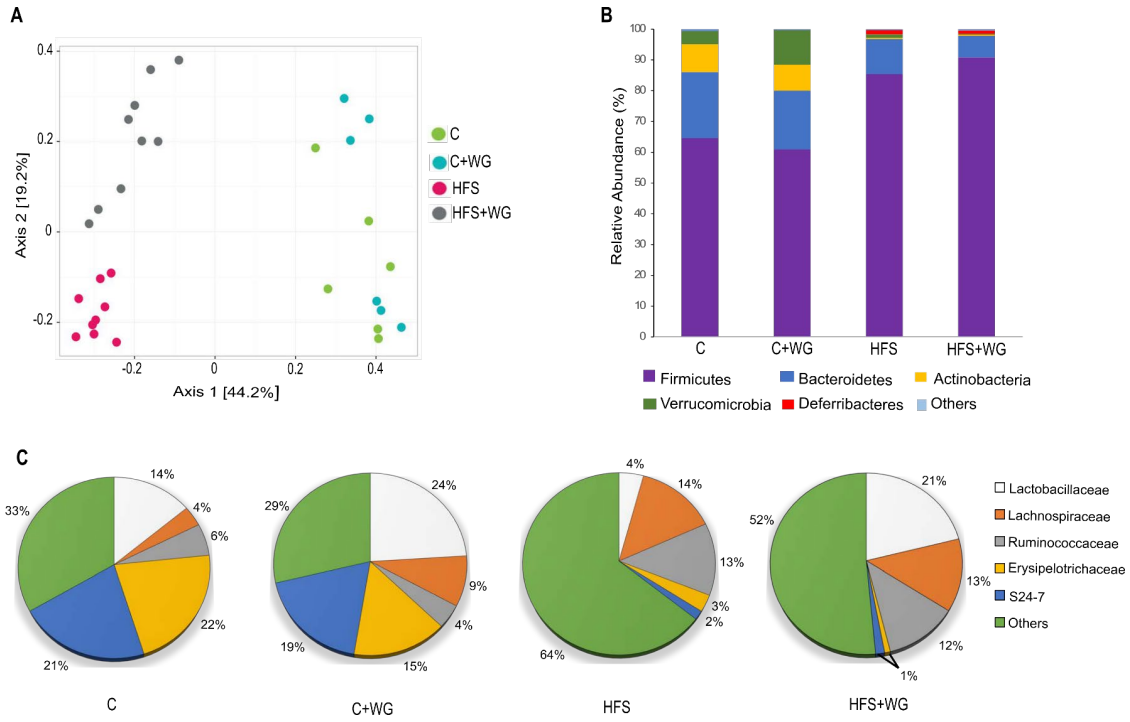
A
Axis 2 [19.2%]
Axis 1 [44.2%]
C
C+WG
HFS
HFS+WG
B
Relative Abundance (%)
C
C+WG
HFS
HFS+WG
Firmicutes
Bacteroidetes
Actinobacteria
Verrucomicrobia
Deferribacteres
Others
C
33%
14%
4%
6%
22%
21%
C+WG
29%
24%
9%
4%
15%
19%
HFS
64%
4%
14%
13%
3%
2%
HFS+WG
52%
21%
13%
12%
1%
Lactobacillaceae
Lachnospiraceae
Ruminococcaceae
Erysipelotrichaceae
S24-7
Others

Figure 2

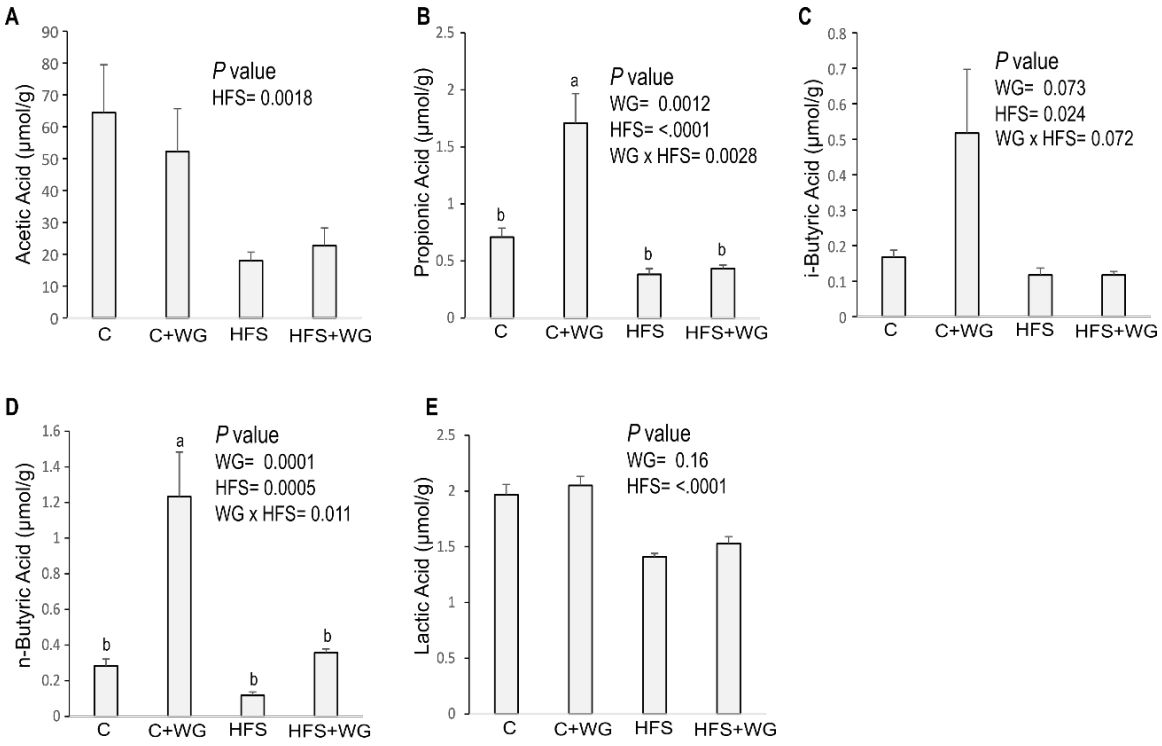
A
Acetic Acid (µmol/g)
P value
HFS= 0.0018
C
C+WG
HFS
HFS+WG
B
Propionic Acid (µmol/g)
P value
WG= 0.0012
HFS= <.0001
WG x HFS= 0.0028
a
b
b
b
C
C+WG
HFS
HFS+WG
C
i-Butyric Acid (µmol/g)
P value
WG= 0.073
HFS= 0.024
WG x HFS= 0.072
C
C+WG
HFS
HFS+WG
D
n-Butyric Acid (µmol/g)
P value
WG= 0.0001
HFS= 0.0005
WG x HFS= 0.011
a
b
b
b
C
C+WG
HFS
HFS+WG
E
Lactic Acid (µmol/g)
P value
WG= 0.16
HFS= <.0001
C
C+WG
HFS
HFS+WG

Figure 3

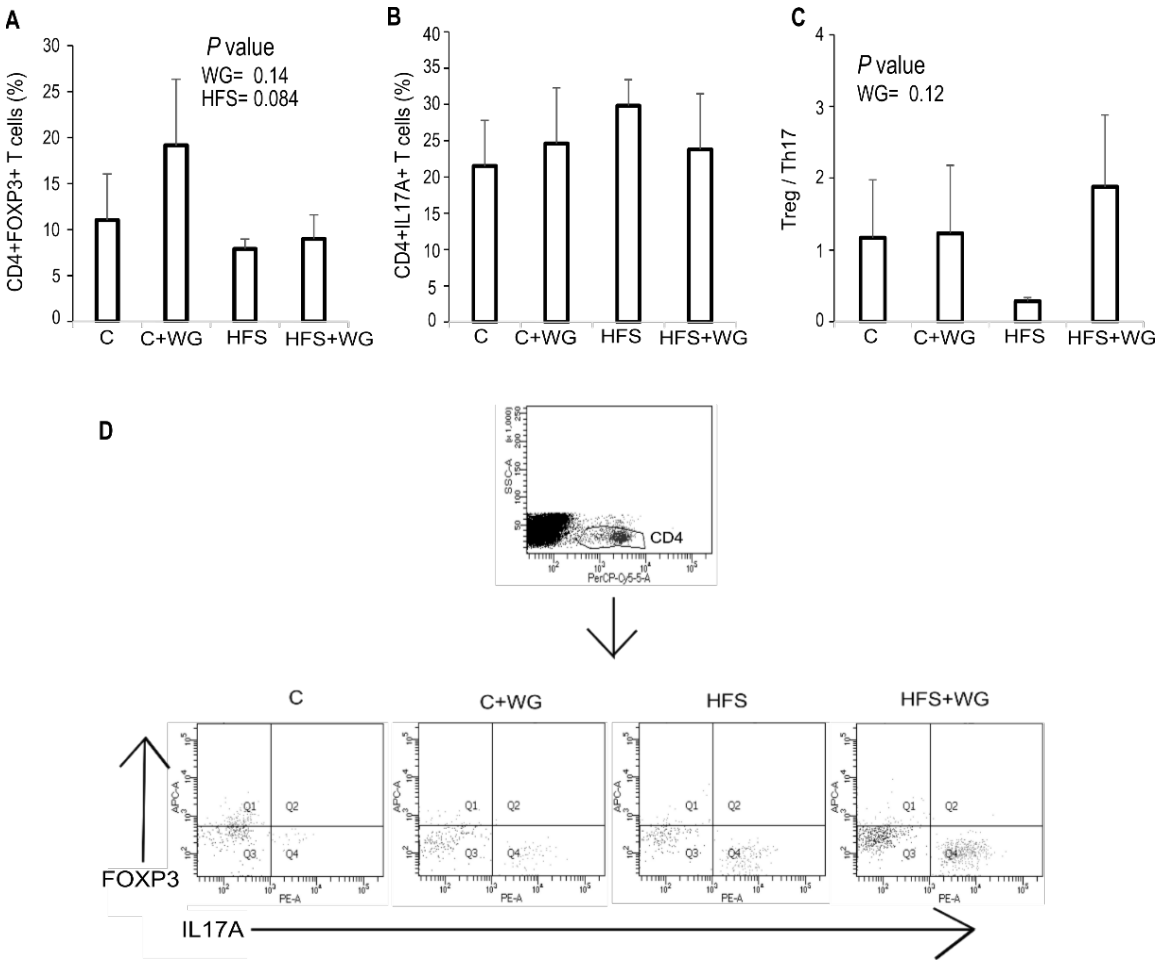
A
CD4+FOXP3+ T cells (%)
P value
WG= 0.14
HFS= 0.084
C
C+WG
HFS
HFS+WG
B
CD4+IL17A+ T cells (%)
C
Treg / Th17
P value
WG= 0.12
D
CD4
FOXP3
IL17A

Figure 4

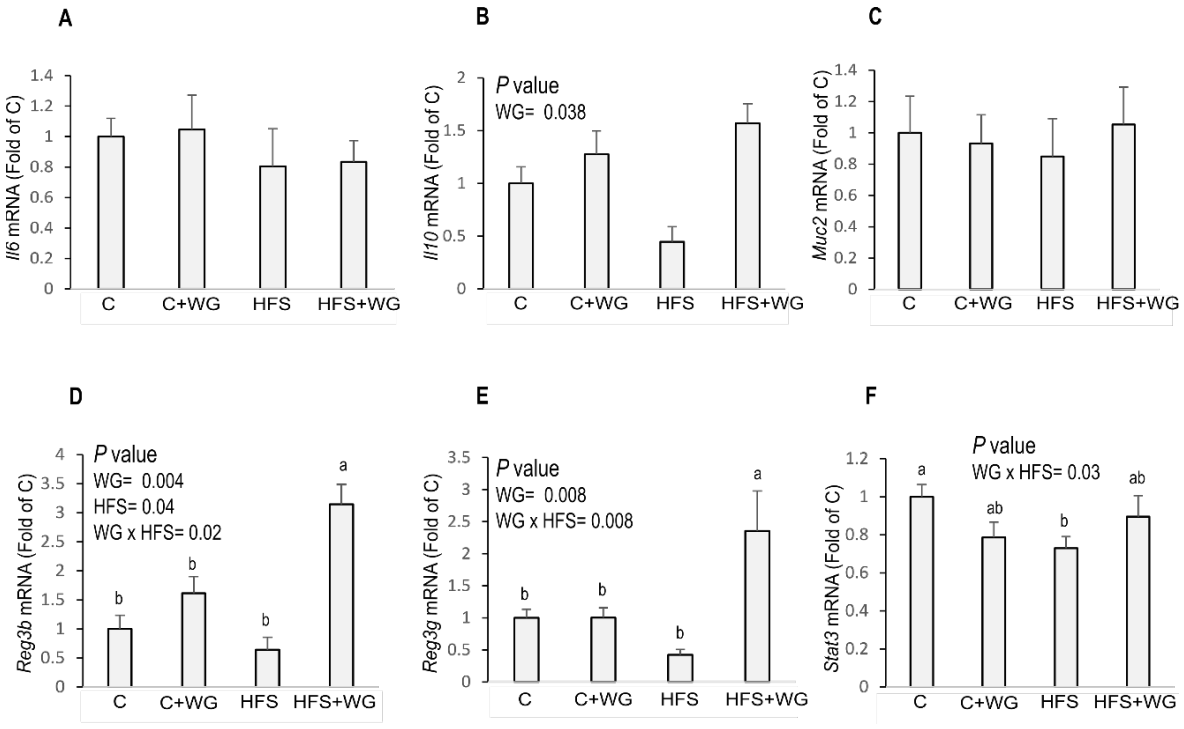
A
Il6 mRNA (Fold of C)
C
C+WG
HFS
HFS+WG
B
Il10 mRNA (Fold of C)
P value
WG= 0.038
C
Muc2 mRNA (Fold of C)
D
Reg3b mRNA (Fold of C)
P value
WG= 0.004
HFS= 0.04
WG x HFS= 0.02
E
Reg3g mRNA (Fold of C)
P value
WG= 0.008
WG x HFS= 0.008
F
Stat3 mRNA (Fold of C)
P value
WG x HFS= 0.03

Figure 5

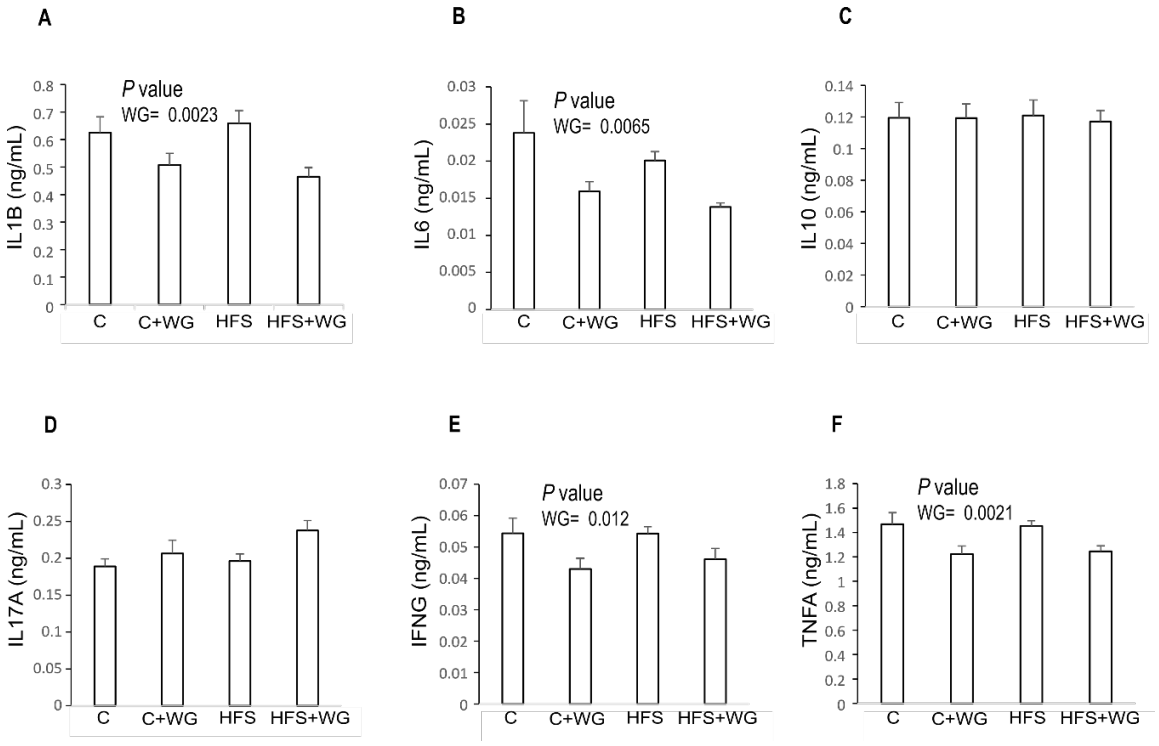
A
IL1B (ng/mL)
P value
WG= 0.0023
C
C+WG
HFS
HFS+WG
B
IL6 (ng/mL)
P value
WG= 0.0065
C
C+WG
HFS
HFS+WG
C
IL10 (ng/mL)
C
C+WG
HFS
HFS+WG
D
IL17A (ng/mL)
C
C+WG
HFS
HFS+WG
E
IFNG (ng/mL)
P value
WG= 0.012
C
C+WG
HFS
HFS+WG
F
TNFA (ng/mL)
P value
WG= 0.0021
C
C+WG
HFS
HFS+WG

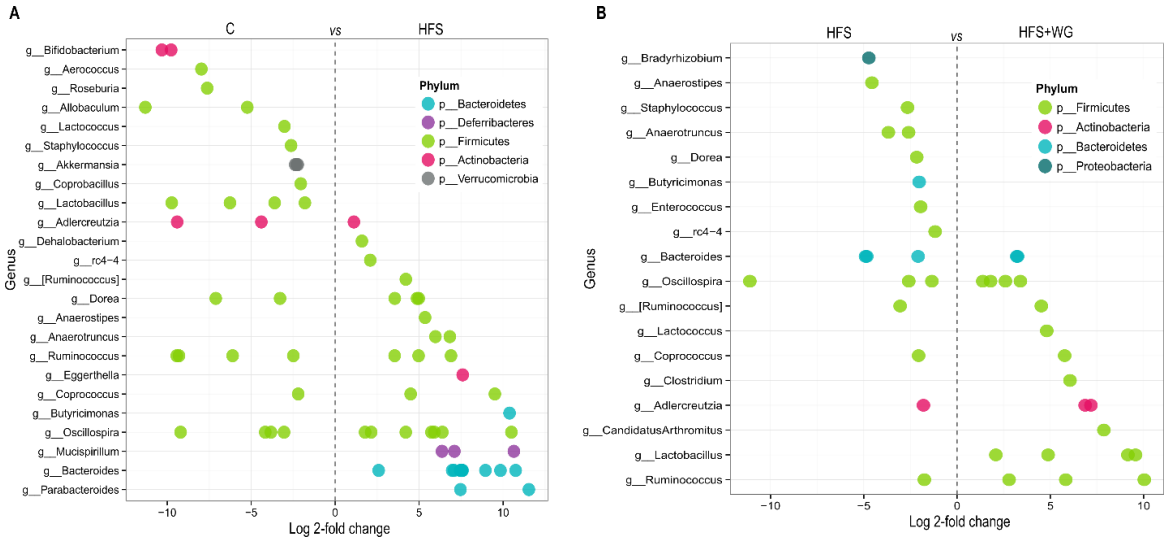

Supplemental Figure 1. Bacteria genera in C57BL/6 mice fed an HFS diet compared with those fed a control diet (A) and HFS+ 10% wheat germ diet (B) for 12 wk (n=6-9 mice / group). Alterations are presented as log 2-fold changes, and points represent OTUs belonging to that genus. Features were considered significant if their false discovery rate-corrected *P* value was < 0.05 and the absolute value of their log 2-fold change was ≥ 1. For clarity, only OTUs classified beyond the family level, and statistically significant are presented.

Tables

Supplemental Table 1: Primer sequences for gene expression analyses

Gene	Forward	Reverse
mCyclo	5`-tgg aga gca cca aga cag aca-3`	5`-tgc cgg agt cga caa tga t-3`
mIl10	5`-ggt tgc caa gcc tta tcg ga-3`	5`-acc tgc tcc act gcc ttg ct-3`
mIl6	5`-gag gat acc act ccc aac aga cc-3`	5`-aag tgc atc atc gtt gtt cat aca-3`
mMuc2	5`-ctg acc aag agc gaa cac aa-3`	5`-cat gac tgg aag caa ctg ga-3`
mReg3β	5`-tgg gaa tgg agt aac aat g-3`	5`-ggc aac ttc acc tca cat-3`
mReg3γ	5`-cca tct tca cgt agc agc-3`	5`-caa gat gtc ctg agg gc-3`
mStat3	5`- cca ttg acc tgc cga tgt c -3`	5`- ctc agc acc ttc acc gtt att tc -3`

Supplemental Table 2 : Enriched or depleted cecal bacterial phyla in C57BL/6 mice fed a C or HFS diet supplemented with 10% WG for 12 wk (n=6-9 mice / group).

	C		HFS		HFS vs CT	
	Mean	SEM	Mean	SEM	changes (%)	$P_{adjusted}$
Firmicutes	64.5	3.89	85.4	1.67	32.40	0.10
Deferribacteres	0.0006	0.0002	1.28	0.52	213233	0.01
Actinobacteria	9	3.93	0.40	0.06	-95.6	0.04

Data are mean percent±SEM. Only significant ($P<0.05$) differences, or mildly significant differences ($P\leq0.1$) between 2 dietary groups are indicated. $P_{adjusted}$ values are based on Kruskal-Wallis rank sum test followed by *post-hoc* analysis using Dunn's test. No significant changes were observed at the phylum level between C vs C+WG, and HF vs HF+WG. C, control; C+WG, control + 10% wheat germ; HFS, high fat and sucrose; HFS+WG, high fat and sucrose + 10% wheat germ.

Supplemental Table 3 : Enriched or depleted cecal bacterial family in C57BL/6 mice fed a C or HFS diet supplemented with 10% WG for 12 wk (n=6-9 mice / group).

	C		C+WG		C+WG vs C	
	Mean	SEM	Mean	SEM	changes (%)	$P_{adjusted}$
Lactobacillaceae	14.00	4.24	24	7.67	71	1
Lachnospiraceae	3.62	0.34	8.94	0.53	146	0.84
Ruminococcaceae	5.72	0.45	4.26	0.78	-26	1
Erysipelotrichaceae	21.8	4.05	15.4	5.4	-29	1
S24-7	21.5	3.02	18.6	2.24	-14	1

	C		HFS		HFS vs CT	
	Mean	SEM	Mean	SEM	changes (%)	$P_{adjusted}$
Lactobacillaceae	14.00	4.24	4.23	0.88	-70	0.32
Lachnospiraceae	3.62	0.34	14.00	1.18	287	**0.0004**
Ruminococcaceae	5.72	0.45	12.80	1.27	124	**0.01**
Erysipelotrichaceae	21.8	4.05	3.05	0.67	-86	**0.06**
S24-7	21.5	3.02	1.61	0.44	-93	**0.004**

	HFS		HFS+WG		HFS+WG vs HFS	
	Mean	SEM	Mean	SEM	changes (%)	$P_{adjusted}$
Lactobacillaceae	4.23	0.88	21.10	3.73	399	**0.007**
Lachnospiraceae	14.00	1.18	13.00	0.84	-7	1
Ruminococcaceae	12.80	1.27	12.00	1.17	-6	1
Erysipelotrichaceae	3.05	0.67	0.93	0.14	-70	0.44
S24-7	1.61	0.44	1.48	0.37	-8	1

Data are mean percent±SE of the 5 most abundant taxa at the family level. $P_{adjusted}$ values are based on Kruskal-Wallis rank sum test followed by *post-hoc* analysis using Dunn's test. C, control; C+WG, control + 10% wheat germ; HFS, high fat and sucrose; HFS+WG, high fat and sucrose + 10% wheat germ.

CHAPTER V

Supplemental Wheat Germ Activates the STAT3-Reg3 pathway in the Gut and Attenuates the Lipopolysaccharide Binding Protein Gene in the Adipose Tissue of Mice Fed a Western Diet

Abstract

The leaky gut phenomenon links obesity to insulin resistance and chronic inflammation in peripheral tissues. *Lactobacillus* produce metabolites that stimulate the release of gut epithelial antimicrobial peptides (AMPs) via the IL22-STAT3 pathway. We have previously reported that wheat germ (WG) selectively increased cecal *Lactobacillus* in obese mice and lessened serum pro-inflammatory markers. This study investigated the effects of WG on gut AMPs (Reg3γ and Reg3β) in the jejunum and its potential to impede Nfκb-activation and immune cell infiltration in the visceral adipose tissue of mice fed a control or a western diet (i.e. high fat and high sucrose, HFS) for 12 wks. Six-wk-old male C57BL/6 mice were randomly assigned to four groups (n=12/group), and fed a control (C, 10% kcal fat, 10% kcal sucrose) or HFS (45% kcal fat, 26% kcal sucrose) diet with or without 10% WG (wt/wt) for 12 wks. The serum was assayed for metabolic parameters. Using immunoblots, we measured STAT3 and NFκB phosphorylation in the jejunum and visceral adipose tissue (VAT), respectively. Gut antimicrobial peptide genes, macrophage and inflammatory markers were measured by qPCR. After 12 wks of dietary treatment, WG significantly improved hyperglycemia, fasting insulin, and HOMA-IR by at least 17% ($P \leq 0034$) in HFS-fed mice. The pore-forming CLAUDIN 2 protein was elevated in the jejunum of HFS-fed mice (≥ 101%; P =0.0016). Supplemental WG upregulated *Il10* and *Il22* genes in the jejunum (≥ 116%; $P \leq 0.035$). The HFS+WG group had a 15-fold increase (P = 0.0012) in pSTAT3 compared to the HFS group in the jejunum. Consequently, the mRNA expression of *Reg3β* and *Reg3γ* were significantly upregulated in the jejunum by WG supplementation (≥ 42%; $P \leq 0.043$). In the VAT, the HFS group had greater NFκBp65 phosphorylation compared to C, while HFS+WG group suppressed this to the level of C (-38%; P = 0.014). In addition, VAT *Il6* and *Lbp* genes were downregulated in the HFS+WG group compared to HFS ($P \leq 0.0032$). Macrophage-related genes, *F4/80*, *Cd11c*, and *iNos*, were repressed (≥ -28%; $P \leq 0.048$) in the VAT of WG-supplemented mice. The stimulatory effects of WG on STAT3 and AMPs in the gut may be vital to reduce the burden of antigen translocation that could initiate adipose tissue inflammation and contribute to obesity-induced insulin resistance.

*This chapter will be submitted to Journal of Nutrition

Introduction

Adipose tissue dysfunction in obesity is characterized by chronic inflammation, which contributes to comorbidities such as insulin resistance (1). Hypertrophic adipocytes secrete chemokines such as the C-C motif chemokine ligand (CCL)2 and (regulated upon activation, normal T cell expressed, and secreted (RANTES) that play a role in monocyte/macrophage and T-cell recruitment, followed by the activation and polarization of macrophages towards an M1 proinflammatory state (1-3). These result in a profound proinflammatory adipose environment characterized by elevated cytokines and adipokines such as tumor necrosis factor (TNF)-α, interleukin (IL)-1β, IL-6, leptin and resistin, which interfere with insulin signaling, and contribute to the inflammatory cytokine pool in the blood (1, 2).

In order to intitate inflammation in peripheral tissues, the specific factors responsible for the activation of cells have been studied over the years. Indeed, animal and clinical studies suggest that obesity disrupt intestinal tight junctions (TJ), allowing for the increased translocation of bacteria and endotoxin (termed bacteremia and endotoxemia, respectively) from the gut into the blood and surrounding tissues which initiates inflammation and insulin resistance (4-8). In response to bacterial endotoxin and pro-inflammatory stimuli, lipopolysaccharide binding protein (LBP) is produced in hepatocytes and adipocytes which increases the severity of toll-like receptor 4 (Tlr4)/ nuclear factor kappa-light-chain-enhancer of activated B cells (Nfκb)-orchestrated inflammation by several folds (9-13). While LBP production may be a beneficial physiological response in cases of acute infection (9, 12), the chronic nature of the obesity-induced leaky gut may continually expose the peripheral tissues to endotoxin

leading to local and systemic chronic inflammation associated with obesity and insulin resistance. As such, LBP may be a marker of obesity-induced insulin resistance even in humans (14). Therefore, strategies that suppress LBP expression in the liver or adipose tissue may alleviate the inflammation and insulin resistance in obesity.

Out of the TJ proteins responsible the maintenance of intestinal TJs, the pore-forming CLAUDIN 2 has received increased attention in recent years (15-19). CLAUDIN 2 is a paracellular cation-water channel mainly expressed in leaky epithelia and impacts its sealing potential and TJ ultrastructure (15, 16). Hence, an increase of CLAUDIN 2 in the gut is associated with several diseases, including inflammatory bowel diseases, infectious diseases, and cancer (15). Additionally, an upregulation of CLAUDIN 2 is observed in the small intestines of high-fat (HF)-fed animals, suggesting an involvement in obesity-induced gut dysbiosis and permeability (16, 17). It is noteworthy that permeability across the intestine may be dependent on region and time (18). Among intestinal sections, jejunum permeability was elevated over time in HF-fed animals (18) and in obese humans (19). Therefore, mitigating permeability in the jejunum may be vital to suppress the inflammatory consequence of bacteremia/endotoxemia in peripheral tissues.

In order to combat systemic inflammation that may be initiated by the epithelial passage of both commensal and pathogenic bacteria, the mamalian gut develops a number of defense mechanisms. Among these are the antimicrobial peptides (AMPs) such as defensins, cryptidins, and the regenerating islet-derived protein (Reg)3 lectins, chiefly produced from the Paneth cells in the intestinal crypts (20). Interestingly, certain commensal bacteria show immunoprotective ability in the gut by metabolizing dietary

factors which stimulate the release of AMPs. For example, gut bacteria-derived butyrate and tryptophan metabolites from *Lactobacillus* protect intestinal integrity by elevating the expression of IL-10 and IL-22 capable of activating the signal transducer and activator of transcription (STAT)3-Reg3 pathway in intestinal epithelial cells (IECs) (21, 22). Consequently, an increase in gut Reg3 lectins prevent bacterial translocation to peripheral tissues (23). Thus, it could be hypothesized that dietary approaches that enhance the production of AMPs in the gut may reduce the impact of HF-induced bacteremia/endotoxemia and suppress inflammation in peripheral tissues.

Accumulating evidence from our group and others show that certain whole foods containing a variety of nutrients possess gut modulatory and prebiotic effects (24-27). For example, wheat germ (WG) is a nutrient-dense component of the wheat grain that contains about 4% fiber, 23% protein, and several bioactive compounds with various health benefits (28, 29). Apart from its fiber component, WG is a rich source of the essential amino acid – tryptophan (30), which could be available for the metabolic survival of certain commensal gut bacteria, including members of the *Lactobacillus* genera (31). Interestingly, WG feeding showed the potential to promote healthy gut bacteria in animals and in humans (26, 32). Our findings showed that in mice fed a 60% fat diet for 12 wks, WG supplementation selectively elevated the commensal gut bacterial family *Lactobacillaceae*, reduced serum profile of proinflammatory cytokines (TNFα, IL6, IL-1β and IL-17), and decreased markers of insulin resistance (26, 29).

Despite these reported health benefits, it is unclear if WG could activate the STAT3-Reg3 pathway in the jejunum and influence adipose tissue inflammation observed in obesity-induced insulin resistance, especially using a western diet model.

This is important, since the dietary factors that induce gut AMPs may abrogate the translocation of gut-derived antigens and suppress their contribution to the initiation of inflammation in peripheral organs (23). Therefore, this study aimed at investigating the effect of WG on the STAT3-Reg3 pathway in the gut, and its potential to reduce inflammation and immune cell infiltration in the visceral adipose tissue of C57BL/6J mice fed a control or a western diet for 12 wks. We **hypothesized** that WG will activate STAT3 in the jejenum and increase the transcription of Reg3 lectins, indicating an enhanced capacity to mitigate HF-induced leaky gut. This effect of WG on the gut would be associated with reduced inflammation and immune cell infiltration in the visceral adipose tissue.

Methods

Animals and Treatment Groups

Animal care was carried out at Oklahoma State University Laboratory Animal Research facility maintained under humidity- and temperature-controlled conditions and a 12-h light–12-h dark cycle. All procedures followed strict guidelines set by the Institution Animal Care of Oklahoma State University.

Six-week-old male C57BL/6 mice (*n*=48) were purchased from Charles River Laboratory (Wilmington, MA). The mice were acclimated for a week and randomly assigned to one of four treatment dietary treatment groups (n = 12/group) in a 2 x 2 factorial design — control (C; 10% kcal fat, 10% kcal sucrose; AIN-93 M), C + 10% WG (C + WG), a western-styled diet with high fat and high sucrose, HFS (45% kcal fat, 26%

kcal sucrose), and HFS + 10% WG (HFS + WG) for 12 wks. Mice were group-housed (4 mice per cage) in wire-bottom cages .

Shawnee Milling Company (Shawnee, OK) graciously provided wheat germ from Oklahoma red winter wheat. WG was analyzed for its nutrient composition (NP Analytical Laboratories, St. Louis, MO) and added to one of the control diets (C+WG, 10% wt:wt) and one of the HFS diets (HFS+WG, 10% wt:wt). The WG dose was based on our previous study that investigated the effect of WG supplementation on the gut microbiome (26). The WG-supplemented diets were adjusted to have the same macronutrient composition, total fiber, calcium, and phosphorus as the unsupplemented diets (**Supplemental Table 1**). Food and water were provided *ad libitum* for 12 wks. Food intake was monitored daily and the body weight of each mouse was measured weekly.

Sample Collection and Processing

For fasting blood glucose measurements, mice were feed-deprived for 6 hours at baseline (Wk 0), mid (Wk 6), and final (Wk 12), and fasting blood glucose was measured from the tail using ReliOn Confirm blood glucose monitoring system (Walmart, USA). A glucose tolerance test (GTT) was conducted at day 80. After taking the baseline fasting glucose measurement, feed-deprived mice were injected with a 20% dextrose solution (2 g /kg body weight) andblood glucose was measured again from tail blood at 15, 30, 60 and 120 min post-glucose injection.

After 12 wks of dietary treatment, mice were feed-deprived for 4 hours and anesthetized using a ketamine/xylazine cocktail (100 mg/10 mg/ kg body weight).

Thereafter, the body composition (lean mass, fat mass, and body fat percentage) of each mouse was assessed using a whole body Piximus densitometer (GE Lunar, Madison, WI). Blood was collected via the carotid artery and serum was processed as described previously (29). The small intestine was flushed with ice cold PBS and excised into three different sections. The jejenum (mid-section) was snapped-frozen in liquid nitrogen and stored at -80^{o} C for further protein and gene expression analyses. The ileum mucosa was collected as previously described (26). The liver, perirenal adipose tissue, pancreas, and spleen were collected, weighed, snap-frozen and stored at -80^{o} C for further analyses. The visceral adipose tissue (VAT) was collected, weighed, and a section was snap-frozen. In preparation for isolating stromal vascular fraction, a section of VAT was dissected and transferred into an ice cold tube containing complete medium (DMEM + 10% FBS + 1% penicillin/streptomycin, 1g fat /10 mL) for further analyses.

Serum Measurements

Serum adipokines, hormones, and lipids were determined as previously described (29). Briefly, total cholesterol, triglycerides were measured using a Biolis 24i automated analyzer (Carolina Chemistry, Brea, CA). Insulin, leptin and resistin were measured as part of the Bio-Plex mouse diabetic markers kit (product no. 171F7001M) using the Bio-Plex MAGPIX Multiplex reader (Bio-Rad Laboratories Inc., Hercules, CA) following the manufacturer's instructions. The homoeostatic model assessment of insulin resistance (HOMA-IR) was used as a surrogate measure of insulin resistance: HOMA-IR= (fasting insulin (μU/ml) × fasting glucose (mg/dl) / 405.

Isolation of Adipose Derived Stromal Vascular Fraction (ADSVF)

The ADSVF was obtained by enzymatic isolation as described previously with few modifications (33). In brief, the VAT was diced into fine pieces and incubated at 37º C in 10 mL digesting medium containing DMEM + 1% FBS + 0.2% Collagenase Type VIII (Sigma, #C2139) while shaking at 300 rpm for 30 mins. The cell suspension was filtered through a 100 um cell strainer (VWR, #10199-658) into 50 mL tube containing equal volume of complete medium (DMEM + 10% FBS + 1% Penicillin/Streptomycin). Each cell suspension was centrifuged (5 min, 1000 rpm), and the cell pellet containing the stromal vascular fraction was incubated with 0.83% NH_4Cl for four mins on ice to lyse the red blood cells. The cell pellets (ADSVF) were washed twice in Dulbecco's Phosphate Buffered Saline (Sigma, #D5652). Radioimmunoprecipitation assay (RIPA) buffer containing 0.5% protease and phosphatase inhibitor cocktails (Sigma, #P8340 #P0044) was added to the ADSVF (70 µL / 3 million cells) for the preparation of total protein following standard procedures.

Gene Expression Analysis

Total RNA was processed from the jejunum, ileum mucosa, and the adipose tissue using Trizol reagent (ThermoFisher, Waltham, MA) following the manufacturer's instructions. Relative abundance of genes encoding antimicrobial peptides (*Reg3b* and *Reg3g*), lipopoly-saccharide biding protein (*Lbp*), *cd14,* Toll-like receptor 4 (*Tlr4),* inflammatory cytokines (*Tnfa, Il6, Il1b, Ifng, Tgfb1, IL22, and Il10*), innate and adaptive immune cell markers (*Cd11c, F4/80, Ccl2, Ccl3, iNos, Arg1, Cd3e, Foxp3*), hypoxia marker (*Hif1a*), angiogenesis and adhesive protein markers (*Vegfa, Icam1, Vcam1*), leptin precursor (*Lep*), and adipose triglyceride lipase (*Pnpla2*) were evaluated using SYBR

Green chemistry on an ABI 7900HT system (Applied Biosystems, Waltham, MA) as previously described (25). The primer sequences used in this study are presented in **Supplemental Table 2**.

Protein Expression Analyses

Total protein extraction and immunoblotting was done as described previously with few modifications (34, 35). Total protein homogenates from the jejunum (20mg), VAT (20 mg), and ADSVF (15 mg) were separated electrophoretically using SDS-PAGE and transferred to PVDF membranes (ThermoScientific, Waltham, MA). Membranes were blocked with 5% nonfat dried milk (Nestle) at room temperature for 1 hour. The membranes were washed twice in PBS and incubated overnight at 4ºC in 5% bovine serum albumin containing the following primary antibodies: CLAUDIN 2 (#sc-293233, Santa Cruz Biotechnology, Dallas, TX), OCCLUDIN (#33-1500, ThermoFisher, Waltham, MA), STAT3 (#4904, Cell Signalling Technology,Danvers, MA), p-STAT3 Tyr705 (#9145, Cell Signalling Technology, Danvers, MA), NFkBp65 (#Ab7970, Abcam,Cambridge, MA), p-NFkBp65 Ser536 (#sc-136548, Santa Cruz Biotechnology, Dallas, TX), FOXP3 (Santa Cruz Biotechnology, Dallas, TX, #sc-53876) and GAPDH (#60004-1, Proteinech, Rosemont IL). Blots were then washed twice with PBS and incubated with an anti-rabbit (#7074, Cell Signaling Technology, Danvers, MA), or anti-mouse (#7076, Cell Signaling Technology, Danvers, MA) IgG HRP-linked antibody. Blots were washed again with PBS, and incubated with SuperSignal West Femto Maximum Sensitivity Substrate (#34095, ThermoScientific,Waltham, MA) for 30 secs – 1 min. The blots were viewed with FluorChem R Imaging System (ProteinSimple, San Jose, CA), and the resulting protein bands were quantified with Image J software, v 1.8.0.

Statistical Analyses

Statistical analyses followed the use of 2-factor ANOVA (factors of HFS and WG). Least squares means were calculated using the mixed model procedure followed by Tukey's post hoc test when the *P* value for interaction was significant. A two-way repeated-measures ANOVA was carried out on the GTT data using the Huynh-Feldt model. Analyses were conducted using SAS software (version 9.4; SAS Institute, Cary, NC). Data are presented as means±SEM, and a P value<0.05 was considered statistically significant. For clarity, *P* values for main effect (HFS, WG) only if there was a significant *P* value ($P < 0.05$), or a trend ($0.05 \leq P \leq 0.14$). Whenever there is a significant *P* value ($P < 0.05$) for interaction (HFS x WG), differences between groups were indicated with letters on the figures.

Results

WG had minimal effects on body weight, tissue weights, and body composition

At the end of the 12 week dietary treatment, WG supplementation had no effect on the HFS-induced weight gain (**Figure 1**A). The HFS-fed group consumed 2% more kilocalories daily than the C group (P=0.022), while WG addition in the HFS+WG group reduced caloric intake to the level of C (**Figure 1**B). In addition, WG supplementation increased lean mass by at least 2% (**Figure 1**C; $P = 0.039$). Supplemental WG showed a modest effect to reduce percent body fat and visceral fat (**Figure 1**C and **1**D; $\boldsymbol{P} \leq 0.14$). However, WG supplementation had no effect on the weights of the liver, spleen, and perirenal fat (**Figure 1**D; $P > 0.05$).

WG supplementation improved glucose homeostasis and reduced serum triglycerides in HFS-fed mice

At wk 6 and wk 12, fasting blood glucose was elevated in the HFS group compared to C by 18% and 23%, respectively ($P \leq 0.047$, **Figure 2**A). On the other hand, WG reduced fasting blood glucose at both time points ($P \leq 0.034$), as evident in a 17% and 19% decrease in the HFS+WG group compared to HFS, at wks 6 and 12, respectively (**Figure 2**A). Glucose area under the curve (AUC) calculated after conducting a glucose tolerance test (**Figure 2**B and C) showed a modest decrease in glucose AUC due to WG supplementation (≤ -8%, $P = 0.079$). Supplemental WG reduced serum fasting insulin by at least 27% ($P = 0.016$; **Figure 2**D), and significantly improved the insulin resistance marker, HOMA-IR by at least -29% ($P = 0.0055$; **Figure 2**E). HFS feeding tended to upregulate the VAT leptin gene ($P = 0.073$) and elevate serum adipokines ($P = 0.13$) while WG had no significant effect (**Supplemental Figure 1**A, **Figure 2**F and G). Moreover, HFS-feeding tended to upregulate the adipose triglyceride lipase gene in the VAT ($P = 0.10$; **Supplemental Figure 1**B). Although not statistically significant, HFS increased serum triglycerides by 43% ($P = 0.18$) compared to the C group, while HFS+WG reduced serum triglycerides by 38% compared to HFS ($P = 0.014$, **Figure 2**I). WG supplementation had no effect on serum cholesterol and non-esterified fatty acids (**Figure 2**H and J; $P > 0.05$).

Supplemental WG modulates the jejunum by activtating STAT3 and upregulating antimicrobial peptide and antiinflammatory genes in mice fed a HFS-diet

As presented in **Figure 3**, WG supplementation upregulated the *Il10* gene in the jejunum by at least 116% ($P = 0.0002$; **Figure 3**A). Similarly, WG showed a main effect of upregulating the *Il22* gene by at least 147 % ($P = 0.035$, **Figure 3**B). Neither WG nor HFS had any effect on *Il6* gene expression (**Figure 3**C). Feeding a HFS diet resulted in elevated levels of CLAUDIN 2 (≥101%, $P = 0.0016$) and OCCLUDIN (≥63%, $P = 0.0064$) proteins in the jejunum compared to the C diets (**Figure 3**D, E, and F.) However, WG supplementation had no effect on both CLAUDIN 2 and OCCLUDIN proteins (**Figure 3**E and F). Compared to the C diet, HFS feeding showed a trend to decrease STAT3 activation as evident in an 89% decrease in STAT3 phosphorylation ($P = 0.088$; **Figure 3**G). Dietary treatments did not impact total STAT3 ($P \geq 0.41$; **Figure 3**H). Consequently, the mRNA expression of *Reg3β* and *Reg3γ* were significantly upregulated by WG supplementation in C and HFS diet (≥42%; $P \leq 0.043$; **Figure 3**I and J). Similarly, WG tended to upregulate *Reg3β* and *Reg3γ* in the ileum ($P \leq 0.078$; **Supplemental Figure 2**A and B).

WG supplementation prevented Nfκbp65 phosphorylation and downregulated *Il6* and *Lbp* genes in the visceral adipose tissue of HFS-fed mice

At the end of the dietary treatment, HFS feeding upregulated *Tlr4* gene in the VAT by ≥60% ($P = 0.034$; **Figure 4**A) while WG had no effect. In addition, the activation of NFκBp65 protein was elevated by 94% in the HFS group compared to control ($P = 0.0019$; **Figure 4**B and **4**C). Interestingly, WG significantly suppressed the HFS-induced

activation of NFκBp65 by 38%, thus bringing it to the level of control (P = 0.014; **Figure 4**B and **4**C). However, there was a main effect of HFS in elevating total NFκBp65 protein in the VAT (P = 0.0028; **Figure 4**B and **4**D). Furthermore, we observed a 3-fold increase of the *Il6* gene in the HFS group compared to the C group (P = 0.0032), while the HFS+WG group downregulated *Il6* gene by 54% compared to the HFS group (P = 0.034; **Figure 4**E). Moreover, HFS feeding significantly upregulated *Il10 gene* (P = 0.018), while WG showed a trend to reduce *Il10* gene expression (P = 0.12) and *Ifng* gene expression (P = 0.13; **Figure 4**E). Interestingly, the expression of *Lbp* gene was signifcantly upregulated by HFS (P = 0.015), while WG supplementation showed a main effect to attenuate *Lbp* expression (P = 0.0021; **Figure 4**F) in VAT. Dietary treatments had no significant effects on *Lbp* gene and other inflammatory gene markers in the liver (P > 0.05; **Figure 4**F, **Supplemental Figure 3** A – E). Finally, WG signifcantly suppressed *Vcam1* gene in the VAT (P = 0.024), but had no effect on the HFS-induced upregulation of *Hif1a* and *Vegfa* (**Supplemental Figure 4**).

Supplemental WG suppressed innate and adaptive immune cells markers in the visceral adipose tissue of HFS-fed mice

As presented in **Figure 5**A, HFS feeding elevated VAT mRNA expression of the chemokine *Ccl2* (≥1.5-fold, P = 0.0026), but not *Ccl3* (P >0.05). On the other hand, WG supplementation showed a trend to decrease *Ccl2* gene (P = 0.10) and significatnly reduced *Ccl3* gene expression (P = 0.037; **Figure 5**A). The gene expression of the macrophage and dendritic cell marker, *Cd11c*, and the macrophage marker *F4/80* in VAT were significantly elevated by HFS feeding (≤ 163%; $P \leq$ 0.023; **Figure 5**A), while WG

supplementation dowbregulated the expression of these genes by at least 28% ($P \leq$ 0.048; **Figure 5**A). The antigen presentation gene marker, H2ab1, which encodes the major histopatibility complex 2 (MHC II), was significantly upregulated in the HFS group compared to the C (1-fold, $P =$ 0.012), while the HFS+WG group significantly repressed the expression of this gene compared to the HFS group (-55%; $P =$ 0.013, **Figure 5**A). Furthermore, WG supplementation significantly downregulated the mRNA expression of the MI macrophage marker, *iNos*, by at least 34% ($P =$ 0.024), while it also showed a tendency to increase the gene expression of *Arg1*, an M2 macrophage marker ($P =$ 0.086; **Figure 5**B). The ratio of *iNos* to *Arg1* gene expression was significantly decreased by supplemental WG ($\geq$ -65%; $P =$ 0.034; **Figure 5**B).

Moreover, data in **Figure 5**C showed that the dietary treatments had no significant impact on the VAT gene expression of the T-cell marker, *Cd3e,* and the T-cell attracttant, *Rantes* ($P \geq$ 0.16; **Figure 5**C). However, the gene expression of *Tgfb1* was significantly higher in the HFS group compared to the HFS+WG group (135% ; $P =$ 0.030; **Figure 5**C). Consequently, HFS feeding significantly upregulated *Foxp3* mRNA ($P =$ 0.042; **Figure 5**C). In addition, HFS feeding showed a tendency to upregulate the protein expression of FOXP3 in the VAT and the ADSVF ($P \leq$ 0.12; **Figure 5**D and E), while WG showed a tendency to reduce FOXP3 protein in the ADSVF ($P =$ 0.058; **Figure 5**E).

Discussion

Diet-induced obesity (DIO) induce a leaky gut which inceases chronic bacteremia and endotoxemia capable of initiating systemic inflammation and insulin resistance via

the activation of the TLR4-NFkB pathway (5, 36). Using a western diet-induced (i.e. HFS) model of obesity, this study investigated the gut-protective mechanism of WG supplementation and the implication on inflammation and immune cell infiltration in the visceral adipose tissue (VAT) of C57BL/6J mice fed a control or a western diet for 12 wk. Although WG had no effect on tight junction proteins in the jejunum, our study demonstrates that WG activates the STAT3 pathway and upregulates antimicrobial peptide genes (Reg3β and Reg3γ) in the jejunum. Consequently, WG attenuated of NFκB phosphorylation in the VAT, together with the downregulation of *Il6* and *Lbp* genes. In addition, WG supplementation resulted in less chemoattractant and macrophage gene markers in the VAT of mice at the end of dietary treatment.

Obesity-induced metabolic syndrome is characterized in part, by insulin resistance, increased abdominal adiposity, and dyslipidemia (37). In mice, various high fat diet compositions have been used to model obesity-induced metabolic syndrome. The degree of response of these animals to high fat diets depend on several factors, including duration and genetic background (38). In this study, we only observed significant HFS effects on few markers of obesity-induced metabolic syndrome, including increased visceral fat, elevated fasting blood glucose (~181 mg/dL), and more glucose intolerance compared to the C diet. In addition, HFS showed modest effects on elevating total body fat, HOMA-IR, fasting triglycerides, and the adipokines, leptin and resistin. Supplemental WG had an opposite effect in most cases, as it significantly reduced fasting glycemia, fasting insulin, HOMA-IR, and serum triglycerides especially in the HFS-fed mice. Considering that the fasting blood glucose of insulin resistant C57BL/6J mice may be greater than 240 mg/dL (39), the overall implication of the metabolic outcomes of the

HFS-fed C57BL/6J mice in our study, especially as it relates to glucose metabolism, suggest that these animals are likely in the early stages of developing obesity-induced insulin resistance. Nevertheless, WG supplementation showed a strong potential to improve glucose metabolic parameters.

Diet-induced obesity (DIO) impair the expression of TJ proteins and impair the normal architecture of gut epithelial TJ (40). As a result, bacteremia and endotoxemia ensue which is associated with the initiation of inflammation in peripheral tissues and insulin resistance (5, 41). While the transcellular pathway allows microbial components through the epithelium by endocytosis (42, 43), elevated expression of the pore-forming claudin 2 is also associated with the leaky gut phenomenon in various diseases (15), including in DIO studies (16, 17). Accordingly, we observed an increase in CLAUDIN 2 expression in the jejunum of HFS mice while WG had no effect. This suggests an increased potential of bacteremia and endotoxemia in the HFS group which could be vital for the initiation of inflammation in peripheral tissues such as the adipose tissue. This notion is in agreement with the finding that HF feeding induces consistent paracellular permeability over time in the jejunum (18). Suprisingly, HFS feeding also increased the protein level of OCCLUDIN in the jejunum which may be a partial compesatory action to restore the jejunum TJs as observed in another study (44). However, this compensatory mechanism may not necessarily be beneficial or effecient in preventing a leaky gut, since elevated OCCLUDIN were observed to be increasingly localized in the cytoplasm rather than the apical cellular border (44, 45).

To reduce bacterial-epithelial interaction and mitigate gut translocation, antimicrobial peptides (AMPs) play a main role by reducing bacterial density within the

mucosal layer (23, 46). Among the AMPs, Reg3β and Reg3γ have been reported for their potent bactericidal action against gram-positive and gram-negative bacteria (46, 47). In the gut, butyrate produced from the bacterial fermentation of dietary fiber activates STAT3 in the epithelium resulting in the generation of the Reg3 lectins (22). Furthermore, indole metabolites derived from tryptophan metabolism by *Lactobacillus*, stimulate the production of IL22 from lamina propria lymphocytes capable of activating the STAT3 - Reg3 pathway (21, 48, 49). We have previously reported that WG Supplementation in HFS-fed mice selectively increased *Lactobacillus* but showed no increase in fecal SCFAs (26). In the present study, WG increased STAT3 phosphorylation and upregulated IL22 and the Reg3 genes in the jejunum. Considering that WG has a modest fiber content (3-4%) but remains one of the richest foods in the tryptophan (28-30), it is plausible that WG's potential to increase Lactobacillus in HF-fed mice resulted in elevated Reg3 AMPs via the IL22-STAT3 pathway. The AMPs may then be vital to reduce the burden of antigen translocation that could initiate inflammation and insulin resistance in peripheral tissues.

Accordingly, our study revealed the ability of WG to modulate adipose tissue inflammation – a classic response in diet-induced obesity. First, we observed an HFS-induced increase in total NFκBp65 in the VAT similar to other studies (50-52). Although WG had no effect on total NFkBp65, supplemental WG attenuated HFS-induced phosphorylation of NFkBp65, a key component of the NFκB complex that drives macrophage recruitment and the transcription of several pro-inflammatory genes (53). Consequently, WG suppressed the HFS-induced upregulation in *Il6, Lbp*, and macrophage-related genes such as *Cd11c* and *F4/80* in the adipose tissue. In addition,

WG downregulated the *Lbp* gene in the VAT. The recognition of pathogen-associated molecular patterns (PAMPs) promote an acute phase response leading to LBP production (54). By recognizing the lipid A moiety of gram negative bacterial cell wall component – lipopolysaccharide (LPS), an LBP-LPS complex is formed that increases the sensitivity of Cd14/TLR4-NFκB pathway to LPS by several folds (9, 10, 12). Furthermore, adipose-derived LBP directs local inflammatory and metabolic responses and may be an early biomarker for adipose tissue dysfunction in obesity (11). Put together, WG's ability to upregulate AMPs in the jejunum in this study may be vital for the prevention of NFκBp65 activation and attenuation of *Il6* and *Lbp* genes in VAT of mice fed a HFS-diet.

In addition, it was intruiging to observe a HFS-induced increase in the anti-inflammatory gene, Il10, in the VAT. The cell population that could contribute to the Il10 pool in the adipose may include macrophages (M2) and T-regulatory (FoxP3+) cells (3). However, WG but not HFS tended to increased M2 macrophage marker gene - *Arg1* in the VAT. On the other hand, FoxP3 gene and protein in the adipose tissue and the stromal vascular fraction showed a strong trend to be higher in the HFS group compared to others. Overall, this is in agreement with studies that show elevated adipose IL10 or FoxP3 in obese animals and humans, suggesting a compensatory effect to the pro-inflammatory environment (55-58). In addition, the initial increase in VAT FOXP3-expressing cells in obese animals progressively reduced over time, which worsened inflammatory and metabolic outcomes (57). It should be noted that the metabolic parameters from our HFS-fed mice suggest that these animals are at the early stages of developing obesity-induced insulin resistance. Thus, our finding of elevated VAT *Il10*

and FOXP3 in the HFS-fed group may be an initial compensatory action that aimed to ameliorate the consequence of the leaky gut-associated production of proinflammatory factors observed also in the HFS group. Importantly, supplemental WG showed no effect to elevate these antiinflammatory factors unlike HFS, due to the less need to combat HFS-induced inflammation.

Some of the limitations of this study include the lack of data related to gut bacterial-derived indole metabolites from tryptophan metabolism. Also, it is still unclear if the effect of WG on STAT3 reported in this study is solely via IL22. Butyrate was not elevated in mice fed HFS supplemented with WG (26), hence the direct effect of WG-induced butyrate on the STAT3 pathway is unlikely. However, IL-10 is also capable of activiating STAT3 in certain models of disease (59, 60). Since supplemental WG also increased *Il10* gene in the jejunum in this study, it is probable that the IL10 pathway contributes to STAT3 activation in the jejunum. Nevertheless, this limitation suggests that whole foods such as WG may be gut protective in HF feeding by various synergistic mechanisms. Therefore, future studies may find it important to clarify these individual mechanisms.

In conclusion, this study showed that in C57BL/6J mice fed a HFS diet for 90 days, WG upregulates the *Il22* gene, activates the STAT3 pathway, and upregulates antimicrobial peptide genes (*Reg3b* and *Reg3g*) in the jejunum. Accordingly, WG attenuated HFS-induced upregulation of *Il6* and *Lbp* genes, and lessened NFκBp65 phosphorylation in the visceral adipose tissue to the level of C. In addition, supplemental WG improved metabolic parameters in HFS-fed animals, including fasting blood glucose and insulin resistance marker (HOMA-IR). Put together, the modulatory effects of WG

on STAT3 and AMPs in the gut may be vital to reduce the burden of antigen translocation that could initiate adipose tissue inflammation and contribute to diet-induced insulin resistance.

Acknowledgements

We appreciate Shawnee Milling Company for providing the wheat germ used in this study.

Abbreviations Used: ADSVF, adipose derived stromal vascular fraction; Arg1, arginase 1; Ccl2, C-C motif chemokine ligand 2; Ccl3, C-C motif chemokine Ligand 3; Cd3e, cluster of differentiation (Cd) 3e; DIO, diet-induced obesity; Foxp3, forkhead box protein 3; H2ab1, histocompatibility 2 class II antigen A; HFS, high fat high sucrose; Hif1a, hypoxia inducible factor 1 subunit alpha; Icam1, intercellular adhesion molecule molecule 1; Ifnγ, interferon gamma; Il22, interleukin (Il) 22; iNos, inducible nitric oxide synthase; LBP, lipopolysaccharide binding protein; Lep, leptin; NFκB, nuclear factor kappa-light-chain-enhancer of activated B cells; Pnpla2, patatin-like phospholipase domain containing 2; Reg3β, regenerating islet-derived protein 3-beta; Reg3γ, regenerating islet-derived protein 3-gamma; TJ, tight junction; Tgfβ1, transforming growth factor beta 1; Tlr4, toll-like receptor 4; Tnfα, tumor necrosis factor alpha; VAT, visceral adipose tissue; Vcam1, vascular cell adhesion molecule 1; Vegfα, vascular endothelial growth factor alpha; WG, wheat germ

References

1. Blüher MJBp, endocrinology rC, metabolism. Adipose tissue dysfunction contributes to obesity related metabolic diseases. 2013;27:163-77.
2. Trayhurn PJAron. Hypoxia and adipocyte physiology: implications for adipose tissue dysfunction in obesity. Annual review of nutrition. 2014;34.
3. Lumeng CN, Bodzin JL, Saltiel ARJTJoci. Obesity induces a phenotypic switch in adipose tissue macrophage polarization. The Journal of clinical investigation. 2007;117:175-84.
4. Moreira APB, Texeira TFS, Ferreira AB, Peluzio MdCG, Alfenas RdCGJBJoN. Influence of a high-fat diet on gut microbiota, intestinal permeability and metabolic endotoxaemia. British Journal of Nutrition. 2012;108:801-9.
5. Cani PD, Amar J, Iglesias MA, Poggi M, Knauf C, Bastelica D, Neyrinck AM, Fava F, Tuohy KM, Chabo CJD. Metabolic endotoxemia initiates obesity and insulin resistance. 2007;56:1761-72.
6. Ding S, Chi MM, Scull BP, Rigby R, Schwerbrock NM, Magness S, Jobin C, Lund PKJPo. High-fat diet: bacteria interactions promote intestinal inflammation which precedes and correlates with obesity and insulin resistance in mouse. 2010;5:e12191.
7. Teixeira TF, Souza NC, Chiarello PG, Franceschini SC, Bressan J, Ferreira CL, Maria do Carmo GPJCn. Intestinal permeability parameters in obese patients are correlated with metabolic syndrome risk factors. Clinical nutrition. 2012;31:735-40.
8. Moreno-Navarrete JM, Sabater M, Ortega F, Ricart W, Fernandez-Real JMJPo. Circulating zonulin, a marker of intestinal permeability, is increased in association with obesity-associated insulin resistance. PloS one. 2012;7:e37160.
9. Knapp S, de Vos AF, Florquin S, Golenbock DT, van der Poll TJI, immunity. Lipopolysaccharide binding protein is an essential component of the innate immune response to Escherichia coli peritonitis in mice. Infection and Immunity. 2003;71:6747-53.
10. Schumann R, Kirschning C, Unbehaun A, Aberle H, Knope H, Lamping N, Ulevitch R, Herrmann FJM, Biology C. The lipopolysaccharide-binding protein is a secretory class 1 acute-phase protein whose gene is transcriptionally activated by APRF/STAT/3 and other cytokine-inducible nuclear proteins. Molecular and Cellular Biology. 1996;16:3490-503.
11. Moreno-Navarrete JM, Escoté X, Ortega F, Serino M, Campbell M, Michalski M-C, Laville M, Xifra G, Luche E, et al. A role for adipocyte-derived lipopolysaccharide-binding protein in inflammation- and obesity-associated adipose tissue dysfunction. Diabetologia. 2013;56:2524-37.
12. Schumann RR. Function of lipopolysaccharide (LPS)-binding protein (LBP) and CD14, the receptor for LPS/LBP complexes: a short review. Research in Immunology. 1992;143:11-5.

13. Jialal I, Devaraj S, Bettaieb A, Haj F, Adams-Huet B. Increased adipose tissue secretion of Fetuin-A, lipopolysaccharide-binding protein and high-mobility group box protein 1 in metabolic syndrome. Atherosclerosis. 2015;241:130-7.
14. Moreno-Navarrete JM, Ortega F, Serino M, Luche E, Waget A, Pardo G, Salvador J, Ricart W, Frühbeck G, et al. Circulating lipopolysaccharide-binding protein (LBP) as a marker of obesity-related insulin resistance. International Journal of Obesity. 2012;36:1442-9.
15. Luettig J, Rosenthal R, Barmeyer C, Schulzke J. Claudin-2 as a mediator of leaky gut barrier during intestinal inflammation. Tissue Barriers. 2015;3:e977176.
16. Ahmad R, Rah B, Bastola D, Dhawan P, Singh AB. Obesity-induces Organ and Tissue Specific Tight Junction Restructuring and Barrier Deregulation by Claudin Switching. Scientific Reports. 2017;7.
17. Xue Y, Wang H, Du M, Zhu M-J. Maternal obesity induces gut inflammation and impairs gut epithelial barrier function in nonobese diabetic mice. The Journal of Nutritional Biochemistry. 2014;25:758-64.
18. Hamilton MK, Boudry G, Lemay DG, Raybould HEJAJoP-G, Physiology L. Changes in intestinal barrier function and gut microbiota in high-fat diet-fed rats are dynamic and region dependent. American Journal of Physiology-Gastrointestinal and Liver Physiology. 2015;308:G840-G51.
19. Genser L, Aguanno D, Soula HA, Dong L, Trystram L, Assmann K, Salem J-E, Vaillant J-C, Oppert J-M, et al. Increased jejunal permeability in human obesity is revealed by a lipid challenge and is linked to inflammation and type 2 diabetes. The Journal of Pathology. 2018;246:217-30.
20. Ayabe T, Ashida T, Kohgo Y, Kono T. The role of Paneth cells and their antimicrobial peptides in innate host defense. Trends in Microbiology. 2004;12:394-8.
21. Hou Q, Ye L, Liu H, Huang L, Yang Q, Turner, Jr., Yu Q. Lactobacillus accelerates ISCs regeneration to protect the integrity of intestinal mucosa through activation of STAT3 signaling pathway induced by LPLs secretion of IL-22. Cell Death & Differentiation. 2018;25:1657-70.
22. Zhao Y, Chen F, Wu W, Sun M, Bilotta AJ, Yao S, Xiao Y, Huang X, Eaves-Pyles TD, et al. GPR43 mediates microbiota metabolite SCFA regulation of antimicrobial peptide expression in intestinal epithelial cells via activation of mTOR and STAT3. Mucosal Immunology. 2018;11:752-62.
23. Wang L, Fouts DE, Stärkel P, Hartmann P, Chen P, Llorente C, DePew J, Moncera K, Ho SB, et al. Intestinal REG3 lectins protect against alcoholic steatohepatitis by reducing mucosa-associated microbiota and preventing bacterial translocation. 2016;19:227-39.
24. Carvalho-Wells AL, Helmolz K, Nodet C, Molzer C, Leonard C, McKevith B, Thielecke F, Jackson KG, Tuohy KMJBjon. Determination of the in vivo prebiotic potential of a maize-based whole grain breakfast cereal: a human feeding study. 2010;104:1353-6.
25. Ojo B, El-Rassi GD, Payton ME, Perkins-Veazie P, Clarke S, Smith BJ, Lucas EAJTJon. Mango supplementation modulates gut microbial dysbiosis and short-chain fatty acid production independent of body weight reduction in C57BL/6 mice fed a high-fat diet. The Journal of Nutrition. 2016;146:1483-91.

26. Ojo BA, O'Hara C, Wu L, El-Rassi GD, Ritchey JW, Chowanadisai W, Lin D, Smith BJ, Lucas EAJTJon. Wheat Germ Supplementation Increases Lactobacillaceae and Promotes an Anti-inflammatory Gut Milieu in C57BL/6 Mice Fed a High-Fat, High-Sucrose Diet. The Journal of Nutrition. 2019.
27. Costabile A, Klinder A, Fava F, Napolitano A, Fogliano V, Leonard C, Gibson GR, Tuohy KMJBjon. Whole-grain wheat breakfast cereal has a prebiotic effect on the human gut microbiota: a double-blind, placebo-controlled, crossover study. 2008;99:110-20.
28. Brandolini A, Hidalgo AJIjofs, nutrition. Wheat germ: not only a by-product. 2012;63:71-4.
29. Ojo B, Simenson AJ, O'Hara C, Wu L, Gou X, Peterson SK, Lin D, Smith BJ, Lucas EAJBJoN. Wheat germ supplementation alleviates insulin resistance and cardiac mitochondrial dysfunction in an animal model of diet-induced obesity. British Journal of Nutrition. 2017;118:241-9.
30. Matej Brestenský SN, Peter Patráš. Wheat Germs and their Protein Quality for Human Nutrition. Nutri Food Sci Int J. 2019;8:555746.
31. Roager HM, Licht TR. Microbial tryptophan catabolites in health and disease. Nature Communications. 2018;9.
32. Moreira-Rosário A, Marques C, Pinheiro H, Norberto S, Sintra D, Teixeira JA, Calhau C, Azevedo LFJEjon. Daily intake of wheat germ-enriched bread may promote a healthy gut bacterial microbiota: a randomised controlled trial. European journal of nutrition. 2019:1-11.
33. Orr JS, Kennedy AJ, Hasty AHJJ. Isolation of adipose tissue immune cells. JoVE (Journal of Visualized Experiments). 2013:e50707.
34. Wu L, Guo X, Lyu Y, Clarke SL, Lucas EA, Smith BJ, Hildebrand D, Wang W, Medeiros DM, Shen XJSr. Targeted metabolomics reveals abnormal hepatic energy metabolism by depletion of β-carotene oxygenase 2 in mice. Scientific Reports. 2017;7:14624.
35. Graef JL, Rendina-Ruedy E, Crockett EK, Ouyang P, King JB, Cichewicz RH, Lucas EA, Smith BJJTJonb. Select polyphenolic fractions from dried plum enhance osteoblast activity through BMP-2 signaling. The Journal of Nutritional Biochemistry. 2018;55:59-67.
36. Saad M, Santos A, Prada PJP. Linking gut microbiota and inflammation to obesity and insulin resistance. Physiology. 2016;31:283-93.
37. Després J-P, Lemieux IJN. Abdominal obesity and metabolic syndrome. 2006;444:881.
38. Rendina-Ruedy E, Hembree KD, Sasaki A, Davis MR, Lightfoot SA, Clarke SL, Lucas EA, Smith BJJJon, metabolism. A comparative study of the metabolic and skeletal response of C57BL/6J and C57BL/6N mice in a diet-induced model of type 2 diabetes. Journal of nutrition and metabolism. 2015;2015.
39. Surwit RS, Kuhn CM, Cochrane C, McCubbin JA, Feinglos MNJD. Diet-induced type II diabetes in C57BL/6J mice. Diabetes. 1988;37:1163-7.
40. Raybould HEJTJop. Gut microbiota, epithelial function and derangements in obesity. The Journal of physiology. 2012;590:441-6.

41. Kim K-A, Gu W, Lee I-A, Joh E-H, Kim D-HJPo. High fat diet-induced gut microbiota exacerbates inflammation and obesity in mice via the TLR4 signaling pathway. PloS one. 2012;7:e47713.
42. Van Itallie CM, Holmes J, Bridges A, Gookin JL, Coccaro MR, Proctor W, Colegio OR, Anderson JMJJocs. The density of small tight junction pores varies among cell types and is increased by expression of claudin-2. Journal of cell science. 2008;121:298-305.
43. Knoop KA, Miller MJ, Newberry RDJCoig. Trans-epithelial antigen delivery in the small intestine: different paths, different outcomes. Current opinion in gastroenterology. 2013;29:112.
44. de La Serre CB, Ellis CL, Lee J, Hartman AL, Rutledge JC, Raybould HEJAJoP-G, Physiology L. Propensity to high-fat diet-induced obesity in rats is associated with changes in the gut microbiota and gut inflammation. 2010;299:G440-G8.
45. Brun P, Castagliuolo I, Leo VD, Buda A, Pinzani M, Palù G, Martines DJAJoP-G, Physiology L. Increased intestinal permeability in obese mice: new evidence in the pathogenesis of nonalcoholic steatohepatitis. 2007;292:G518-G25.
46. Miki T, Hardt W-DJPo. Outer membrane permeabilization is an essential step in the killing of gram-negative bacteria by the lectin RegIIIβ. PloS one. 2013;8:e69901.
47. van Ampting MT, Loonen LM, Schonewille AJ, Konings I, Vink C, Iovanna J, Chamaillard M, Dekker J, van der Meer R, et al. Intestinally secreted C-type lectin Reg3b attenuates salmonellosis but not listeriosis in mice. Infection and immunity. 2012;80:1115-20.
48. Parks OB, Pociask DA, Hodzic Z, Kolls JK, Good M. Interleukin-22 Signaling in the Regulation of Intestinal Health and Disease. Frontiers in cell and developmental biology. 2016;3.
49. Zelante T, Rossana, Cunha C, Antonella, Giovannini G, Pieraccini G, Zecchi R, D'Angelo C, Massi-Benedetti C, et al. Tryptophan Catabolites from Microbiota Engage Aryl Hydrocarbon Receptor and Balance Mucosal Reactivity via Interleukin-22. Immunity. 2013;39:372-85.
50. Zou B, Ge Z-z, Zhang Y, Du J, Xu Z, Li C-mJF, function. Persimmon tannin accounts for hypolipidemic effects of persimmon through activating of AMPK and suppressing NF-κB activation and inflammatory responses in high-fat diet rats. Food and Function. 2014;5:1536-46.
51. Sahin K, Orhan C, Akdemir F, Tuzcu M, Sahin N, Yılmaz I, Juturu VJF, Toxicology C. β-Cryptoxanthin ameliorates metabolic risk factors by regulating NF-κB and Nrf2 pathways in insulin resistance induced by high-fat diet in rodents. Food and Chemical Toxicology. 2017;107:270-9.
52. Tuzcu M, Sahin N, Orhan C, Agca CA, Akdemir F, Tuzcu Z, Komorowski J, Sahin KJN, metabolism. Impact of chromium histidinate on high fat diet induced obesity in rats. Nutrition and metabolism. 2011;8:28.
53. Baker RG, Hayden MS, Ghosh SJCm. NF-κB, inflammation, and metabolic disease. 2011;13:11-22.
54. Geller DA, Kispert PH, Su GL, Wang SC, Di Silvio M, Tweardy DJ, Billiar TR, Simmons RLJAoS. Induction of hepatocyte lipopolysaccharide binding protein in models of sepsis and the acute-phase response. Archives of Surgery. 1993;128:22-8.

55. Juge-Aubry CE, Somm E, Pernin A, Alizadeh N, Giusti V, Dayer J-M, Meier CAJC. Adipose tissue is a regulated source of interleukin-10. Cytokine. 2005;29:270-4.
56. Pereira S, Teixeira L, Aguilar E, Oliveira M, Savassi-Rocha A, Pelaez JN, Capettini L, Diniz MT, Ferreira A, Alvarez-Leite J. Modulation of adipose tissue inflammation by FOXP3+ Treg cells, IL-10, and TGF-β in metabolically healthy class III obese individuals. Nutrition. 2014;30:784-90.
57. Feuerer M, Herrero L, Cipolletta D, Naaz A, Wong J, Nayer A, Lee J, Goldfine AB, Benoist C, Shoelson SJNm. Lean, but not obese, fat is enriched for a unique population of regulatory T cells that affect metabolic parameters. Nature Medicine. 2009;15:930.
58. Van Der Weerd K, Dik WA, Schrijver B, Schweitzer DH, Langerak AW, Drexhage HA, Kiewiet RM, Van Aken MO, Van Huisstede A, et al. Morbidly Obese Human Subjects Have Increased Peripheral Blood CD4+ T Cells With Skewing Toward a Treg- and Th2-Dominated Phenotype. Diabetes. 2012;61:401-8.
59. Nguyen PM, Putoczki TL, Ernst M. STAT3-Activating Cytokines: A Therapeutic Opportunity for Inflammatory Bowel Disease? Journal of Interferon & Cytokine Research. 2015;35:340-50.
60. Dudakov JA, Hanash AM, van den Brink MRJAroi. Interleukin-22: immunobiology and pathology. 2015;33:747-85.

Figures

FIGURE 1: Effects of wheat germ (WG) supplementation on body composition and food intake in C57BL/6J mice fed a control (C) or high fat and sugar (HFS) diet for 12 wks. A) Initial (Wk 0) and final body weights (Wk 12), B) Average daily caloric intake, C) Body composition, and D) Tissue weights. Data are means ± SEM. Differences between groups are indicated with letters when the HFS x WG interaction was significant ($P < 0.05$, 2-way ANOVA). Labelled means without a common letter are significantly different from each other ($P<0.05$). n=10-12 mice/group

FIGURE 2: Effects of wheat germ (WG) on metabolic parameters in C57BL/6J mice fed a control (C) or high fat and sucrose (HFS) diet supplemented with 10% WG for 12 wks. A) Fasting blood glucose on Wk 0, 6, and 12, B) Glucose tolerance test, C) Glucose area under the curve, D) Fasting serum insulin, E) HOMA-IR, F) Serum leptin, G) Serum resistin, H) Serum total cholesterol, I) Serum triglycerides, and J) Serum NEFA. Data are means ± SEM. Differences between groups are indicated with letters when the HFS x WG interaction was significant ($P < 0.05$, 2-way ANOVA). Labelled means without a common letter are significantly different from each other ($P<0.05$). A-C, H-J (n=10-12/group). D-G (n=8/group). HOMA-IR, Homeostatic model assessment of insulin resistance; NEFA, non-esterified fatty acids

FIGURE 3: Effects of wheat germ (WG) on jejunal protein and gene expression in C57BL/6J mice fed a control (C) or high fat and sucrose (HFS) diet supplemented with

10% WG for 12 wks. A) *Il10* mRNA, B) *Il22* mRNA, C) *Il6* mRNA, D) Representative immunoblots, E) CLAUDIN 2 protein, F) OCCLUDIN protein, G) phosphorylated STAT3, H) Total STAT3 protein, I) *Reg3β* mRNA, and J) *Reg3γ* mRNA expression. Data are means ± SEM. Differences between groups are indicated with letters when the HFS x WG interaction was significant ($P < 0.05$, 2-way ANOVA). Labelled means without a common letter are significantly different from each other ($P<0.05$). n=6/group. IL10, interleukin 10; IL22, interleukin 22; Reg3b, regenerating islet-derived protein 3-beta; Reg3g, regenerating islet-derived protein 3-gamma; STAT3, Signal Transducer And Activator Of Transcription 3

FIGURE 4: Effects of wheat germ (WG) on inflammatory markers in the visceral adipose tissue (VAT) of C57BL/6J mice fed a control (C) or high fat and sucrose (HFS) diet supplemented with 10% WG for 12 wks. A) *Cd14* and *Tlr4* mRNA, B) Representative immunoblots, C) phosphorylated NFkBp65 protein, D) total NFkBp65 protein, E) *Tnfa, Il1b, Ifng, Il6, Il10* mRNA, and F) *Lbp* mRNA in the liver and VAT. Data are means ± SEM. Differences between groups are indicated with letters when the HFS x WG interaction was significant ($P < 0.05$, 2-way ANOVA). Labelled means without a common letter are significantly different from each other ($P<0.05$). n=6/group. Cd14, cluster of differentiation 14; Ifnγ, interferon gamma; Lbp, lipopolysaccharide binding protein; NFkB, nuclear factor kappa-light-chain-enhancer of activated B cells, Tlr4, toll-like receptor 4; Tnfα, tumor necrosis factor alpha

FIGURE 5: Effects of wheat germ (WG) on macrophage and T-cell related markers in the visceral adipose tissue (VAT) and adipose derived stromal vascular fraction *(*ADSVF) of C57BL/6J mice fed a control (C) or high fat and sucrose (HFS) diet supplemented with 10% WG for 12 wks. A) VAT *Ccl2, Ccl3, Cd11c, F4/80, H2ab1* mRNA, B) VAT mRNA expression of *iNos, Arg1*, and *iNOS-Arg1* mRNA expression ratio, C) VAT mRNA expression of *Rantes, Cd3e, Tgfb1, Foxp3*, D) VAT FOXP3 protein expression, and E) FOXP3 protein expression in the ADSVF. Data are means ± SEM. Differences between groups are indicated with letters when the HFS x WG interaction was significant ($P < 0.05$, 2-way ANOVA). Labelled means without a common letter are significantly different from each other ($P<0.05$). A-D (n=6/group), E (n=5/group). Arg1, arginase 1; Cd3e, cluster of differentiation 3e; Ccl2, C-C motif chemokine ligand 2; Foxp3, forkhead box protein 3, iNos, inducible nitric oxide synthase; Tgfβ1, transforming growth factor beta 1

Figure 1

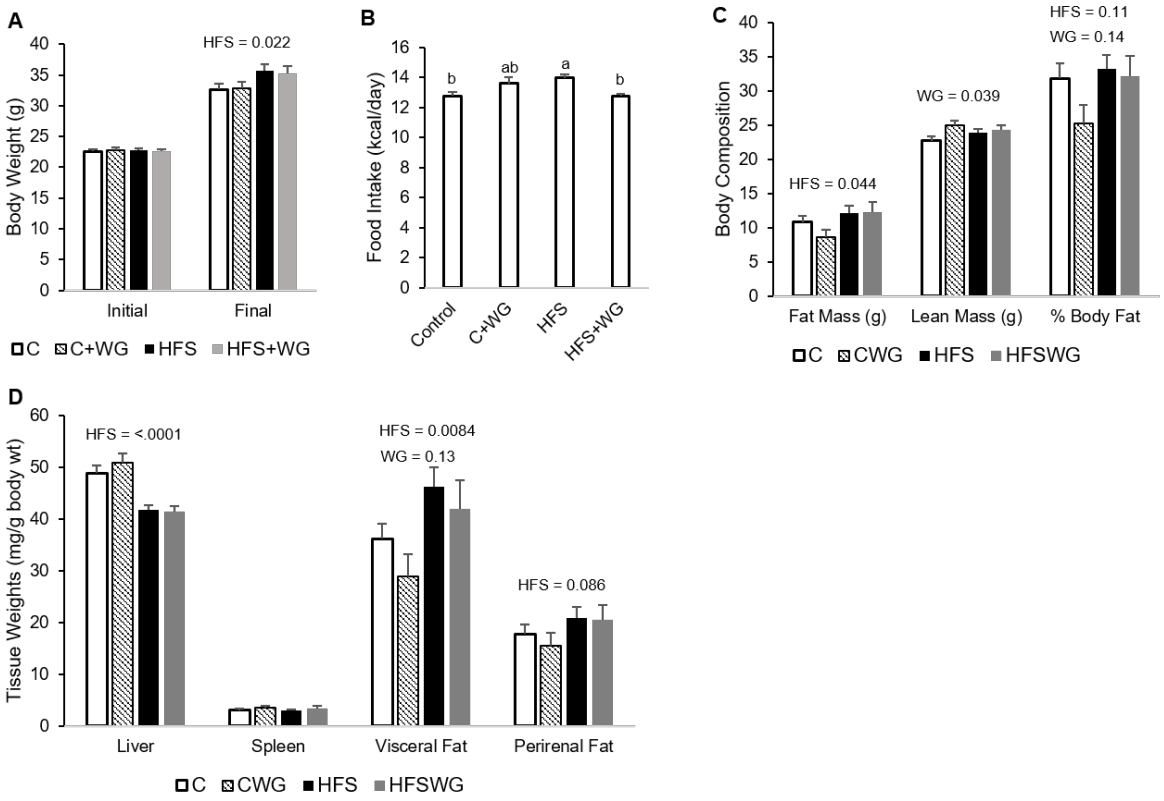
A
Body Weight (g)
HFS = 0.022
Initial
Final
C C+WG HFS HFS+WG
B
Food Intake (kcal/day)
b
ab
a
b
Control
C+WG
HFS
HFS+WG
C
Body Composition
HFS = 0.11
WG = 0.14
WG = 0.039
HFS = 0.044
Fat Mass (g)
Lean Mass (g)
% Body Fat
C CWG HFS HFSWG
D
Tissue Weights (mg/g body wt)
HFS = <.0001
HFS = 0.0084
WG = 0.13
HFS = 0.086
Liver
Spleen
Visceral Fat
Perirenal Fat
C CWG HFS HFSWG

Figure 2

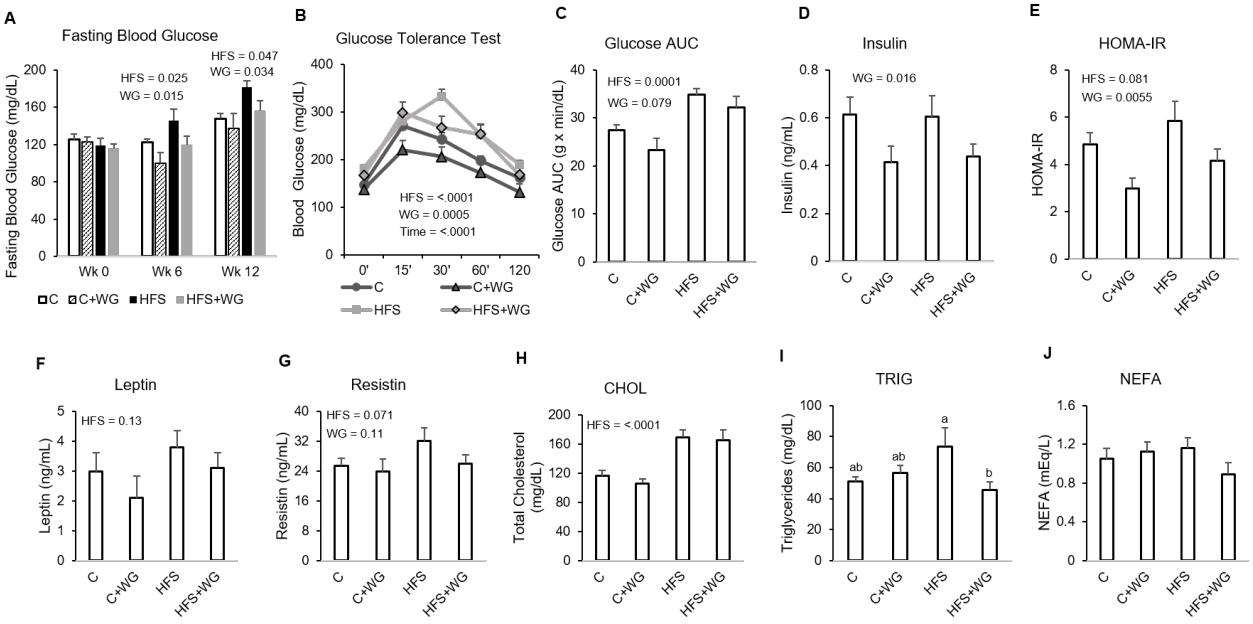
A
Fasting Blood Glucose
Fasting Blood Glucose (mg/dL)
HFS = 0.025
WG = 0.015
HFS = 0.047
WG = 0.034
Wk 0
Wk 6
Wk 12
C C+WG HFS HFS+WG
B
Glucose Tolerance Test
Blood Glucose (mg/dL)
HFS = <.0001
WG = 0.0005
Time = <.0001
0' 15' 30' 60' 120
C C+WG HFS HFS+WG
C
Glucose AUC
Glucose AUC (g x min/dL)
HFS = 0.0001
WG = 0.079
D
Insulin
Insulin (ng/mL)
WG = 0.016
E
HOMA-IR
HOMA-IR
HFS = 0.081
WG = 0.0055
F
Leptin
Leptin (ng/mL)
HFS = 0.13
G
Resistin
Resistin (ng/mL)
HFS = 0.071
WG = 0.11
H
CHOL
Total Cholesterol (mg/dL)
HFS = <.0001
I
TRIG
Triglycerides (mg/dL)
ab
ab
a
b
J
NEFA
NEFA (mEq/L)
C C+WG HFS HFS+WG

Figure 3

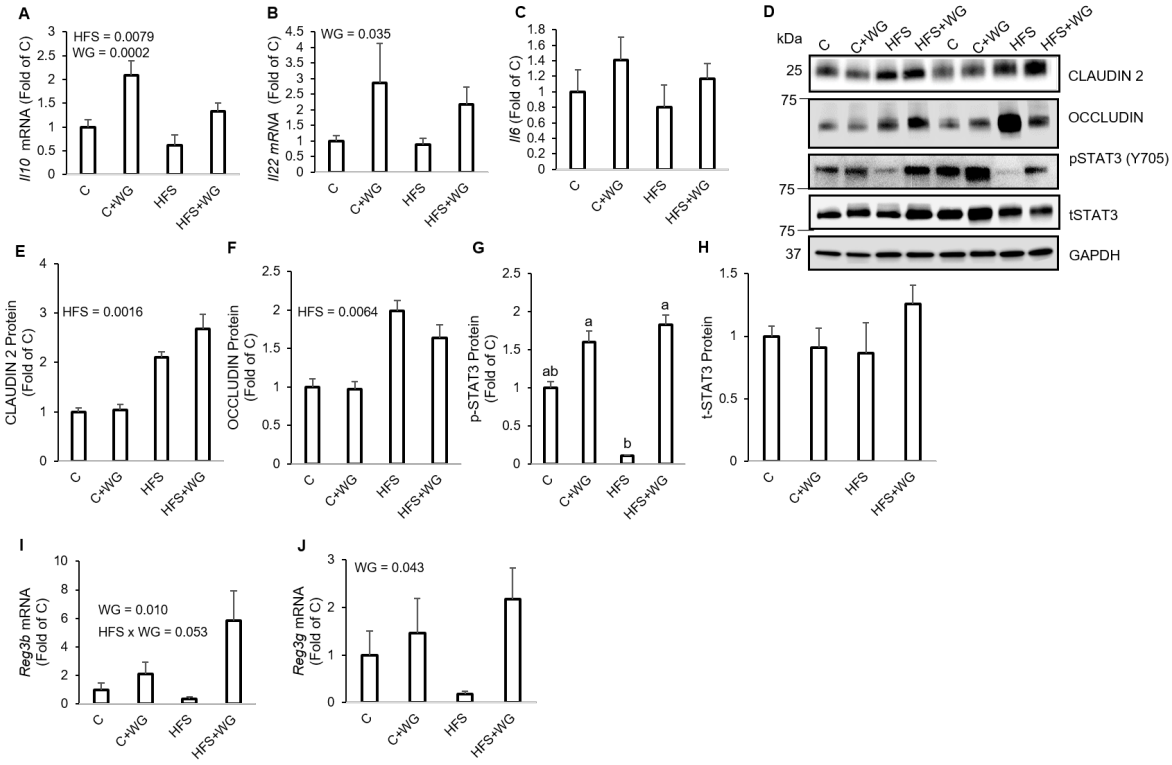
A
Il10 mRNA (Fold of C)
HFS = 0.0079
WG = 0.0002
B
Il22 mRNA (Fold of C)
WG = 0.035
C
Il6 (Fold of C)
D
kDa
CLAUDIN 2
OCCLUDIN
pSTAT3 (Y705)
tSTAT3
GAPDH
E
CLAUDIN 2 Protein (Fold of C)
HFS = 0.0016
F
OCCLUDIN Protein (Fold of C)
HFS = 0.0064
G
p-STAT3 Protein (Fold of C)
H
t-STAT3 Protein
I
Reg3b mRNA (Fold of C)
WG = 0.010
HFS x WG = 0.053
J
Reg3g mRNA (Fold of C)
WG = 0.043
C
C+WG
HFS
HFS+WG

Figure 4

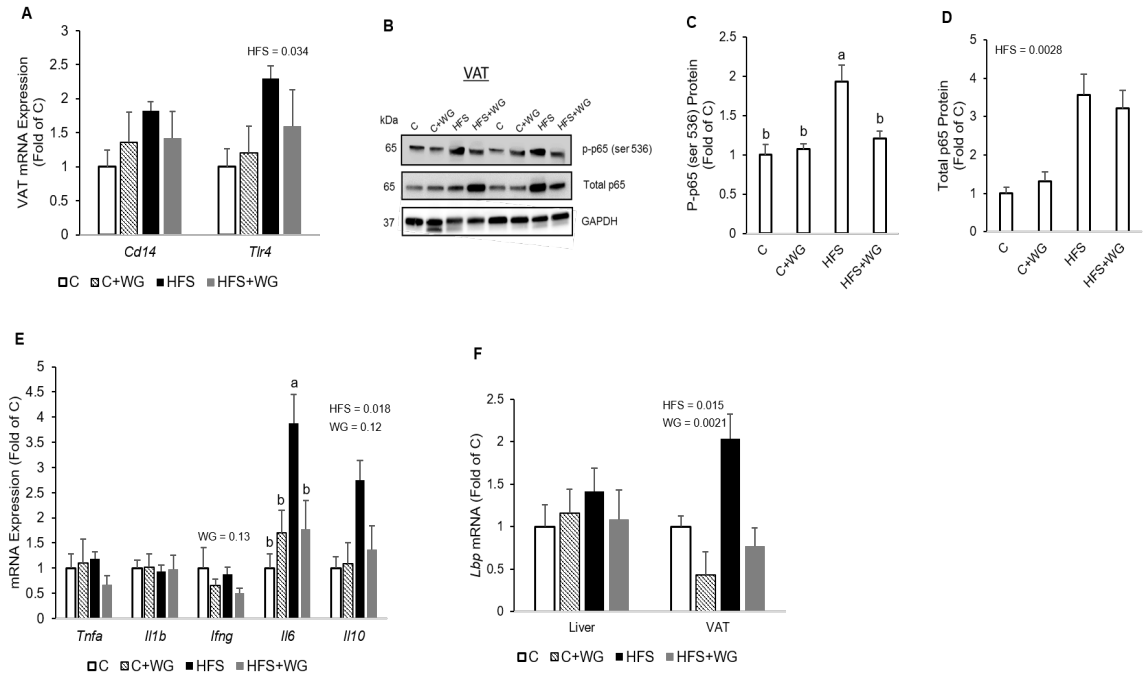
A
VAT mRNA Expression (Fold of C)
HFS = 0.034
Cd14
Tlr4
C C+WG HFS HFS+WG
B
VAT
kDa
C C+WG HFS HFS+WG C C+WG HFS HFS+WG
65
p-p65 (ser 536)
65
Total p65
37
GAPDH
C
P-p65 (ser 536) Protein (Fold of C)
a
b
b
b
C C+WG HFS HFS+WG
D
Total p65 Protein (Fold of C)
HFS = 0.0028
C C+WG HFS HFS+WG
E
mRNA Expression (Fold of C)
HFS = 0.018
WG = 0.12
WG = 0.13
a
b
b
Tnfa
Il1b
Ifng
Il6
Il10
C C+WG HFS HFS+WG
F
Lbp mRNA (Fold of C)
HFS = 0.015
WG = 0.0021
Liver
VAT
C C+WG HFS HFS+WG

Figure 5

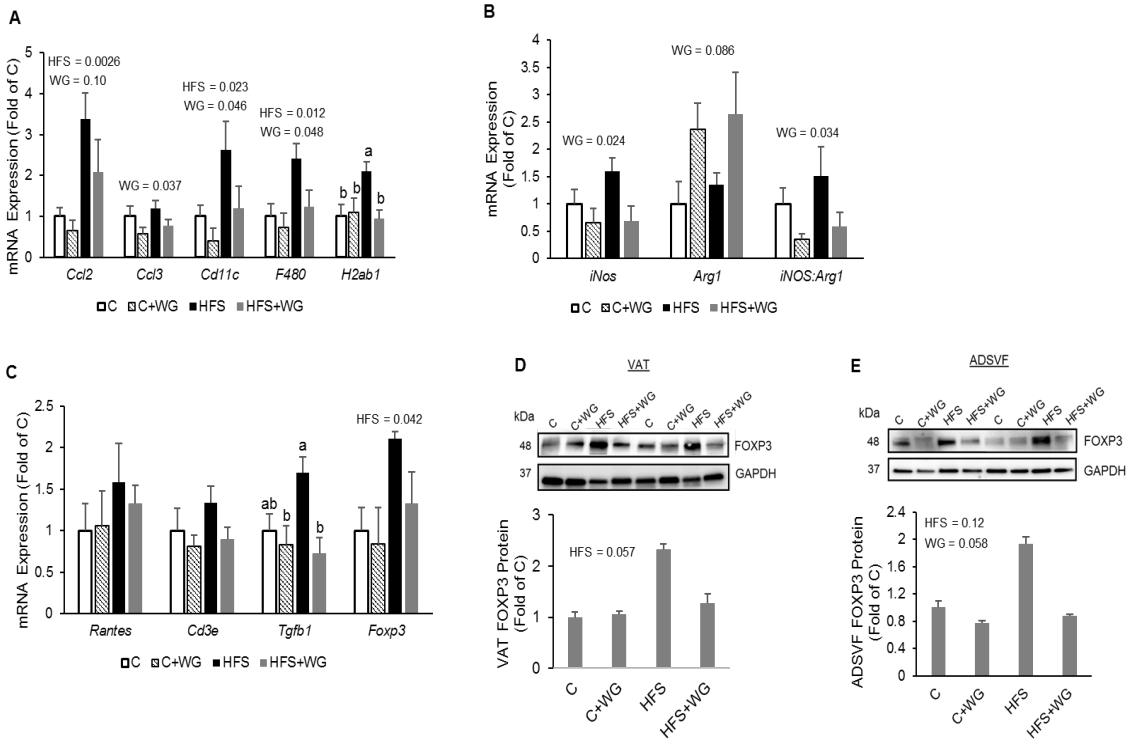
A
mRNA Expression (Fold of C)
HFS = 0.0026
WG = 0.10
WG = 0.037
HFS = 0.023
WG = 0.046
HFS = 0.012
WG = 0.048
a
b
b
b
Ccl2
Ccl3
Cd11c
F480
H2ab1
C C+WG HFS HFS+WG
B
mRNA Expression (Fold of C)
WG = 0.024
WG = 0.086
WG = 0.034
iNos
Arg1
iNOS:Arg1
C C+WG HFS HFS+WG
C
mRNA Expression (Fold of C)
HFS = 0.042
ab
b
a
b
Rantes
Cd3e
Tgfb1
Foxp3
C C+WG HFS HFS+WG
D
VAT
kDa
C C+WG HFS HFS+WG C C+WG HFS HFS+WG
48
FOXP3
37
GAPDH
VAT FOXP3 Protein (Fold of C)
HFS = 0.057
C
C+WG
HFS
HFS+WG
E
ADSVF
kDa
C C+WG HFS HFS+WG C C+WG HFS HFS+WG
48
FOXP3
37
GAPDH
ADSVF FOXP3 Protein (Fold of C)
HFS = 0.12
WG = 0.058
C
C+WG
HFS
HFS+WG

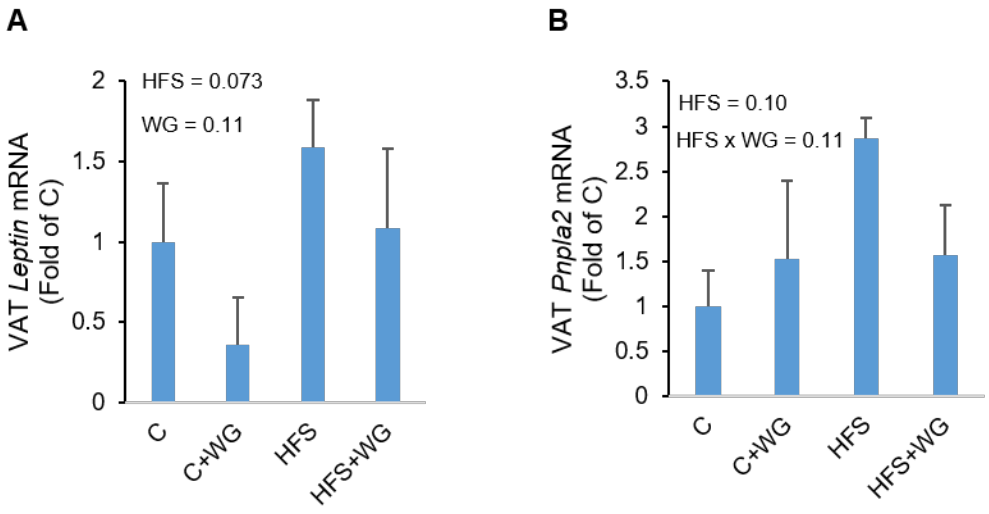

Supplemental Figure 1: Effects of wheat germ (WG) on (A) Leptin mRNA and (B) adipose triglyceride lipase gene, *Pnpla2,* in the visceral adipose tissue (VAT) of C57BL/6J mice fed a control (C) or high fat and sucrose (HFS) diet supplemented with 10% WG for 12 wks. Main effects were considered statistically significant when $P < 0.05$ (2-way ANOVA). n=6/group. Pnpla2, patatin-like phospholipase domain containing 2

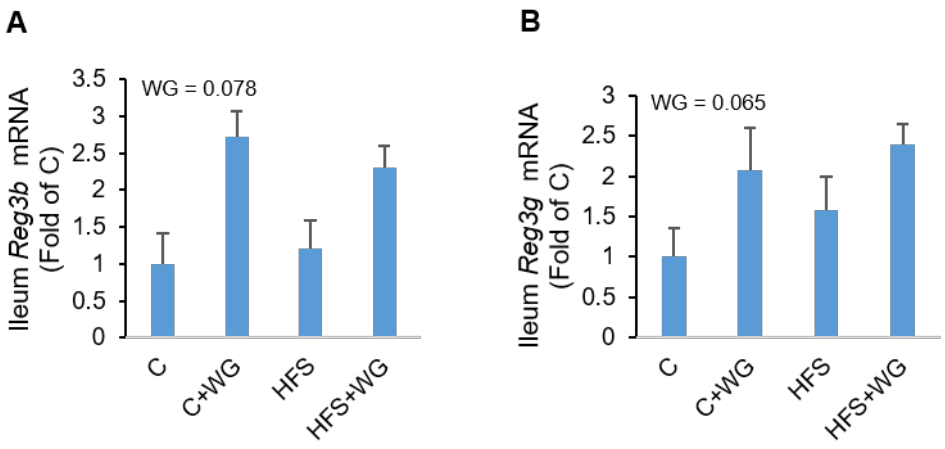

Supplemental Figure 2: Effects of wheat germ (WG) on (A) *Reg3b* mRNA and (B) *Reg3γ,* in the ileum of C57BL/6J mice fed a control (C) or high fat and sucrose (HFS) diet supplemented with 10% WG for 12 wks. n=6/group. Main effects were considered statistically significant when $P < 0.05$ (2-way ANOVA). Reg3β, regenerating islet-derived protein 3-beta; Reg3γ, regenerating islet-derived protein 3-gamma

Supplemental Figure 3

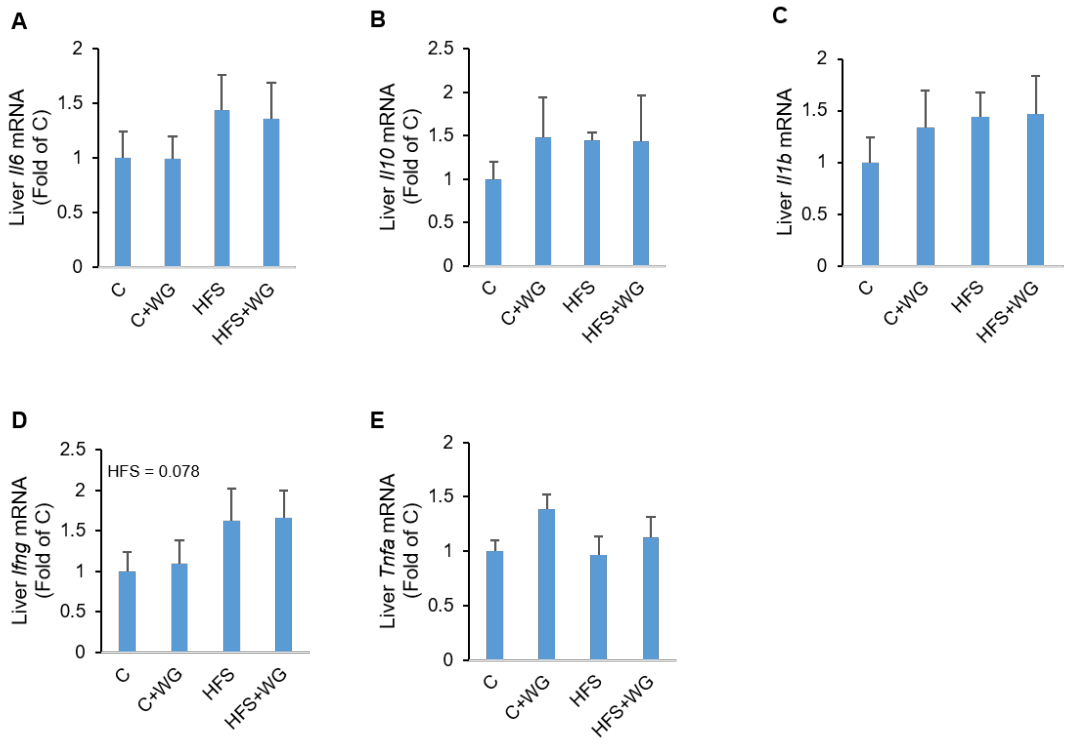

Effects of wheat germ (WG) on (A) *Il6* mRNA and (B) *Il10* mRNA, (C) *Il1β* mRNA, (D) *Ifnγ* mRNA, and (E) *Tnfα* mRNA in the liver of C57BL/6J mice fed a control (C) or high fat and sucrose (HFS) diet supplemented with 10% WG for 12 wks. Main effects were considered statistically significant when $P < 0.05$ (2-way ANOVA). n=6/group. Il6, interleukin 6; Ifnγ, interferon gamma; Tnfα, tumor necrosis factor alpha

Supplemental Figure 4

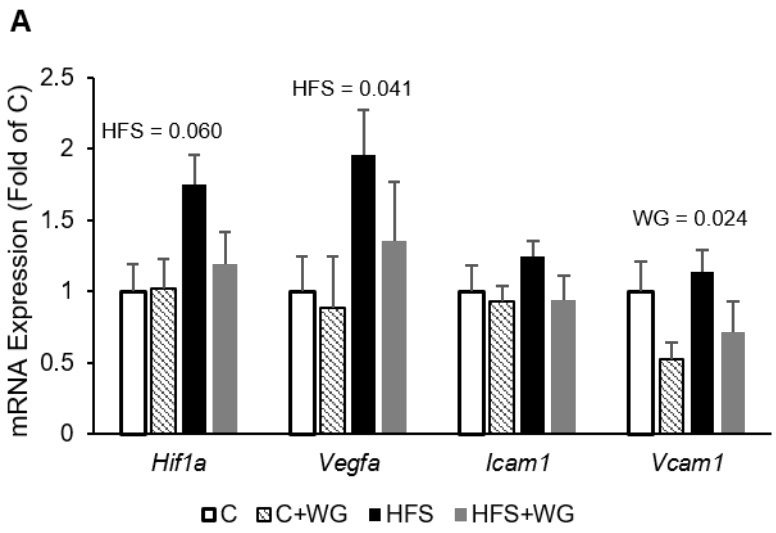

Effects of wheat germ (WG) on *Hif1α, Vegfα, Icam1,* and *Vcam1* mRNA expression in the VAT of C57BL/6J mice fed a control (C) or high fat and sucrose (HFS) diet supplemented with 10% WG for 12 wks. Main effects were considered statistically significant when $P < 0.05$ (2-way ANOVA). n=6/group. Il6, interleukin 6; Hif1α, hypoxia inducible factor 1 subunit alpha; Icam, intercellular adhesion molecule molecule 1; Vcam1, vascular cell adhesion molecule 1; Vegfα, vascular endothelial growth factor alpha;

Tables

Supplemental Table 1: Diet Composition (g/kg)

	C	C+WG	HFS	HFS+WG
Wheat Germ (WG)[1]	--	100	--	100
Carbohydrates				
Total	721	721	466.1	466.1
Cornstarch	466	413	34	0
Sucrose	100	100	308.6	308.6
Dextrinized Cornstarch	155	155	123.5	106.9
WG[1]	--	50.6	--	50.6
Protein				
Total	140	140	172.8	172.8
Casein	140	116.6	172.8	149.2
WG[1]	--	23.6	--	23.6
Fat				
Total	40	40	238.3	238.3
Soybean Oil	40	32.3	49.4	41.69
Lard	0	0	188.9	188.9
WG[1]	--	7.71	--	7.71
Fiber				
Total	50	50	61.7	61.7
Cellulose	50	46.9	61.7	58.6
WG[1]	--	3.1	--	3.1
Vitamin Mix[2]	10	10	12.3	12.3
Mineral Mix[3]				
Total	35	35	43.2	43.2
Calcium	25.9	25.8	31.97	31.83
Calcium from WG[1]	--	0.06	--	0.06
Sodium Phosphate	5.6	3.48	6.91	4.78
Potassium Phosphate	2.4	1.49	2.96	2.04
Phosphorous from WG[1]	--	0.93	--	0.93
Sucrose	1.1	3.29	1.36	3.57
L-Cystine	1.8	1.8	3.1	3.1
Choline bitartrate	2.5	2.5	2.2	2.2
Tert-butylhydroquinone	0.01	0.01	0.01	0.01
Kcal/g	3.96	3.96	4.62	4.62

[1]WG composition (Shawnee Mills, OK, USA) was analyzed by NP Analytical Laboratory (St. Louis, MO, USA): carbohydrates, 50.6%; protein, 23.6%; fat, 7.71%; fiber, 3.10%; calcium, 0.056%; and phosphorus, 0.93%.
[2]Harlan-Teklad Laboratories (TD 94047, WI, USA).
[3]Complete mineral mix (TD94049, Harlan-Teklad Laboratories) was used for the control diet (C) and a calcium and phosphorus deficient mineral mix (TD 98057, Harlan-Teklad Laboratories) was used for the C+WG and the high fat and sugar (HFS) diets.
[2,3]Compositions of the vitamin and mineral mix has been previously published (25).

Supplemental Table 2: Primer Sequence for Gene Expression Analyses

Gene	Forward	Reverse
mArg1	5'-cagtctggcagttggaagca-3`	5'-gcatccacccaaatgacaca-3`
mCcl2	5'-cttcctccaccaccatgca-3`	5'-ccagccggcaactgtga-3`
mCcl3	5`-ttcatcgttgactattttgaaacca-3`	5`-gccggtttctcttagtcaggaa-3`
mCd3e	5`-tagccagtgctgggacattg-3`	5`-caatctcagcagcctgattcttt-3`
mCd11c	5'-cttcattctgaagggcaacct-3`	5`-cactcaggagcaacacctttttt-3`
mCd14	5'-gccgccaccgcttct-3`	5'-acacgttgcggaggttca-3`
mCyclo	5`-tgg agagca cca aga cag aca-3`	5`-tgc cgg agt cga caa tga t-3`
mF4/80	5`-tggccaagattctcttcctcac-3`	5`-gcctccactagcatccagaaga-3`
mFoxp3	5`-ggcccttctccaggacaga-3`	5`-ggcatgggcatccacagt-3`
mH2ab1	5`-gcctgaagagccccatcac-3`	5`-tgccgctcaacattttgct-3`
mHif1a	5'-caacgtggaaggtgcttca-3`	5'-tgaggttggttactgttggtatca-3`
mIcam1	5'-ggaggtggcgggaaagtt-3`	5'-tccagccgaggaccatacag-3`
mIfng	5`-atgaacgctacacactgcatc-3`	5`-ccatccttttgccagttcctc-3`
mIl1b	5'-caaccaacaagtgatattctccatg-3'	5'-gatccacactctccagctgca-3`
mIl10	5`-ggt tgc caa gcc tta tcg ga-3`	5`-acc tgc tcc act gcc ttg ct-3`
mIl6	5`-gag gat acc act ccc aac aga cc-3`	5`-aag tgc atc atc gtt gtt cat aca-3`
mIl22	5`-atgagtttttcccttatggggac-3`	5`-gctggaagttggacacctcaa-3`
miNos	5'-caggaggagagagatccgattta-3`	5'-gcattagcatggaagcaaaga-3`
mLbp	5`-gtcctgggaatctgtccttg-3`	5`-ccggtaaccttgctgttgtt-3`
mLep	5`-ctccatctggccttctc-3`	5`-catccaggctctctggcttct-3`
mPnpla2	5`-aaggacctgatgaccaccct-3`	5`-ccaacaagcggatggtgaag-3`
mRantes	5'-ggagtatttctacaccagcagcaa-3`	5'-ggcggttccttcgagtga-3`
mReg3β	5`-tgg gaa tgg agt aac aat g-3`	5`-ggc aac ttc acc tca cat-3`
mReg3γ	5`-cca tct tca cgt agc agc-3`	5`-caa gat gtc ctg agg gc-3`
mTgfb1	5`-ctcccgtggcttctagtgc-3`	5`-gccttagtttggacaggatctg-3`
mTlr4	5'-actgttcttctcctgcctgaca-3`	5'-tgatccatgcattggtaggtaata-3`
mTnfa	5`-ctgaggtcaatctgcccaagtac-3`	5`-cttcacagagcaatgactccaaag-3`
mVcam1	5`-tgaacccaaacagaggcagagt-3`	5`-ggtatcccatcacttgagcagg-3`
mVegfa	5`-cgctggtagacgtccatga-3`	5`-cacgacagaaggagagcagaa-3`

CHAPTER VI

Pinto Beans Modulate the Gut Microbiome and Augment MHC II and Antimicrobial Peptide Expression at the Early Onset of Glucose Intolerance in Mice fed a Normal or Western-Style Diet

Abstract

The onset of type 2 diabetes in obesity is associated with gut dysbiosis and a failure to restrict the gut bacteria and toxins to the gut while prebiotics may prevent these effects. This study evaluated the early protective effects of pinto beans (PB) supplementation on the cecal bacteria, short chain fatty acids (SCFA), antigen presentation marker (MHC II) and antimicrobial peptide genes in the distal ileum, and the implication on glucose tolerance and adipose inflammation in C57BL/6J mice fed either a control (C) or a high-fat, high sucrose (HFS) diet for 4 weeks. Six-wk-old, male C57BL/6J mice were randomly assigned to four groups (n=12/group), and fed a control or HFS diet with or without freeze-dried cooked PB (10%, wt/wt) for 4 weeks. Results showed that supplemental PB in both C and HFS diets decreased the abundance of Tenericutes and the sulfate-reducing bacteria *Bilophila*. In contrast, PB raised the abundance of taxa within the SCFA-producing family, *Lachnospiraceae*, compared to groups without PB. Consequently, fecal butyric acid was significantly higher in PB-supplemented groups over the study duration. In the distal ileum, PB reversed the HFS-induced ablation of STAT3 phosphorylation, and upregulated Reg3γ, Reg3κ, and Il-10 genes. Furthermore, the expression of major histocompatibility complex (MHC) II protein was elevated in the PB supplemented groups compared to C and HFS. Tenericutes and *Bilophilia* negatively correlated with activated STAT3 and MHC II proteins. Finally, supplemental PB improved fasting blood glucose, glucose tolerance and suppressed tumor necrosis factor (TNF)-α and inducible nitric oxide synthase (iNos) in the visceral adipose tissue. Put together, PB supplementation induced favorable shifts in the gut that may be central to its potential to protect against diet-induced inflammation and glucose intolerance.

*This chapter will be submitted to Journal of Nutritional Biochemistry.

1. Introduction

Obesity remains a global epidemic that drives the development of other chronic diseases, including type 2 diabetes (T2D) [1]. One of the hallmarks of obesity is the persistent activation of immune cells, leading to chronic inflammation. Indeed, a typical event in fat accumulation observed in obesity is the infiltration of the adipose tissue by macrophages [2]. Classically activated macrophages express inducible nitric oxide synthase (iNos) and significantly contribute to chronic inflammation via the production of several pro-inflammatory cytokines such as interleukin (IL) 1β, IL-6 and tumor necrosis factor (TNF)α [3, 4]. These proinflammatory factors are implicated in the disruption of insulin signaling pathways– a key connection between obesity and the onset of T2D characterized by glucose intolerance [2].

Interestingly, the mammalian gut is a significant source of the signals that initiate inflammation in peripheral tissues [5-7]. Although the gastrointestinal tract is equipped with several physical and biochemical protective features, high fat (HF) diet-induced obesity ablates some of these features leading to increased gut translocation [7]. Specifically, the onset of type 2 diabetes in obesity is preceded by impaired antigen presentation signals in the ileum, increased gut permeability to bacteria and endotoxin (termed bacteremia and endotoxemia, respectively), coupled with the disruption of the structural composition of the commensal gut bacteria disruption (dysbiosis) [5, 6, 8]. Some of the characteristic changes in gut dysbiosis may include the loss of several taxa within the short-chain fatty acids (SCFAs)-producing family, *Lachnospiraceae* [9] along with an increase in detrimental taxa within the Proteobacteria phylum [9, 10].

SCFAs (primarily acetate, propionate and butyrate) confer several protective benefits to the host [11-14]. For example, butyrate is a preferred energy source for epithelial cells and are vital for the maintenance of intestinal tight junctions [11]. Further, through the activation of the transcription factor signal transducer and activator of transcription (STAT)3 in intestinal epithelial cells, butyrate may mediate the production of antimicrobial peptides (AMPs) which are vital in the restriction of the commensal bacteria to the intestinal lumen [12]. Butyrate and propionate also promote gut tolerance by stimulating the differentiation of IL10-producing T cells, and reducing gut inflammation and oxidative stress [13, 14]. Moreover, butyrate improved antigen-presenting capacity in the gut by elevating the recruitment of major histocompatibility complex (MHC)II^+ cells in the gut, which conferred protection against HFdiet-induced malignancy [15]. Thus, gut dysbiosis deprives the intestinal environment of vital bacterial-derived SCFAs, which are important for the maintenance of intestinal tight junctions, gut tolerance, efficient antigen presentation, and the induction of antimicrobial peptides. As a result, increased bacteremia and endotoxemia ensues leading to chronic activation of immune cells and inflammation associated with the onset of obesity-induced T2D [5, 8]. Therefore, strategies that increase SCFAs in the gut may be vital to improve the consequences of diet-induced obesity.

Prebiotics are substrates that can be utilized by the gut bacteria and confer a health benefit to the host [16]. The prebiotic potential of non-digestible carbohydrates (NDCs), such as inulin, oligofructose, galactooligosaccharides, and human milk oligosaccharide, have been widely studied [16]. These NDCs prevent gut bacterial dysbiosis and confer several health benefits in obesity mostly by increasing SCFA

production [17]. In contrast to the prebiotic pills and supplements widely available in the marketplace, whole foods may as well show several prebiotic potential [18]. The global alteration in food supply characterized by increased western-style diets (high in fat and sugar) has been a major driver of the obesity epidemic [19]. Hence, incorporating whole foods in the diet may be an efficient and cost-effective means to prevent gut dysbiosis, improve gut homeostasis, and mitigate the detrimental health implications of obesity.

Among whole foods, dietary pulses (peas, lentils, dry beans) have been studied for their ability to improve several consequences of obesity and its comorbidities [20]. Of these, the dry edible beans (*Phaseolus vulgaris L*), are nutrient dense foods that provide high quality protein, low in fat, rich in phenolic compounds, and contain the most fermentable fiber content, (15-45% wt/wt) depending on the variety, and may improve diet quality [21-23]. As such, studies have reported the anti-inflammatory and gut modulatory potential of certain bean varieties in models of obesity [24] and colitis [25, 26]. Specifically, the pinto beans (PB) variety – commonly produced in the United States [23] – increased *in vitro* SCFA production [27], and modulated postprandial glucose response in T2D patients [28]. It is unclear if these beneficial effects of PB is due to it robust impact on the gut microbiome, and innate gut protective factors (i.e., antimicrobial peptides, improved tight junction, and antigen surveillance).

Since our recent understanding indicates that the disruption of the gut immune defense and gut microbiota precedes the onset of high fat-induced chronic inflammation and T2D [5, 8], the impact of PB on these gut regulatory mechanisms from a preventive standpoint is not fully understood and warrants further investigation. Hence, this study evaluated the early protective effects of PB supplementation on the cecal microbiome,

antigen presentation marker (MHC II), and antimicrobial peptide expression in the gut of mice fed either a control or a high fat, high sucrose (HFS) diet for 4 weeks. Moreover, we sought to investigate the implication of these gut changes on immune cell recruitment and local inflammation in the visceral adipose tissue (VAT). Due to its rich fermentable-fiber component, we hypothesized that supplemental PB will prevent gut dysbiosis and increase SCFAs, improve MHC II protein in the gut, and enhance AMP transcription. These PB effects in the gut of HFS-fed mice may then explain the prevention of glucose intolerance and lesser proinflammatory milieu in the VAT.

2. Methods

2.1 Diet preparation and experimental design

Four-week-old male C57BL/6 mice (*n*=48) were purchased from Charles River Laboratory (Wilmington, MA) and were acclimated for one week. This was followed by random assignment into one of four treatment dietary treatment groups (n = 12/group) in a 2 x 2 factorial design — control (C; 10% kcal fat, 10% kcal sucrose; AIN-93 G), C + 10% PB (C + PB), a western-style diet with high fat and high sucrose, HFS (45% kcal fat, 26% kcal sucrose), and HFS + 10% PB (HFS + PB)— for 30days. Mice were group-housed (4 mice per cage) in wire-bottom cages. Animal care was carried out at Oklahoma State University Laboratory Animal Research facility maintained under humidity- and temperature-controlled conditions and a 12-h light–12-h dark cycle. Food and water was provided *ad libitum* for 4 weeks. Food intake was monitored daily and the body weight of each mouse was measured weekly. All procedures followed strict guidelines set by the Institution Animal Care of Oklahoma State University.

Raw pinto bean (PB) samples obtained from a local grocery store was prepared to mimic human consumption pattern as described by Zhang et al [26] and Kutos et al [29]. Briefly, pinto beans was soaked in water overnight at room temperature (300 mL H2O per 100 g dried beans) and cooked in the soaking water (98ºC -100ºC) for 40 mins. The resulting beans and water mixture was freeze-dried and ground. Nutrient composition of the bean powder was determined (NP Analytical Laboratories, St Louis, MO) and added to the C and HFS diet (10% wt/wt). The PB dose is less than to those used in previous animal studies of dietary bean intake [24-26] and it is relevant to legume intake levels (~ 1cup/day) in humans [30, 31]. We adjusted the PB-supplemented diets to consist of the same macronutrient composition, total fiber, calcium, and phosphorus as the unsupplemented diets (**Suppl. Table 1**).

2.2 Glucose homeostasis

On the 27th day of dietary treatment, mice were fasted for 6 hours and a fasting blood glucose was measure from the tail blood using the ReliOn Confirm blood glucose monitoring system (Walmart, USA). This was followed by an intraperitoneal injection with a 20% dextrose solution (2g/kg body weight). Thereafter, blood glucose was measured at 15, 30, 60, and 120 min post-injection.

2.3 Tissue collection

Fecal samples were collected per cage before the commencement (baseline) and at the end (final) of dietary treatment, and stored at -80º C. After 30days of dietary treatment, mice were deprived of food for 3 hours and anesthetized with a ketamine/xylazine cocktail (100 mg/10 mg/ kg body weight). Thereafter, a whole body Piximus

densitometer (GE Lunar, Madison, WI) was used to measure body composition. The liver, visceral and perirenal fat, and spleen were collected, weighed, flash-frozen in liquid nitrogen, and stored at -80° C. Cecal contents were processed as described previously [32]. The small intestine was flushed in ice cold phosphate buffered saline and the Peyer's Patches were excised. A portion of the distal ileum (2 cm from cecum) were stored in RNALater (Invitrogen, Carlsbad, CA) overnight, and subsequently stored at -80° C for gene and protein expression analyses. Further, a portion of the distal ileum was fixed in 10% neutral buffered formalin (NBF) for immunofluorescence staining.

2.4 Gut microbiota analyses

Nucleic acid isolation was carried out on frozen cecal samples using the QIAamp PowerFecal DNA kit (Qiagen) according to manufacturer's instructions. Sample library preparation and sequencing were performed at the Mouse Metabolic Phenotyping Center, University of California, Davis (Davis, CA). The DNA samples were purified and PCR-amplified on the V4 region of the 16S rRNA genes using the F319-R806 primers (F319, 5'-ACTCCTACGGGAGGCAGCAGT-3'; R806, 5'-GGACTACNVGGGTWTCTAAT-3'). Thereafter, paired-end high-throughput sequencing (250-bp) was performed on the Illumina Miseq platform. Data processing followed the use of the QIIME2 pipeline [33]. Paired-end sequences were demultiplexed and quality filtered followed by the prediction of operational taxonomic units (OTUs) using the DADA2 package [34]. Taxonomic classification of OTUs was done with the Naïve Bayes classifier trained against the Silva 128 97% OTU database. Raw sequence reads for this project can be found at https://www.ncbi.nlm.nih.gov/sra under the SRA accession number PRJNA527838.

2.5 Fecal SCFA analyses

Fecal samples collected at baseline and at the end of treatment were processed and analyzed in duplicates. The concentrations of acetic, propionic, butyric, and valeric acids were evaluated using gas chromatography as previously described [35].

2.6 Gene expression analysis

Total RNA was isolated from the ileum and visceral adipose tissue (VAT) using the Trizol reagent (ThermoFisher). Thereafter, the relative abundance of genes encoding antimicrobial peptides (Reg3b and Reg3g), lipopolysaccharide binding protein (Lbp), inflammatory cytokines (Tnfa, Il6, Ifng, Tgfb1, and Il10), chemokines (Ccl2 and Ccl3), innate immune cell markers (Cd11c, F4/80, iNos, Arg1), and forkhead box protein 3 (Foxp3), were evaluated using SYBR Green chemistry on an ABI 7900HT system (Applied Biosystems) as previously described [36]. The primer sequences used in this study can be found in **Suppl. Table 2.**

2.7 Immunoblotting

Total protein was prepared from the ileum using the radioimmunoprecipitation assay (RIPA) buffer containing 0.5% protease and phosphatase inhibitor cocktails (Sigma, #P8340 #P0044) following standard procedures. The samples for MHC II experiment were not heated in order to detect SDS-stable α/β dimers [37], while that of other experiments were heated (80° C, 3 minutes). Protein homogenates were separated on 4-20% polyacrylamide gels (BioRad) using SDS-PAGE and immunoblotting on PVDF membranes (ThermoScientific) as previously described [38, 39]. Primary antibodies diluted in 5% bovine serum albumin (BSA) include: MHC Class II I-A/I-E

(ThermoFisher, #14-5321-82), claudin 4 (ThermoFisher, #36-4800), occludin (ThermoFisher, #33-1500), STAT3 (Cell Signalling, #4904), p-STAT3 Tyr705 (Cell Signalling, #9145), and beta-actin (Cell Signaling, #8457). Blots were then washed twice with PBS and incubated with an anti-rabbit (Cell Signaling, #7074), or anti-mouse (Cell Signaling, #7076) IgG HRP-linked antibody. Proteins were detected using the SuperSignal West Femto maximum sensitivity substrate (ThermoScientific, #34095) for 30 secs – 1 min. Imaging followed with the FluorChem R Imaging System (ProteinSimple), and the resulting protein bands were quantified with Image J software, v 1.8.0.

2.8 Immunofluorescence analysis

The distal ileum samples stored in 10% NBF were paraffin-embedded. Slides containing 5 micrometer tissue sections were incubated (65-68°C, 30 min), dewaxed and rehydrated using xylene and ethanol gradients. Immunofluorescence analyses of the sections followed as previously described [40] with few modifications. Briefly, the samples were washed 3x with Millipore water, and incubated in 10 mM citrate buffer for antigen retrieval. The tissue sections were pre-incubated in 1% BSA for one hour, followed by overnight incubation with MHC Class II I-A/I-E antibody (1:500, ThermoFisher). Thereafter, the samples were washed 3x in phosphate buffered saline tween 20 (PBST, 5 min each) and incubated in Alexa Fluor 488 antibody (1:400, Invitrogen). The sections were counterstained with 4′-6-diamidino-2-phenylindole (DAPI, 1:4000, Calbiochem) for 1 min in the dark. The samples were rinsed 3x with PBST in the dark, mounted, and examined for fluorescence using a Keyence all-in-one

fluorescence microscope (BZ-X710) with images taken] with the KEYENCE BZ-X Viewer.

2.9 Statistical analyses

For the microbiome data, beta diversity analyses was carried out using the Bray-Curtis matrix. Principal coordinate analyses (PCoA) of the first two coordinates were plotted and comparison between groups was performed in R software (v.3.6.1) with permutational multivariate analysis of variance (PERMANOVA). Using the generated tables of relative taxonomic frequencies, differences between the dietary treatment groups were determined using the Kruskal-Wallis test (SAS version 9.4, Cary, NC). Statistically significant results were further subjected to a post-hoc analysis using Dunn's test (Dunn.test package in R software). *P*-values were false discovery (FDR)-corrected with the Benjamini-Hochberg procedure (p.adjust function in R software).

For other data, 2-factor analysis of variance (factors of HFS and PB) was conducted using the mixed model procedure followed by Tukey's post hoc test when the *P* value for interaction (HFS x PB) was significant. A repeated-measures ANOVA was carried out on the GTT and SCFA data using the Huynh-Feldt and variance component model, respectively. Analyses were conducted using SAS software (version 9.4; SAS Institute). Data are presented as means±SEM, and a P value <0.05 was considered statistically significant. For clarity, P values for main effect (HFS, PB) were presented only if $P < 0.05$ or a trend ($0.05 \leq P \leq 0.10$). Whenever $P < 0.05$ for interaction (HFS x PB or HFS x PB x Time), differences between groups were indicated with letters or

symbols on the figures. Finally, Spearman correlation matrix and visualization was carried out using the *ggcorrplot* package in R software (v. 3.6.1).

3. Results

3.1. Pinto Bean (PB) supplementation had no effect on body weight and body composition

After 30 days of dietary treatment, mice consuming the HFS diets had higher weight change than those consuming the C diets (**Fig. 1A**). Similarly, mice fed the HFS diets had greater energy intake that those fed on the C diets (**Fig. 1B**). Correspondingly, an increase in total fat mass and percent body fat was observed in mice fed the HFS diets (**Fig. 1C**). In addition, relative weights of the visceral fat, spleen, and perirenal fat were increased due to the consumption of the HFS diets (**Fig 1D**). Generally, supplemental PB had no effect on any of these parameters.

3.2 PB supplementation improves glucose homeostasis

After 27 days of dietary treatment, mice were fasted for 6 hours, followed by a fasting blood glucose (FBG) assessment and intraperitoneal glucose tolerance test (GTT). Our results showed an increase in FBG due to HFS feeding while PB supplementation significantly reduced fasting blood glucose by up to 13% in the HFS mice (**Fig. 2A**). Similarly, the GTT results showed that the HFS group had significantly high blood glucose that the C and C+PB groups at 30 and 120 minutes post-glucose injection (**Fig. 2B**). Consequently, HFS-feeding significantly increased glucose area under the curve (AUC), while supplemental PB significantly decreased glucose AUC by at least 8% (**Fig. 2C**).

3.3 Supplemental PB for 30 days significantly modulates the gut microbiota to favor SCFA-producing families

Cecal microbiome analysis of β-diversity using the Bray-Curtis distance metrics revealed a notable clustering among the PB supplemented groups and the non-supplemented groups (**Fig 3A**). However, PERMANOVA showed a significant ($p < 0.01$) β–diversity for each pairwise comparison. At the phylum level, HFS-feeding had no significant effect of the cecal bacteria, while PB significantly modulated some low-abundance phyla (**Fig 3B, 3D-F**). Tenericutes (o_Mollicutes RF9) were significantly reduced in the C+PB and HFS+PB groups compared to C and HFS respectively, by at least 55% ($p < 0.01$, **Fig 3B and 3D**). In addition, PB feeding in the HFS+PB group lowered members of the Proteobacteria and Verrucomicrobia phyla compared to the HFS group (Fig. 3B, 3E-F). Relative abundance at the family level (**Fig. 3C**) showed an elevation in the SCFA-producing bacteria family, *Lachnospiraceae*, in the PB supplemented groups compared to the respective controls by at least 48% ($p \leq 0.01$, Fi**g. 3C and 3G**). Similarly, *Bacteroidales S24-7* group had a higher abundance in the C+PB group compared to C, with a modest effect of PB to raise this family in animals fed the HFS diet (**Fig. 3C** and **3H)**. In this study, a significant early effect of HFS in disrupting the gut bacteria was observed in the abundance of the *Clostridales vadin BB60* group, which was reduced in the HFS group compared to control (-98%, $p < 0.001$, Fig 3C and 3I). The abundance of the *Clostridales vadin BB60* group in the HFS+PB was significantly higher than in the HFS group (**Fig. 3I**). The abundance of the *Ruminococcaceae* family was significantly suppressed by PB supplementation under C

and HFS dietary conditions (**Fig. 3J**). Analysis of bacteria genera showed that supplemental PB raised the abundance of *Lachnospiraceae NK4A136* group by over 1-fold compared to the respective C and HFS diets (**Fig. 3K, Supplementary Figure 1**). The *Roseburia* genera (f_*Lachnospiraceae*) was not detected in either C or HFS group but detected in all C+PB samples and half of the HFS+PB samples (*data not shown*). Moreover, mice fed a HFS diet had a modest elevation ($p = 0.07$) in the sulphate reducing bacteria (SRB)- *Bilophilia* (f_*Desulfovibrionaceae*) compared to the C group (**Fig. 3L**). On the other hand, PB supplementation in both C and HFS diets significantly lowered the abundance of this SRB-genus ($\geq$ -51%, $p < 0.05$, **Fig. 3L**). Lastly, the HFS+PB group had a lower abundance of the *Ruminococcaceae UCG-014* genus compared to the HFS group (**Fig. 3M**).

3.4 PB supplementation in mice fed C and HFS diets increased fecal butyrate concentrations over time.

Baseline (day 0) fecal samples and final fecal samples (day 30) were analyzed for their SCFA concentrations and subjected to repeated measures analysis of variance. At baseline, there were no differences in the measured SCFAs (**Fig 4**). At the end of the study, our results showed that total SCFA and acetic acid were elevated over time in all groups, although the effect size of HFS group was lower than that of the other groups (**Fig. 4A and 4B**). Final fecal concentrations of propionic acid was significantly higher in the C+PB group compared to C and HFS group ($p \leq 0.029$), but not to the HFS+PB group ($p > 0.05$, **Fig. 4C**). In addition, fecal butyric acid was significantly higher in C+PB compared to all other groups ($\geq$ 50%, $p \leq 0.001$, **Fig. 4D**). Interestingly, butyric acid was also significantly higher in the HFS+PB group compared to the C and HFS groups ($\geq$

52%, $p \leq 0.01$, **Fig. 4D**). Finally, valeric acid showed an increase over time in all groups while PB supplementation further increased its fecal concentration (**Fig. 4E**).

3.5 Supplemental PB increased STAT3 activation, elevated antimicrobial peptide genes, and MHC II protein in the distal ileum of HFS-fed mice

At the end of the 30-day dietary treatment, we evaluated proteins and genes partly responsible for the maintenance of gut homeostasis. Our results showed that in the distal ileum, STAT3 phosphorylation was suppressed in the HFS group while PB supplementation reversed this effect to the level of the C group (**Fig. 5A-5D**). The antimicrobial peptide genes, Reg3β and Reg3γ, were significantly upregulated in the PB supplemented groups compared to C and HFS groups (**Fig. 5E and 5F**). Furthermore, HFS-feeding significantly downregulated Ifnγ mRNA in the distal ileum, while there was a modest PB effect to upregulate the Ifnγ gene (**Fig. 5G**). Moreover, total MHC II protein in the distal ileum was higher in the PB-supplemented groups (**Fig 5H**). Immunofluorescence images showed more of a discontinuous MHC II staining along the epithelium of the C and HFS group, compared to the PB supplemented groups (**Fig. 5I**). In addition, Il-10 mRNA was significantly higher in the PB-supplemented groups (> 1-fold, **Fig. 5J**). The tight junction (TJ) protein- OCCLUDIN, tended to be lower due to HFS-feeding while PB supplementation showed a tendency to increase this TJ protein in the ileum (**Fig 5K and 5L**). On the other hand, CLAUDIN 4 was unaffected by the dietary treatments at the end of the 30-day feeding (Fig. 5K and 5M). Lastly, there was a tendency ($P = 0.07$) for HFS-feeding to downregulate Tnf-α and Tgfβ1 genes in the

ileum (**Supplementary Fig. 2A and 2B**), while no effect was observed on Il6 gene in the ileum (**Supplementary Fig. 2C**).

3.6 Dietary modification of the cecal gut microbiota significantly correlates with pSTAT3, MHC II, and antimicrobial peptide genes in the distal ileum.

We conducted a Spearman correlation analysis in order to find relationships between significantly changed gut bacteria taxa and ileal protein and genes (**Fig. 6**). The Tenericutes phylum negatively correlated with pSTAT3, MHC II, and the Reg3 genes (**Fig. 6**). On the other hand, the Lachnospiraceae family positively correlated with Reg3β and Reg3γ , similar to the S24-7 group which positively correlated with Reg3β (**Fig. 6**). Further, *Clostridiales vadin BB60* group positively correlated with Ifng gene while Ruminococcaceae negatively correlated with pSTAT3, Reg3γ and Ifnγ genes (**Fig. 6**). At the genus level, *Lachnospiraceae NK4A136* group positively correlated with Reg3β (Fig. 5). Lastly, we observed a significant negative correlation of *Bilophilia* with pSTAT3 and MHC II (**Fig. 6**).

3.7 PB supplementation attenuated Tnf-α and iNos gene expression in the visceral adipose tissue (VAT) of mice fed a C and HFS diet.

At the end of the 30-day feeding, we observed an HFS-induced upregulation in the mRNA of the chemokine Ccl2, and macrophage marker genes, (Cd11c and F4/80) in the VAT with no PB effect (**Fig. 7A**). Further, PB reduced Tnf-α mRNA, but had no effect on HFS-induced expression of Il-6 and Il-10 mRNA (**Fig. 7B**). Moreover, the gene expression of Lbp was modestly (P= 0.11) upregulated by HFS-feeding (**Fig. 7C**). Similarly, HFS diet tended (P= 0.089) to increase the mRNA expression of the M1

macrophage marker, iNos, but supplemental PB significantly reduced iNos gene expression (**Fig 7D**). The mRNA of M2 macrophage marker, Arg1, was not impacted by dietary treatment (**Fig 7D**). Finally, Foxp3 mRNA was significantly upregulated in the VAT by HFS feeding while PB had no effect (**Fig. 7E**).

4. Discussion

Using a western diet model of obesity and glucose intolerance, the present study sought to evaluate the effects of pinto beans (PB) on the gut microbiome and their fermentative capacity, and the implication on gut antimicrobial peptide expression, overall antigen-detecting capacity in the gut, and adipose tissue inflammation. Our results showed that after 4 weeks of HFS diet-feeding, PB had no effect on early weight gain or fat accumulation but improved glucose intolerance. Moreover, supplemental PB in the HFS diet modulated several aspects of the cecal microbiota, including an increase the SCFA-producing Lachnospiraceae, and a decrease in Proteobacteria. Consequently, PB significantly raised fecal SCFAs levels, especially butyrate in both the C and HFS diets. Furthermore, PB restored STAT3 activation in the HFS diet, coupled with an upregulation in antimicrobial peptide genes (Reg3y and Reg3b). In addition, supplemental PB tended to augment the TJ protein,occludin, and significantly elevated IL-10 gene and MHC II protein in the ileum of both C and HFS-fed mice. Irrespective of a significant HFS-effect, PB downregulated the gene expression of Tnf-α and iNos in the visceral adipose tissue.

Inclusion of non-digestible carbohydrates (NDCs) in the diet serve as substrates for the growth and maintenance of the commensal gut bacteria [16]. In turn, the gut

bacteria ferments the NDCs to produce short chain fatty acids (SCFAs) which confer several health benefits to the host [16, 41]. Our analysis showed that the PB used in this study had 24 g/100g total dietary fiber content, where 23% of that comprise of soluble fiber that could be available for gut bacterial fermentation. Interestingly, our 2x2 factorial model that consisted of a C and HFS group strongly showed the prebiotic potential of PB on the gut bacteria and SCFAs. Indeed, supplemental PB mostly modulated the gut bacteria and SCFAs (especially butyrate) similarly regardless of dietary fat or sugar content. For example, HFS feeding tended to raise the levels of sulfate-reducing bacteria (SRB), *Bilophilia* (p_Proteobacteria) similar with other long term studies [42-44]. Conversely, PB supplementation suppressed these genera in both the C and HFS diets, similar to prebiotic treatment in the study of Everard an colleagues [45]. This finding is significant since an increase in Proteobacteria, particularly in the SRB genera are associated with gut dysbiosis and inflammatory bowel diseases [10, 46]. Considering that higher doses of other bean varieties were beneficial in models of colitis [25, 26], future studies may evaluate if PB supplementation could have protective properties in colitis models.

Moreover, PB supplementation in both C and HFS diets increased the abundance of the *Lachnospiraceae* family, which harbors several SCFA-producing taxa [9, 47]. Accordingly, PB significantly increased fecal concentrations of butyrate over the treatment period in both C and HFS diets. This finding could have several implications. First, butyrate is a preferred source of energy for intestinal epithelial cells (IECs) and hence, vital for the maintenance of intestinal tight junctions [48, 49]. Consequently, the tendency of HFS diet to lower the expression of occludin, a TJ protein, was modestly

reversed by PB supplementation. Secondly, butyrate may participate in limiting gut translocation by stimulating AMP expression via STAT3 activation in IECs [12]. Indeed, expression of the Reg3 antimicrobial peptides in the gut improved steatohepatitis in mice by preventing bacterial translocation [50]. In this study, Reg3β and Reg3γ genes were significantly upregulated by PB. Since HFS-feeding suppressed STAT3 phosphorylation in the ileum, it is plausible that the PB-induced increase in butyrate contributed to STAT3 activation and the subsequent expression of the Reg3 genes that are part of the defense against gut translocation.

While the ideal situation is to restrict bacteria and endotoxin to the gut lumen under gut homeostasis, gut-derived bacteria still translocated under normal conditions as detected in the blood and adipose tissue of animals fed a normal chow diet [51]. Therefore, apart from the intestinal physical barrier and the biochemical secretions for apical gut defense (i.e AMPs, mucins, IgA), immune cells and signals within the lamina propria may also contribute to gut homeostasis [52]. The contribution may include mechanisms that induce tolerance to commensal bacteria, or preventing translocation by efficient detection of virulent bacteria by antigen presenting cells (APCs, MHC II^+ cells) and the subsequent clearance of the antigen [53]. Interestingly, SCFAs such as butyrate participate in some of these processes as reported in its ability to induce gut tolerance and an anti-inflammatory gut environment by increasing the differentiation of IL-10-expressing lymphocytes [13]. In this study, PB supplementation significantly upregulated the Il-10 gene in both C and HFS-fed mice in a similar pattern to our result on butyrate, suggesting an anti-inflammatory and tolerogenic potential of PB in the gut.

Further, Garidou et al showed that mice fed a HF diet for 10 or 30 days reduced the number of APCs and antigen-clearance capacity in the ileum, which contributed to the early onset of HF-induced insulin resistance [8]. Moreover, these changes were associated with the abundance of the *Porphyromonadaceae* bacteria family (also called *S24-7 group* depending on the taxonomic database classifier used [54, 55], or more recently proposed as *Muribaculaceae* [56]. In contrast, a tumorigenic mouse model showed that butyrate administration increased MHC II signals in the gut to improve disease outcomes through yet unclear mechanisms [15]. In a similar pattern to the butyrate result in our study, MHC II immunoblots showed a significant PB effect to elevate MHC II protein in the distal ileum but did not show a significant HFS effect. The lack of an HFS effect could possibly be due to different models of obesity (72% fat [8] versus 45% in our study), or due to different methods of detection (flow cytometry versus immunoblotting). Nevertheless, supplemental PB in our study raised the abundance of the *S24-7* bacteria, and correlated significantly with MHC II protein, similar to a previous observation [8]. It is noteworthy that our sample immunofluorescence staining for the unsupplemented mice (C and HFS groups) showed discontinuous MHC II staining along the ileum epithelia unlike the PB-supplemented groups. The continuous epithelial staining observed in the PB-supplemented groups may serve a gut protective role, since specific ablation of MHC II on intestinal epithelial cells resulted in increased susceptibility to colitis [57]. Put together, supplemental PB expands the overall antigen presenting capacity in the ileum that may potentiate efficient clearance of translocated antigens. However, future studies are needed to further clarify these mechanisms.

Short-term diet-induced obesity (DIO) studies show that bacteremia or endotoxemia initiate insulin resistance and inflammation in peripheral tissues [5, 8, 51]. More evidence from germ-free (GF) mice showed that in comparison to conventionally raised mice, GF mice were resistant to obesity, were more glucose tolerant, and had less adipose inflammation [58-60]. Apart from our observation of elevated VAT inflammation and macrophage accumulation in the HFS-groups, we observed an early tendency of HFS to increase iNos gene while PB supplementation significantly suppressed this effect. Considering the gut modulatory effects of PB seen in this study, this effect of PB in the VAT may be due to less endotoxin signal in the adipose tissue, since innate immune response to bacteria and endotoxin require iNos expression, as part of the mechanisms of pathogen elimination [61-64]. However, this concept as it relates specifically to the effects of PB needs to be expatiated in future studies.

Certainly, a main limitation of this study is our inability to attribute these robust PB effects to a single bioactive component (i.e fiber) since other components such as polyphenols also possess gut-modulatory potentials that may confer a health benefit [41]. However, it is vital to reiterate that these beneficial effects were observed using PB prepared similar to human consumption patterns. If replicated in humans, these findings imply that the incorporation of pinto beans in the diet may improve several facets of our gut health when consuming either a balanced diet or western-styled diets. In conclusion, PB showed a robust potential to influence the gut-adipose axis at the early stage of HFS-feeding, which may be vital for the prevention of obesity-induced chronic inflammation that is typically associated with the induction of glucose intolerance in the long term.

Acknowledgement

We thank Drs. Helen Raybould, Trina Knotts, and Michael Goodson of the University of California Davis' Microbiome and Host Response Core (RRID:SCR_015361, supported by NIH grant U24-DK092993) for their assistance with the microbiome analysis. Funding was provided in part by the Northarvest Bean Growers Association and by the Oklahoma State University College of Human Sciences. The funding agencies had no part in study design, data collection or analysis. The authors have no conflicts of interest to disclose.

Abbreviations Used: Arg1, arginase 1; Ccl2, C-C motif chemokine ligand 2; Ccl3, C-C motif chemokine Ligand 3; DIO, diet-induced obesity; Foxp3, forkhead box protein 3; HFS, high fat high sucrose; Ifng, interferon gamma; iNos, inducible nitric oxide synthase; Lbp, lipopolysaccharide binding protein; MHC II, major histocompatibility complex class II, PB, pinto bean; Reg3b, regenerating islet-derived protein 3-beta; Reg3g, regenerating islet-derived protein 3-gamma; TJ, tight junction; Tgfb1, transforming Growth Factor Beta 1; Tnfa, tumor necrosis factor alpha; VAT, visceral adipose tissue

References

1. Hu FBJDc. Globalization of diabetes: the role of diet, lifestyle, and genes. Diabetes care. 2011;34:1249-57.
2. Olefsky JM, Glass CKJArop. Macrophages, inflammation, and insulin resistance. Annual review of physiology. 2010;72:219-46.
3. Lumeng CN, Bodzin JL, Saltiel ARJTJoci. Obesity induces a phenotypic switch in adipose tissue macrophage polarization. The Journal of clinical investigation. 2007;117:175-84.
4. Xue Q, Yan Y, Zhang R, Xiong H. Regulation of iNOS on Immune Cells and Its Role in Diseases. International Journal of Molecular Sciences. 2018;19:3805.
5. Cani PD, Amar J, Iglesias MA, Poggi M, Knauf C, Bastelica D, et al. Metabolic endotoxemia initiates obesity and insulin resistance. Diabetes. 2007;56:1761-72.
6. Ding S, Chi MM, Scull BP, Rigby R, Schwerbrock NM, Magness S, et al. High-fat diet: bacteria interactions promote intestinal inflammation which precedes and correlates with obesity and insulin resistance in mouse. PloS one. 2010;5:e12191.
7. Moreira APB, Texeira TFS, Ferreira AB, Peluzio MdCG, Alfenas RdCGJBJoN. Influence of a high-fat diet on gut microbiota, intestinal permeability and metabolic endotoxaemia. British Journal of Nutrition. 2012;108:801-9.
8. Garidou L, Pomié C, Klopp P, Waget A, Charpentier J, Aloulou M, et al. The gut microbiota regulates intestinal CD4 T cells expressing RORγt and controls metabolic disease. Cell metabolism. 2015;22:100-12.
9. Kriss M, Hazleton KZ, Nusbacher NM, Martin CG, Lozupone CAJCoim. Low diversity gut microbiota dysbiosis: drivers, functional implications and recovery. Current opinion in microbiology. 2018;44:34-40.
10. Shin N-R, Whon TW, Bae J-WJTib. Proteobacteria: microbial signature of dysbiosis in gut microbiota. Trends in biotechnology. 2015;33:496-503.
11. Kelly CJ, Zheng L, Campbell EL, Saeedi B, Scholz CC, Bayless AJ, et al. Crosstalk between microbiota-derived short-chain fatty acids and intestinal epithelial HIF augments tissue barrier function. Cell Host & Microbe. 2015;17:662-71.
12. Zhao Y, Chen F, Wu W, Sun M, Bilotta AJ, Yao S, et al. GPR43 mediates microbiota metabolite SCFA regulation of antimicrobial peptide expression in intestinal epithelial cells via activation of mTOR and STAT3. Mucosal immunology. 2018;11:752.
13. Arpaia N, Campbell C, Fan X, Dikiy S, van der Veeken J, Deroos P, et al. Metabolites produced by commensal bacteria promote peripheral regulatory T-cell generation. Nature. 2013;504:451.
14. Tong L-c, Wang Y, Wang Z-b, Liu W-y, Sun S, Li L, et al. Propionate ameliorates dextran sodium sulfate-induced colitis by improving intestinal barrier function and reducing inflammation and oxidative stress. Frontiers in pharmacology. 2016;7:253.

15. Schulz MD, Atay Ç, Heringer J, Romrig FK, Schwitalla S, Aydin B, et al. High-fat-diet-mediated dysbiosis promotes intestinal carcinogenesis independently of obesity. Nature. 2014;514:508.
16. Gibson GR, Hutkins R, Sanders ME, Prescott SL, Reimer RA, Salminen SJ, et al. Expert consensus document: The International Scientific Association for Probiotics and Prebiotics (ISAPP) consensus statement on the definition and scope of prebiotics. Nature reviews Gastroenterology. 2017;14:491.
17. Delcour JA, Aman P, Courtin CM, Hamaker BR, Verbeke KJAiN. Prebiotics, fermentable dietary fiber, and health claims. Advances in Nutrition. 2016;7:1-4.
18. Graf D, Di Cagno R, Fåk F, Flint HJ, Nyman M, Saarela M, et al. Contribution of diet to the composition of the human gut microbiota. Microbial ecology in health. 2015;26:26164.
19. Zobel EH, Hansen TW, Rossing P, von Scholten BJJCor. Global changes in food supply and the obesity epidemic. Current obesity reports. 2016;5:449-55.
20. Marinangeli CP, Jones PJJBJoN. Pulse grain consumption and obesity: effects on energy expenditure, substrate oxidation, body composition, fat deposition and satiety. British Journal of Nutrition. 2012;108:S46-S51.
21. Messina VJTAjocn. Nutritional and health benefits of dried beans. The American journal of clinical nutrition. 2014;100:437S-42S.
22. Hernández-Salazar M, Osorio-Diaz P, Loarca-Piña G, Reynoso-Camacho R, Tovar J, Bello-Pérez LAJJotSoF, et al. In vitro fermentability and antioxidant capacity of the indigestible fraction of cooked black beans (Phaseolus vulgaris L.), lentils (Lens culinaris L.) and chickpeas (Cicer arietinum L.). Journal of the Science of Food and Agriculture. 2010;90:1417-22.
23. Câmara CR, Urrea CA, Schlegel VJA. Pinto beans (Phaseolus vulgaris L.) as a functional food: Implications on human health. Agriculture. 2013;3:90-111.
24. Monk JM, Wu W, Lepp D, Wellings HR, Hutchinson AL, Liddle DM, et al. Navy bean supplemented high-fat diet improves intestinal health, epithelial barrier integrity and critical aspects of the obese inflammatory phenotype. The Journal of nutritional biochemistry. 2019;70:91-104.
25. Monk JM, Zhang CP, Wu W, Zarepoor L, Lu JT, Liu R, et al. White and dark kidney beans reduce colonic mucosal damage and inflammation in response to dextran sodium sulfate. The Journal of nutritional biochemistry. 2015;26:752-60.
26. Zhang C, Monk JM, Lu JT, Zarepoor L, Wu W, Liu R, et al. Cooked navy and black bean diets improve biomarkers of colon health and reduce inflammation during colitis. British Journal of Nutrition. 2014;111:1549-63.
27. Finley JW, Burrell JB, Reeves PGJTJon. Pinto bean consumption changes SCFA profiles in fecal fermentations, bacterial populations of the lower bowel, and lipid profiles in blood of humans. The Journal of nutrition. 2007;137:2391-8.
28. Thompson SV, Winham DM, Hutchins AMJNj. Bean and rice meals reduce postprandial glycemic response in adults with type 2 diabetes: a cross-over study. Nutrition journal. 2012;11:23.
29. Kutoš T, Golob T, Kač M, Plestenjak AJFc. Dietary fibre content of dry and processed beans. Food chemistry. 2003;80:231-5.
30. Olmedilla-Alonso B, Pedrosa MM, Cuadrado C, Brito M, Asensio-S-Manzanera C, Asensio-Vegas CJJotSoF, et al. Composition of two Spanish common dry beans

(Phaseolus vulgaris),‘Almonga’and ‘Curruquilla’, and their postprandial effect in type 2 diabetics. Journal of the Science of Food. 2013;93:1076-82.
31. Jenkins DJ, Kendall CW, Augustin LS, Mitchell S, Sahye-Pudaruth S, Mejia SB, et al. Effect of legumes as part of a low glycemic index diet on glycemic control and cardiovascular risk factors in type 2 diabetes mellitus: a randomized controlled trial. Archives of internal medicine. 2012;172:1653-60.
32. Ojo B, El-Rassi GD, Payton ME, Perkins-Veazie P, Clarke S, Smith BJ, et al. Mango supplementation modulates gut microbial dysbiosis and short-chain fatty acid production independent of body weight reduction in C57BL/6 mice fed a high-fat diet. The Journal of Nutrition. 2016;146:1483-91.
33. Bolyen E, Rideout JR, Dillon MR, Bokulich NA, Abnet CC, Al-Ghalith GA, et al. Reproducible, interactive, scalable and extensible microbiome data science using QIIME 2. Nature biotechnology. 2019;37:852-7.
34. Callahan BJ, McMurdie PJ, Rosen MJ, Han AW, Johnson AJA, Holmes SPJNm. DADA2: high-resolution sample inference from Illumina amplicon data. Nature methods. 2016;13:581.
35. Ojo BA, O'Hara C, Wu L, El-Rassi GD, Ritchey JW, Chowanadisai W, et al. Wheat Germ Supplementation Increases Lactobacillaceae and Promotes an Anti-inflammatory Gut Milieu in C57BL/6 Mice Fed a High-Fat, High-Sucrose Diet. The Journal of Nutrition. 2019.
36. Ojo B, Simenson AJ, O’Hara C, Wu L, Gou X, Peterson SK, et al. Wheat germ supplementation alleviates insulin resistance and cardiac mitochondrial dysfunction in an animal model of diet-induced obesity. British Journal of Nutrition. 2017;118:241-9.
37. Kitamura H, Kamon H, Sawa S-i, Park S-J, Katunuma N, Ishihara K, et al. IL-6-STAT3 controls intracellular MHC class II αβ dimer level through cathepsin S activity in dendritic cells. Immunity. 2005;23:491-502.
38. Graef JL, Rendina-Ruedy E, Crockett EK, Ouyang P, King JB, Cichewicz RH, et al. Select polyphenolic fractions from dried plum enhance osteoblast activity through BMP-2 signaling. The Journal of Nutritional Biochemistry. 2018;55:59-67.
39. Wu L, Guo X, Lyu Y, Clarke SL, Lucas EA, Smith BJ, et al. Targeted metabolomics reveals abnormal hepatic energy metabolism by depletion of β-carotene oxygenase 2 in mice. Scientific Reports. 2017;7:14624.
40. Pervin M, Hasnat MA, Lim J-H, Lee Y-M, Kim EO, Um B-H, et al. Preventive and therapeutic effects of blueberry (Vaccinium corymbosum) extract against DSS-induced ulcerative colitis by regulation of antioxidant and inflammatory mediators. The Journal of nutritional biochemistry. 2016;28:103-13.
41. Laparra JM, Sanz Y. Interactions of gut microbiota with functional food components and nutraceuticals. Pharmacological Research. 2010;61:219-25.
42. Schneeberger M, Everard A, Gómez-Valadés AG, Matamoros S, Ramírez S, Delzenne NM, et al. Akkermansia muciniphila inversely correlates with the onset of inflammation, altered adipose tissue metabolism and metabolic disorders during obesity in mice. Scientific reports. 2015;5:16643.
43. Bruce-Keller AJ, Salbaum JM, Luo M, Blanchard IV E, Taylor CM, Welsh DA, et al. Obese-type gut microbiota induce neurobehavioral changes in the absence of obesity. Biological psychiatry. 2015;77:607-15.

44. Natividad JM, Lamas B, Pham HP, Michel M-L, Rainteau D, Bridonneau C, et al. Bilophila wadsworthia aggravates high fat diet induced metabolic dysfunctions in mice. Nature communications. 2018;9:2802.
45. Everard A, Lazarevic V, Gaïa N, Johansson M, Ståhlman M, Backhed F, et al. Microbiome of prebiotic-treated mice reveals novel targets involved in host response during obesity. The ISME journal. 2014;8:2116.
46. Rizzatti G, Lopetuso LR, Gibiino G, Binda C, Gasbarrini A. Proteobacteria: A Common Factor in Human Diseases. BioMed Research International. 2017;2017:1-7.
47. Ríos-Covián D, Ruas-Madiedo P, Margolles A, Gueimonde M, de los Reyes-Gavilán CG, Salazar NJFim. Intestinal short chain fatty acids and their link with diet and human health. Frontiers in microbiology. 2016;7:185.
48. Ma X, X. Fan P, Li L, Qiao S, Zhang G, Li DJJoas. Butyrate promotes the recovering of intestinal wound healing through its positive effect on the tight junctions. Journal of animal science. 2012;90:266-8.
49. Bauer E, Williams BA, Smidt H, Mosenthin R, Verstegen MWJNrr. Influence of dietary components on development of the microbiota in single-stomached species. Nutrition research reviews. 2006;19:63-78.
50. Wang L, Fouts DE, Stärkel P, Hartmann P, Chen P, Llorente C, et al. Intestinal REG3 lectins protect against alcoholic steatohepatitis by reducing mucosa-associated microbiota and preventing bacterial translocation. Cell host. 2016;19:227-39.
51. Amar J, Chabo C, Waget A, Klopp P, Vachoux C, Bermúdez-Humarán LG, et al. Intestinal mucosal adherence and translocation of commensal bacteria at the early onset of type 2 diabetes: molecular mechanisms and probiotic treatment. EMBO molecular medicine. 2011;3:559-72.
52. Kato LM, Kawamoto S, Maruya M, Fagarasan SJIr. The role of the adaptive immune system in regulation of gut microbiota. Immunological reviews. 2014;260:67-75.
53. Maynard CL, Elson CO, Hatton RD, Weaver CTJN. Reciprocal interactions of the intestinal microbiota and immune system. Nature. 2012;489:231.
54. Wang Q, Garrity GM, Tiedje JM, Cole JRJAEM. Naive Bayesian classifier for rapid assignment of rRNA sequences into the new bacterial taxonomy. Appl Environ Microbiol. 2007;73:5261-7.
55. Quast C, Pruesse E, Yilmaz P, Gerken J, Schweer T, Yarza P, et al. The SILVA ribosomal RNA gene database project: improved data processing and web-based tools. Nucleic acids research. 2012;41:D590-D6.
56. Lagkouvardos I, Lesker TR, Hitch TC, Gálvez EJ, Smit N, Neuhaus K, et al. Sequence and cultivation study of Muribaculaceae reveals novel species, host preference, and functional potential of this yet undescribed family. Microbiome. 2019;7:28.
57. Thelemann C, Eren RO, Coutaz M, Brasseit J, Bouzourene H, Rosa M, et al. Interferon-γ Induces Expression of MHC Class II on Intestinal Epithelial Cells and Protects Mice from Colitis. PloS One. 2014;9:e86844.

58. Rabot S, Membrez M, Bruneau A, Gérard P, Harach T, Moser M, et al. Germ-free C57BL/6J mice are resistant to high-fat-diet-induced insulin resistance and have altered cholesterol metabolism. The FASEB Journal. 2010;24:4948-59.
59. Tran H, Bretin A, Adeshirlarijaney A, San Yeoh B, Vijay-Kumar M, Zou J, et al. "Western-diet"-induced adipose inflammation requires a complex gut microbiota. Cellular and molecular gastroenterology and hepatology. 2019.
60. Bäckhed F, Manchester JK, Semenkovich CF, Gordon JIJPotNAoS. Mechanisms underlying the resistance to diet-induced obesity in germ-free mice. Proceedings of the National Academy of Sciences. 2007;104:979-84.
61. Shiloh MU, MacMicking JD, Nicholson S, Brause JE, Potter S, Marino M, et al. Phenotype of mice and macrophages deficient in both phagocyte oxidase and inducible nitric oxide synthase. Immunity. 1999;10:29-38.
62. Chakravortty D, Hensel MJM, infection. Inducible nitric oxide synthase and control of intracellular bacterial pathogens. Microbes. 2003;5:621-7.
63. Serbina NV, Salazar-Mather TP, Biron CA, Kuziel WA, Pamer EGJI. TNF/iNOS-producing dendritic cells mediate innate immune defense against bacterial infection. Immunity. 2003;19:59-70.
64. MacMicking JD, Nathan C, Hom G, Chartrain N, Fletcher DS, Trumbauer M, et al. Altered responses to bacterial infection and endotoxic shock in mice lacking inducible nitric oxide synthase. Cell. 1995;81:641-50.

Figures

FIG. 1: Effects of pinto beans (PB) supplementation on body composition and food intake in C57BL/6J mice fed a control (C) or high fat and sugar (HFS) diet for 30 days. A) Percent weight change over the study period, B) Average daily caloric intake, C) Body composition, and D) Tissue weights. Data are means ± SEM, $P < 0.05$ is considered statistically significant, 2-way ANOVA, n=12 mice/group.

FIG. 2: Effects of pinto beans (PB) on glucose homeostasis in C57BL/6J mice fed a control (C) or high fat and sucrose (HFS) diet for 30 days. A) Fasting blood glucose on Wk 4, B) Glucose tolerance test, and C) Glucose area under the curve. Data are means ± SEM. Differences between groups are indicated with symbols when the HFS x PB x Time interaction was significant ($P < 0.05$, repeated measures ANOVA). * HFS vs C and C+PB; # HFS vs C+PB. (n=11-12/group).

FIG. 3: Effects of pinto beans (PB) on the gut microbiome in C57BL/6J mice fed a control (C) or high fat and sucrose (HFS) diet for 30 days. A) Microbiome beta-diversity based on Bray-Curtis distance of operational taxonomic units, B) taxonomic abundance at the phylum level, C) top 20 bacterial taxa at the family level, D-M) significantly different taxa at the D-F) phylum, G-J) family, and K-M) genus level. n=6/group. Differences between groups are indicated with symbols when the Kruskal-Wallis test and Dunn's *post-hoc* tests were significant (*$P < 0.05$, **$P < 0.01$, ***$P < 0.001$).

FIG. 4: Effects of pinto beans (PB) on fecal short chain fatty acids (SCFAs) over time in C57BL/6J mice fed a control (C) or high fat and sucrose (HFS) diet for 30 days. A) total SCFA, B) acetic acid, C) propionic acid, D) butyric acid, and E) valeric acid. Data are means ± SEM. (n = 3 cages/group, 4 mice/cage). Differences between groups are indicated with symbols when the HFS x PB x Time interaction was significant ($P < 0.05$, repeated measures ANOVA). * C+PB vs C and HFS; # C+PB vs other groups; † HFS+PB vs C and HFS.

FIG. 5: Effects of pinto beans (PB) on gene and protein expression in the distal ileum of C57BL/6J mice fed a control (C) or high fat and sucrose (HFS) diet for 30 days. A) representative blots of B) phosphorylated STAT3 protein and C) total STAT3 protein, D) ratio of pSTAT3 to tSTAT3, mRNA expression of E) Reg3 beta, F) Reg3γandG) interferon γ, H) MHC II protein expression, I) sample immunofluorescence images of MHC II. Magnification=20x, Scale bar = 50um, DAPI = Blue, MHC II = Green, J) interleukin 10 mRNA expression, and K) representative blots of L) Occludin and M) Claudin 4 proteins. Data are means ± SEM. n = 7-9 mice/group for A-D, H, K-M. n=6 mice/group for E-G and J. Differences between groups are indicated with letters when the HFS x PB interaction was significant ($P < 0.05$, 2-way ANOVA). Labelled means without a common letter are significantly different from each other ($P<0.05$).

FIG. 6: PB-induced changes in the cecal microbiome correlates with protein and gene expression in the distal ileum. Spearman correlation was perform and visualized using R software. * indicates $R \geq 0.50$, $p \leq 0.01$

FIG. 7: Effects of pinto beans (PB) on markers related to immune cell accumulation and inflammation in the visceral adipose tissue (VAT) of C57BL/6J mice fed a control (C) or high fat and sucrose (HFS) diet for 30 days. Visceral adipose tissue (VAT) mRNA expression of (A) *Ccl2, Ccl3, Cd11c, F4/80*, (B) Tnf-a, Ifny, Il-6, Il-10, (C) Lbp, (D) *iNos, Arg1,* and (E) *Foxp3*. Data are means ± SEM. n= 6 mice/group.

Suppl. Fig. 1: Effects of pinto beans (PB) on the abundance of cecal bacterial genera in C57BL/6J mice fed a control (C) or high fat and sucrose (HFS) diet for 30 days. n=6/group.

Suppl. Fig. 2: Effects of pinto beans (PB) on the mRNA expression of (A) Tnf-a, (B) Tgfb1, and (C) Il-6, in the distal ileum of C57BL/6J mice fed a control (C) or high fat and sucrose (HFS) diet for 30 days. Data are means ± SEM. n = 6 mice/group.

Fig. 1

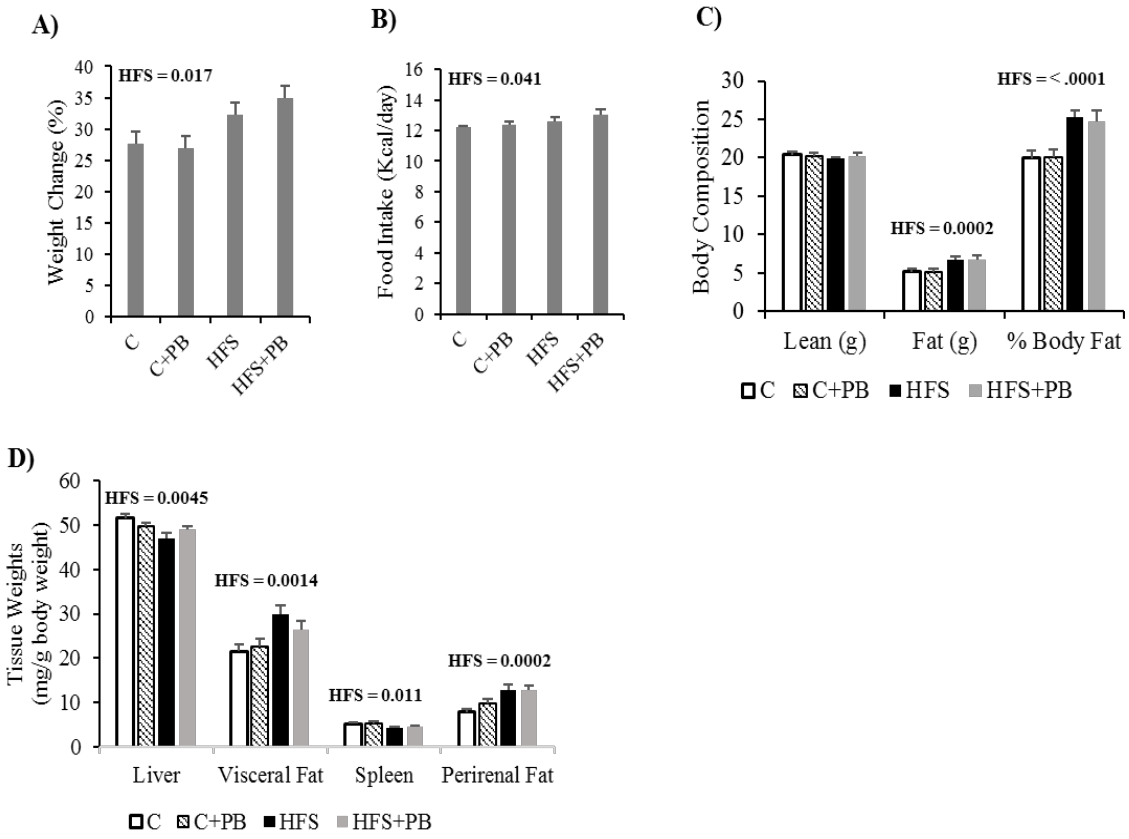
A)
Weight Change (%)
HFS = 0.017
C
C+PB
HFS
HFS+PB
B)
Food Intake (Kcal/day)
HFS = 0.041
C)
Body Composition
HFS = < .0001
HFS = 0.0002
Lean (g)
Fat (g)
% Body Fat
C C+PB HFS HFS+PB
D)
Tissue Weights (mg/g body weight)
HFS = 0.0045
HFS = 0.0014
HFS = 0.011
HFS = 0.0002
Liver
Visceral Fat
Spleen
Perirenal Fat
C C+PB HFS HFS+PB

Fig. 2

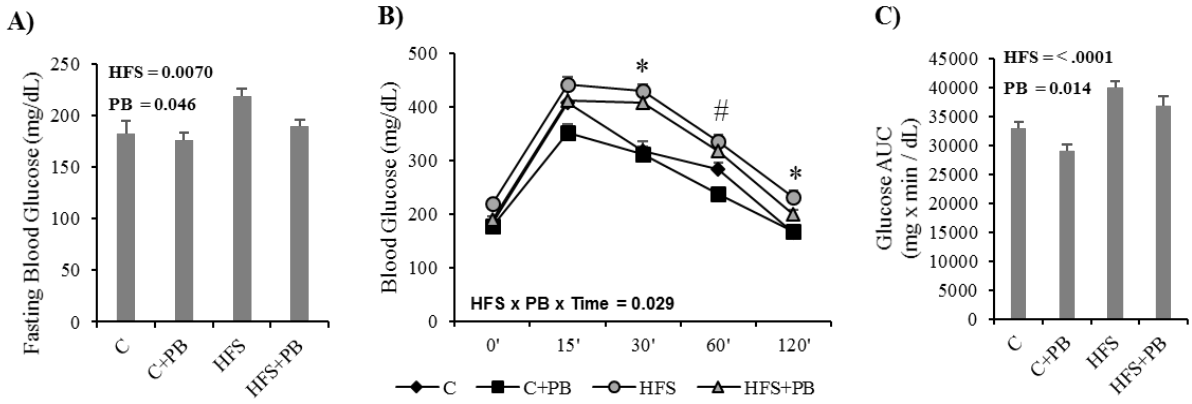
A)
Fasting Blood Glucose (mg/dL)
HFS = 0.0070
PB = 0.046
C
C+PB
HFS
HFS+PB
B)
Blood Glucose (mg/dL)
HFS x PB x Time = 0.029
0'
15'
30'
60'
120'
C
C+PB
HFS
HFS+PB
C)
Glucose AUC (mg x min / dL)
HFS = < .0001
PB = 0.014

Fig. 3

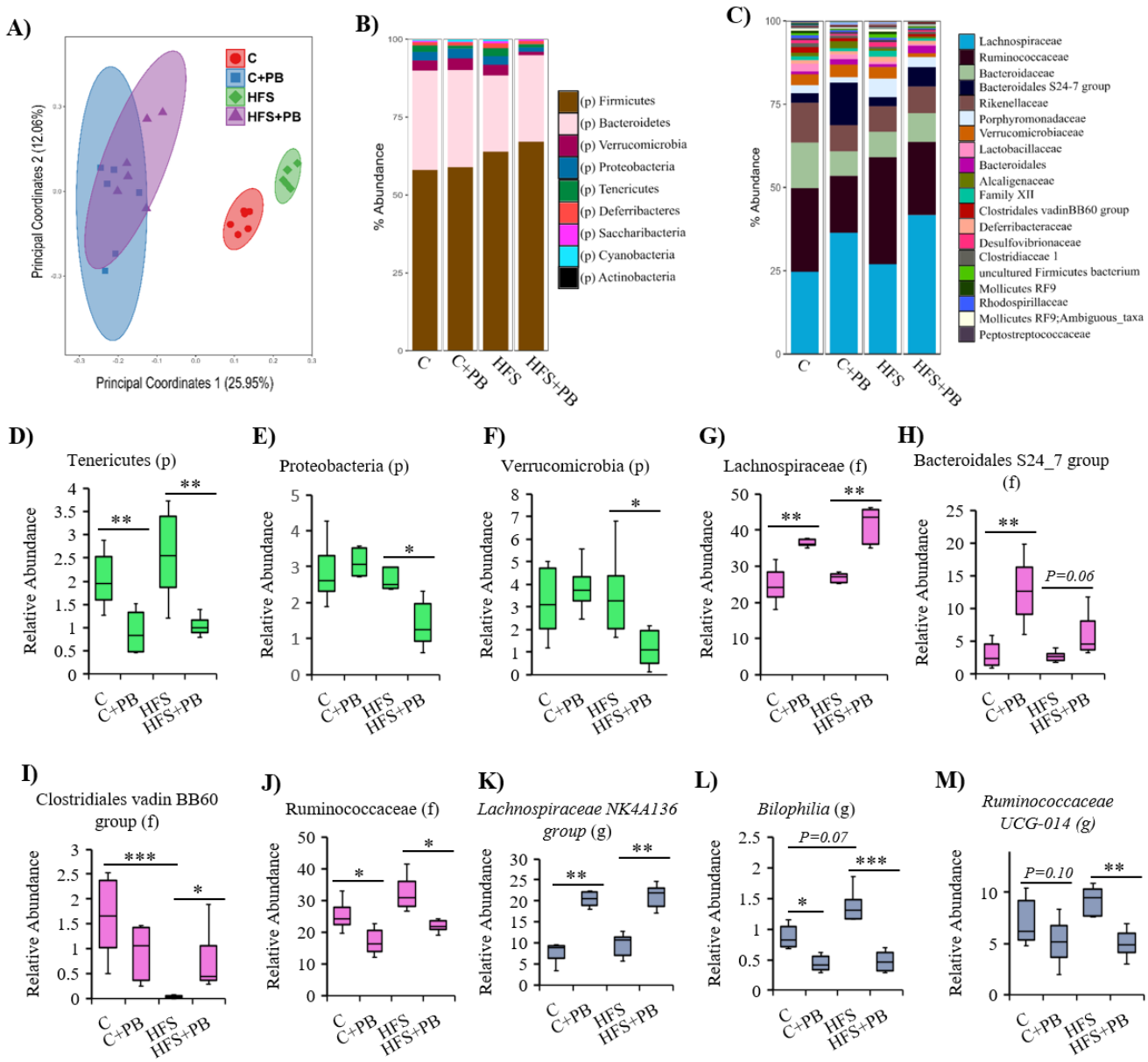
A)
C
C+PB
HFS
HFS+PB
Principal Coordinates 2 (12.06%)
Principal Coordinates 1 (25.95%)
B)
% Abundance
(p) Firmicutes
(p) Bacteroidetes
(p) Verrucomicrobia
(p) Proteobacteria
(p) Tenericutes
(p) Deferribacteres
(p) Saccharibacteria
(p) Cyanobacteria
(p) Actinobacteria
C)
% Abundance
Lachnospiraceae
Ruminococcaceae
Bacteroidaceae
Bacteroidales S24-7 group
Rikenellaceae
Porphyromonadaceae
Verrucomicrobiaceae
Lactobacillaceae
Bacteroidales
Alcaligenaceae
Family XII
Clostridiales vadinBB60 group
Deferribacteraceae
Desulfovibrionaceae
Clostridiaceae 1
uncultured Firmicutes bacterium
Mollicutes RF9
Rhodospirillaceae
Mollicutes RF9;Ambiguous_taxa
Peptostreptococcaceae
D)
Tenericutes (p)
E)
Proteobacteria (p)
F)
Verrucomicrobia (p)
G)
Lachnospiraceae (f)
H)
Bacteroidales S24_7 group (f)
P=0.06
I)
Clostridiales vadin BB60 group (f)
J)
Ruminococcaceae (f)
K)
Lachnospiraceae NK4A136 group (g)
L)
Bilophilia (g)
P=0.07
M)
Ruminococcaceae UCG-014 (g)
P=0.10
Relative Abundance
C
C+PB
HFS
HFS+PB

Fig. 4

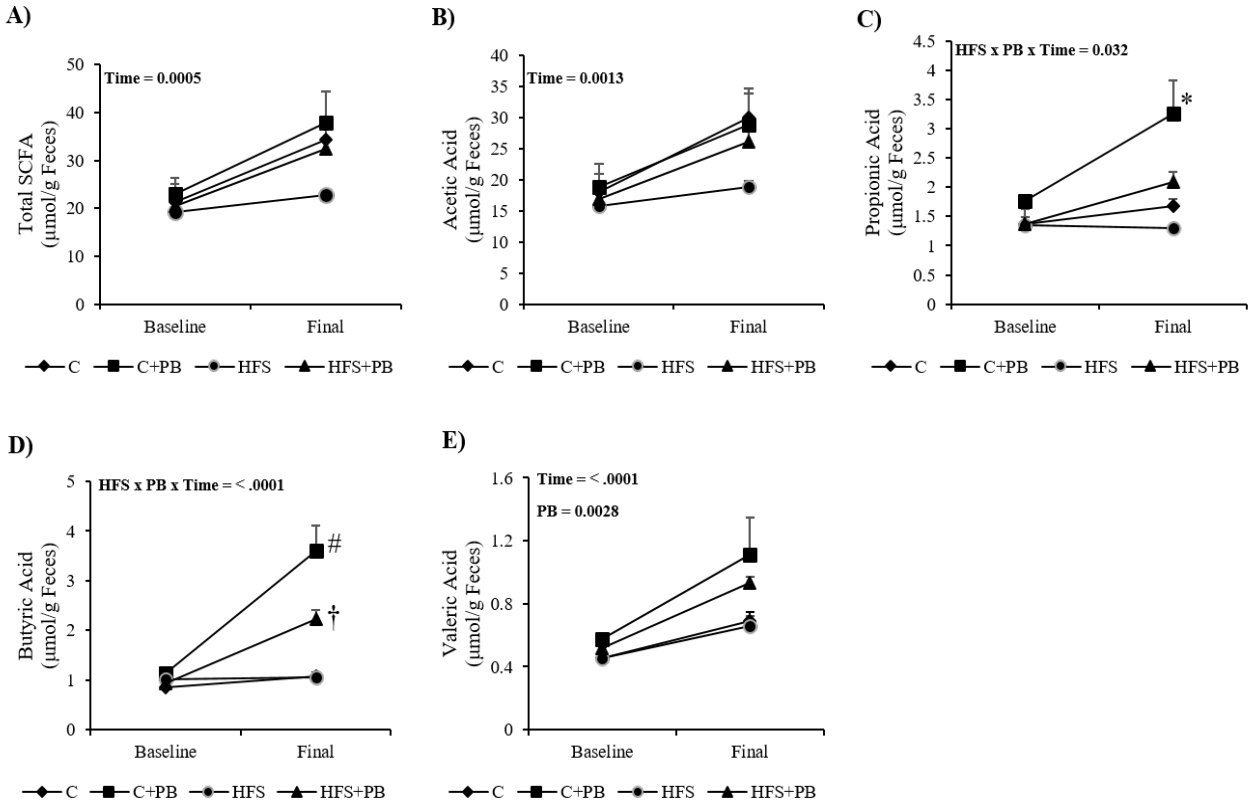
A)
Time = 0.0005
Total SCFA (µmol/g Feces)
Baseline
Final
C
C+PB
HFS
HFS+PB
B)
Time = 0.0013
Acetic Acid (µmol/g Feces)
C)
HFS x PB x Time = 0.032
Propionic Acid (µmol/g Feces)
*
D)
HFS x PB x Time = < .0001
Butyric Acid (µmol/g Feces)
#
†
E)
Time = < .0001
PB = 0.0028
Valeric Acid (µmol/g Feces)

Fig. 5

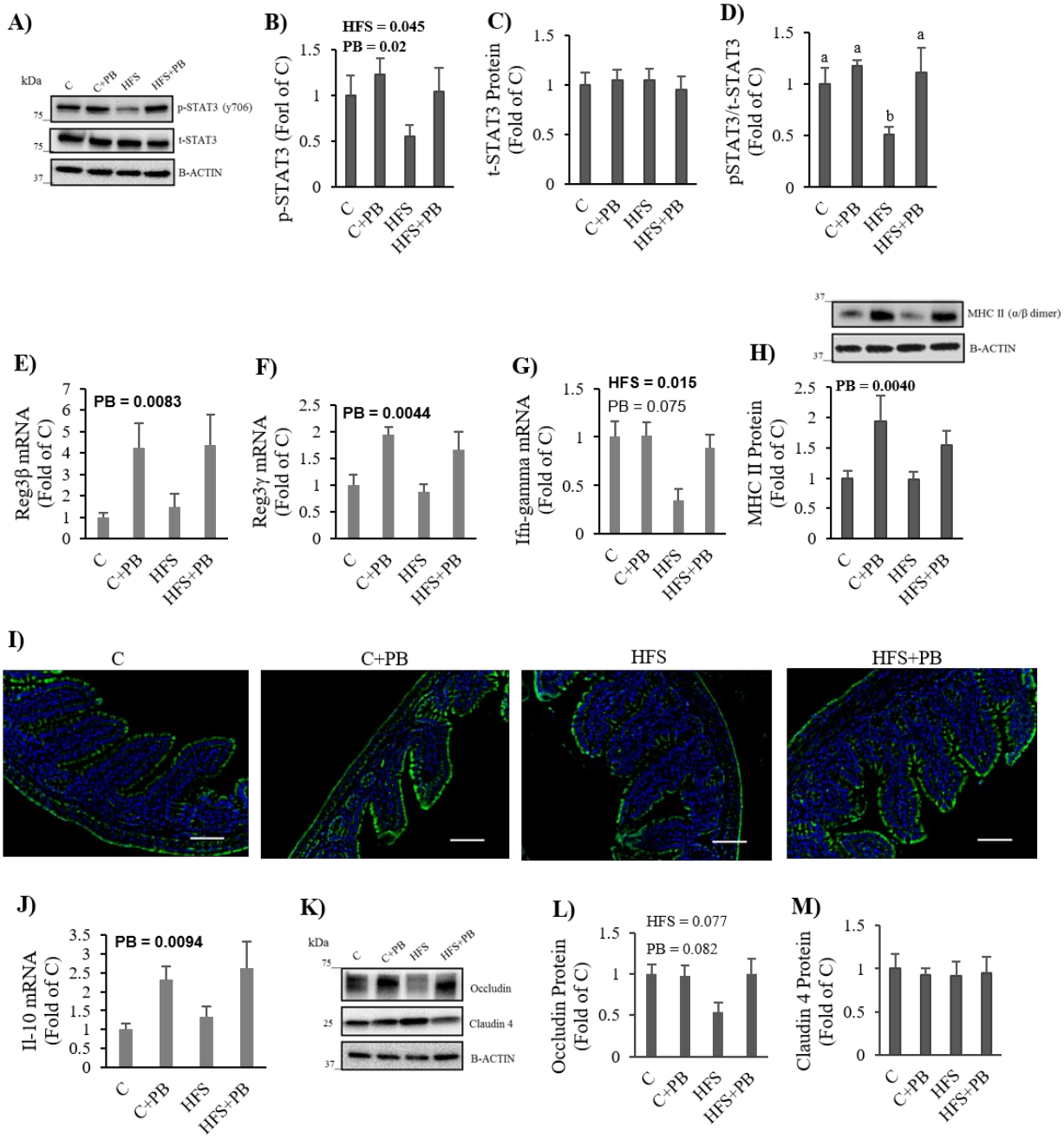
A)
kDa
C
C+PB
HFS
HFS+PB
75
p-STAT3 (y706)
75
t-STAT3
37
B-ACTIN
B)
HFS = 0.045
PB = 0.02
p-STAT3 (Forl of C)
C)
t-STAT3 Protein (Fold of C)
D)
pSTAT3/t-STAT3 (Fold of C)
a
a
b
a
E)
PB = 0.0083
Reg3β mRNA (Fold of C)
F)
PB = 0.0044
Reg3γ mRNA (Fold of C)
G)
HFS = 0.015
PB = 0.075
Ifn-gamma mRNA (Fold of C)
H)
37
MHC II (α/β dimer)
37
B-ACTIN
PB = 0.0040
MHC II Protein (Fold of C)
I)
C
C+PB
HFS
HFS+PB
J)
PB = 0.0094
Il-10 mRNA (Fold of C)
K)
kDa
75
Occludin
25
Claudin 4
37
B-ACTIN
L)
HFS = 0.077
PB = 0.082
Occludin Protein (Fold of C)
M)
Claudin 4 Protein (Fold of C)

Fig. 6

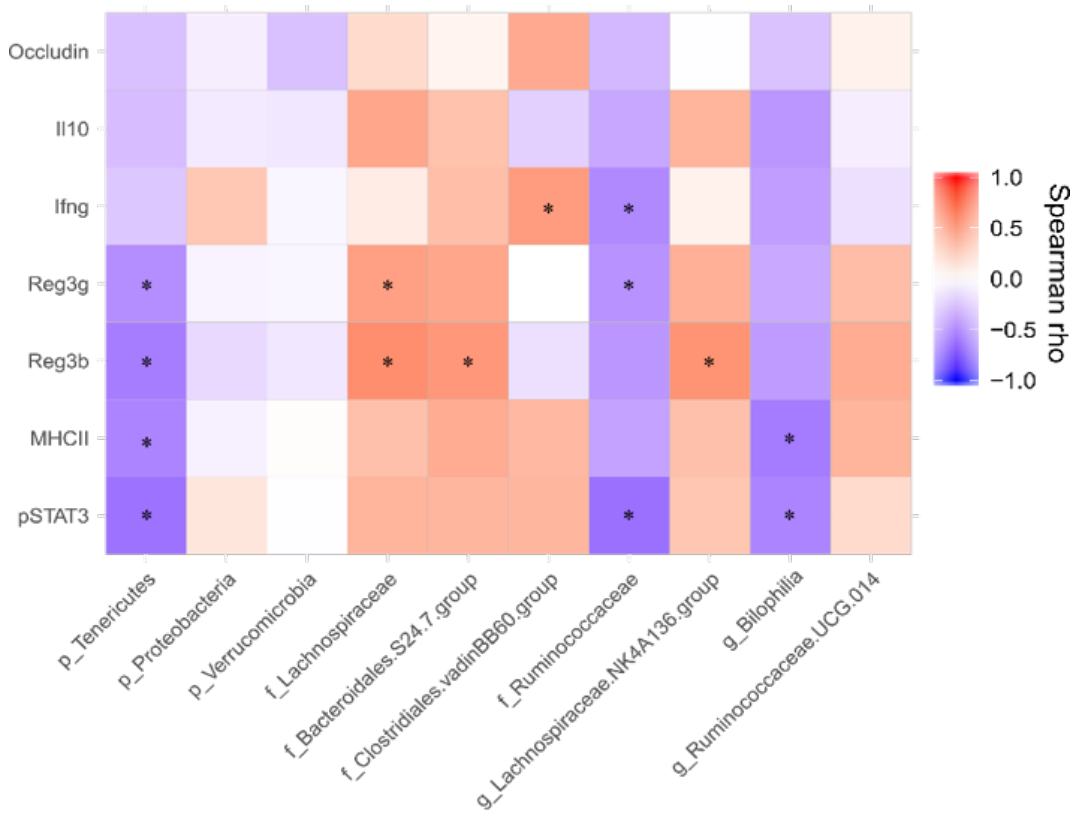
Occludin
Il10
Ifng
Reg3g
Reg3b
MHCII
pSTAT3
p_Tenericutes
p_Proteobacteria
p_Verrucomicrobia
f_Lachnospiraceae
f_Bacteroidales.S24.7.group
f_Clostridiales.vadinBB60.group
f_Ruminococcaceae
g_Lachnospiraceae.NK4A136.group
g_Bilophila
g_Ruminococcaceae.UCG.014
1.0
0.5
0.0
−0.5
−1.0
Spearman rho

Fig. 7

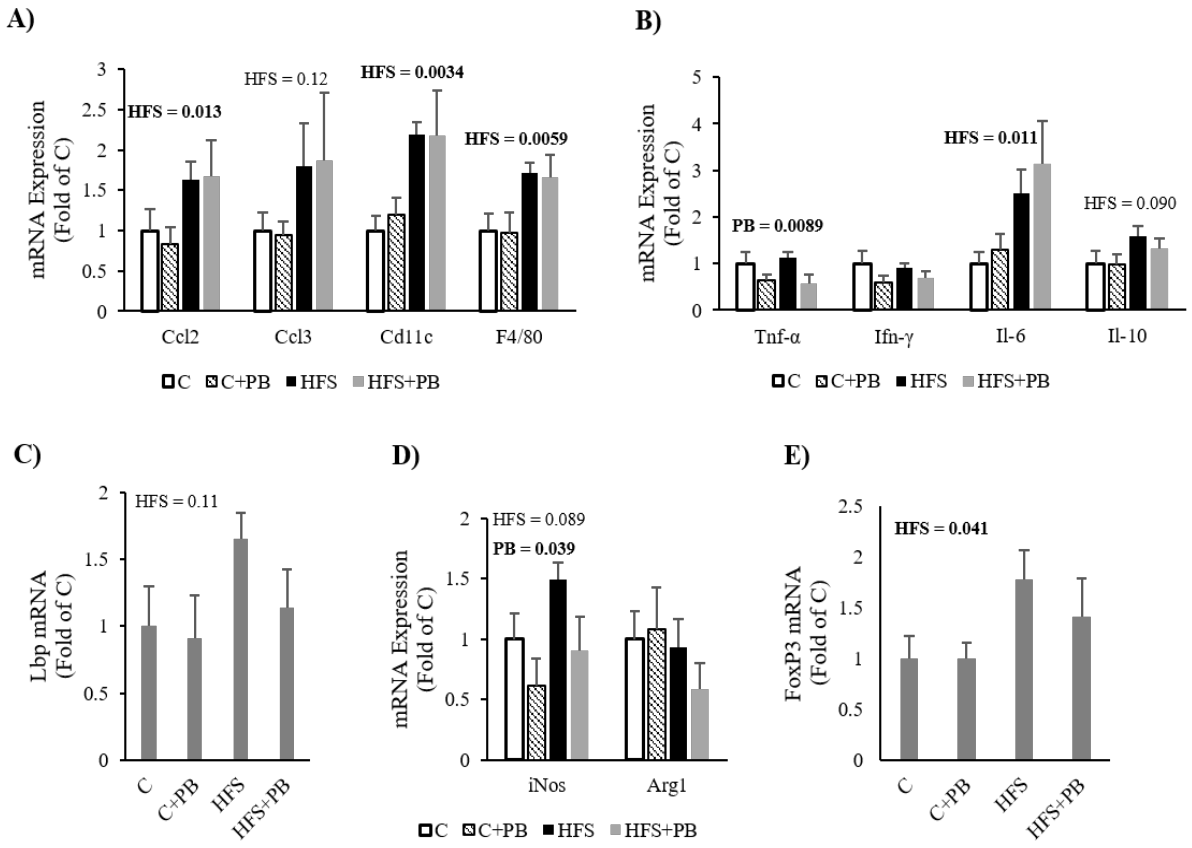
A)
mRNA Expression (Fold of C)
HFS = 0.013
HFS = 0.12
HFS = 0.0034
HFS = 0.0059
Ccl2
Ccl3
Cd11c
F4/80
C C+PB HFS HFS+PB
B)
mRNA Expression (Fold of C)
PB = 0.0089
HFS = 0.011
HFS = 0.090
Tnf-α
Ifn-γ
Il-6
Il-10
C C+PB HFS HFS+PB
C)
Lbp mRNA (Fold of C)
HFS = 0.11
C
C+PB
HFS
HFS+PB
D)
mRNA Expression (Fold of C)
HFS = 0.089
PB = 0.039
iNos
Arg1
C C+PB HFS HFS+PB
E)
FoxP3 mRNA (Fold of C)
HFS = 0.041
C
C+PB
HFS
HFS+PB

Supplementary Materials

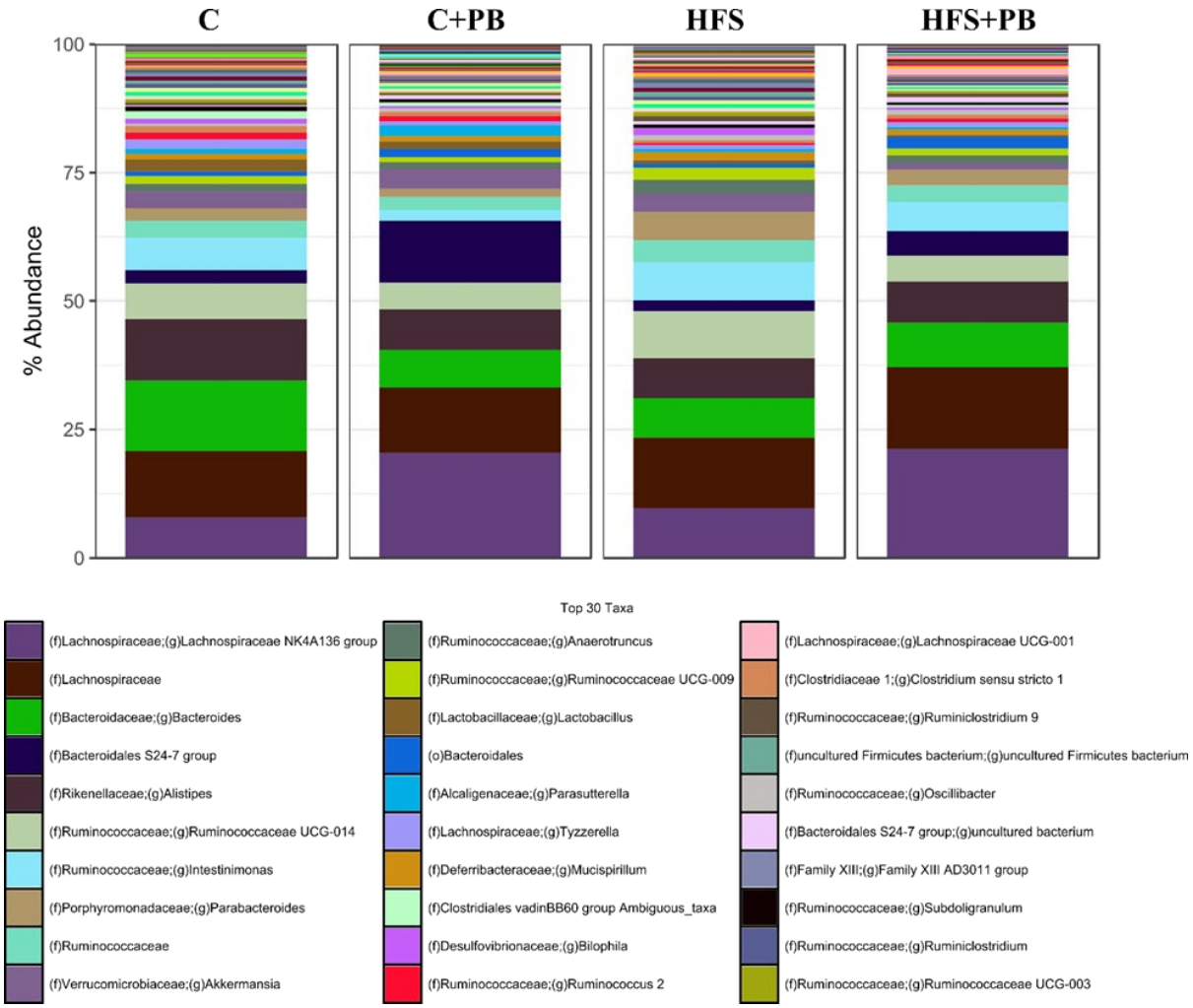

Suppl. Fig. 1: Effects of pinto beans (PB) on the abundance of cecal bacterial genera in C57BL/6J mice fed a control (C) or high fat and sucrose (HFS) diet for 30 days. n=6/group.

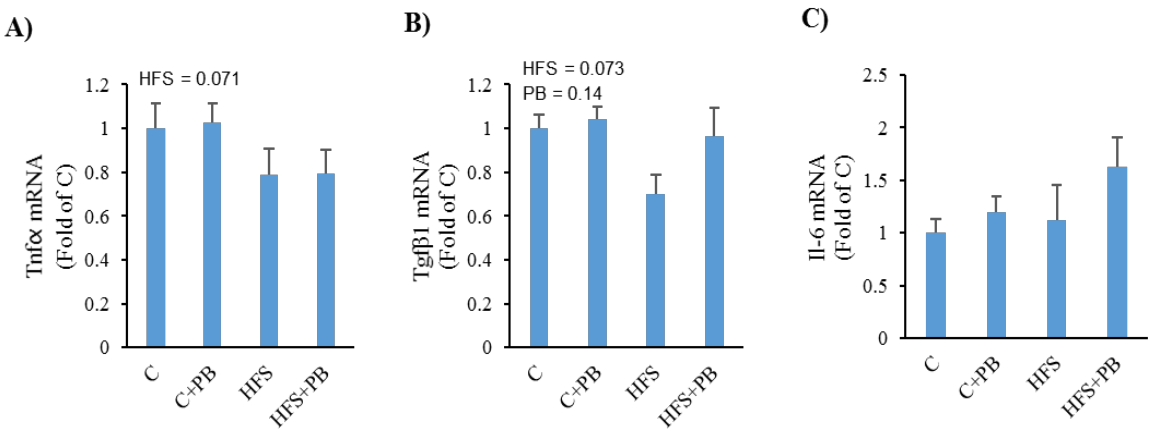

Suppl. Fig. 2: Effects of pinto beans (PB) on the mRNA expression of (A) Tnf-a, (B) Tgfb1, and (C) Il-6, in the distal ileum of C57BL/6J mice fed a control (C) or high fat and sucrose (HFS) diet for 30 days. Data are means ± SEM. n = 6 mice/group.

Tables

Suppl. Table 1: Diet Composition (g/kg)

	C	C+PB	HFS	HFS+PB
Pinto Bean (PB)[1]	--	100	--	100
Carbohydrates				
Total	629.5	629.5	400	400
Cornstarch	397.5	350.5	88.5	41.5
Sucrose	100	100	200	200
Dextrinized Cornstarch	132	132	115	115
PB[1]	--	47	--	47
Protein				
Total	200	200	245	245
Casein	200	181.2	245	226.2
PB[1]	--	18.8	--	18.8
Fat				
Total	70	70	225	225
Soybean Oil	70	67.15	30	27.15
Lard	0	0	195	195
PB[1]	--	2.85	--	2.85
Fiber				
Total	50	50	58	58
Cellulose	50	25.7	58	33.7
PB[1]	--	24.3	--	24.3
Vitamin Mix[2]	10	10	19	19
Mineral Mix[3]				
Total	35	35	43	43
Calcium Carbonate	12.5	12.24	15.35	15.09
Calcium Phosphate, dibasic	0	0	3.4	3.4
Calcium from PB[1]	--	0.103	--	0.103
Sodium Phosphate	4.38	3.41	5.39	4.41
Potassium Phosphate	1.88	1.46	2.32	1.90
Phosphorous from PB[1]	--	0.482	--	0.482
Sucrose	2.84	3.91	0.07	1.14
L-Cystine	3	3	3.5	3.5
Choline bitartrate	2.5	2.5	3	3
Tert-butylhydroquinone	0.01	0.01	0.01	0.01
Kcal/g	3.96	3.96	4.62	4.62

[1]Pinto bean composition was analyzed by NP Analytical Laboratory (St. Louis, MO, USA): carbohydrates, 47%; protein,18.8%; fat, 2.85%; total dietary fiber, 24.3% (soluble, 5.6%); calcium, 0.103%; and phosphorus, 0.482%.

[2]Harlan-Teklad Laboratories (TD 94047, WI, USA).

[3]Complete mineral mix (TD94049, Harlan-Teklad Laboratories) was used for the control diet (C) and a calcium and phosphorus deficient mineral mix (TD 98057, Harlan-Teklad Laboratories) was used for the C+PB and the HFS diets.

[2,3]Compositions of the vitamin and mineral mix has been previously published (32).

C, control; C+PB, control + 10% pinto beans; HFS, high fat and sucrose; HFS+PB, high fat and sucrose + 10% pinto beans

Supplemental Table 2: Primer Sequence for Gene Expression Analyses

Gene	Forward	Reverse
mArg1	5'-cagtctggcagttggaagca-3`	5'-gcatccacccaaatgacaca-3`
mCcl2	5'-cttcctccaccaccatgca-3`	5'-ccagccggcaactgtga-3`
mCcl3	5`-ttcatcgttgactattttgaaacca-3`	5`-gccggtttctcttagtcaggaa-3`
mCd11c	5'-cttcattctgaagggcaacct-3`	5`-cactcaggagcaacacctttttt-3`
mCyclo	5`-tgg agagca cca aga cag aca-3`	5`-tgc cgg agt cga caa tga t-3`
mF4/80	5`-tggccaagattctcttcctcac-3`	5`-gcctccactagcatccagaaga-3`
mFoxp3	5`-ggcccttctccaggacaga-3`	5`-ggcatgggcatccacagt-3`
mIfng	5`-atgaacgctacacactgcatc-3`	5`-ccatccttttgccagttcctc-3`
mIl10	5`-ggt tgc caa gcc tta tcg ga-3`	5`-acc tgc tcc act gcc ttg ct-3`
mIl6	5`-gag gat acc act ccc aac aga cc-3`	5`-aag tgc atc atc gtt gtt cat aca-3`
miNos	5'-caggaggagagagatccgattta-3`	5'-gcattagcatggaagcaaaga-3`
mLbp	5`-gtcctgggaatctgtccttg-3`	5`-ccggtaaccttgctgttgtt-3`
mReg3β	5`-tgg gaa tgg agt aac aat g-3`	5`-ggc aac ttc acc tca cat-3`
mReg3γ	5`-cca tct tca cgt agc agc-3`	5`-caa gat gtc ctg agg gc-3`
mTnfa	5`-ctgaggtcaatctgcccaagtac-3`	5`-cttcacagagcaatgactccaaag-3`

CHAPTER VII

SUMMARY, CONCLUSIONS, AND RECOMMENDATIONS

Summary

Several studies have extensively shown that high fat (HF) diets elevate intestinal permeability due to the failure to restrict the commensal bacteria and endotoxins to the gut lumen (5-7. This in-turn activates endotoxin-responsive cells in peripheral tissues such as the adipose and liver, leading to chronic inflammation and the induction of insulin resistance. One of the gut-protective mechanisms for preventing translocation is the secretion of antimicrobial peptides (AMPs). Upon translocation across the gut epithelium, antigen-presenting cells are necessary for the efficient detection and elimination of most invaders, and this process is deficient in HF feeding. Signal transducer and activator of transcription (STAT)3 is reported to be central to the stimulation of some protective effects within the small intestine, including the induction of antimicrobial peptides. Present knowledge shows that STAT3 could be activated via gut bacterial-derived metabolites from certain dietary sources, including fiber and tryptophan. Due to their nutrient variety, incorporation of beneficial whole foods in the diet may potentially improve several facets of our gut and systemic health when consuming either a normal diet or western-style diets.

Hence, the current studies were designed to understand the effect of two whole foods – wheat germ (WG) and pinto beans (PB) – on the gut bacteria and intestinal defense markers against diet-induced maladies. In addition, the studies examined

potential mechanisms of effect within the gut and the implication of these on adipose tissue inflammation. Together, results from the WG studies showed that in the animals fed a western-style diet, WG selectively increased the abundance of *Lactobacillaceae,* whose taxa are capable of metabolizing dietary tryptophan to stimulate interleukin (IL)22-STAT3 pathway in the gut. In turn, WG up-regulated IL22 gene and increased STAT3 phosphorylation in the jejunum, followed by an upregulation of the AMP genes (Reg3β and Reg3γ), which are vital for restricting commensal bacterial-derived antigens to the gut lumen. The effect of WG on AMPs is more likely via the IL22 pathway since butyrate known to also activate the STAT3 pathway was not impacted by supplemental WG. Furthermore, supplemental WG influenced several facets of the western diet-induced dysfunction in the visceral adipose tissue, including macrophage infiltration, the suppression of NFκB activation, and downregulation of IL6 and lipopolysaccharide binding protein (Lbp) mRNA expression. Accordingly, WG supplementation improved insulin resistance which may be attributed to the lesser burden of inflammation in the WG-fed group.

Interestingly, our PB results showed similar pattern on STAT3 and AMPs in the gut. After a short-term feeding of an HFS diet (4 weeks), STAT3 phosphorylation was suppressed by high fat and sucrose (HFS) diet feeding in the ileum while PB significantly prevented this effect. Consequently, the mRNA expression of Reg3β and Reg3γ were elevated in the PB-fed groups. However, this effect of PB on STAT3 is likely due to butyrate, since PB raised fecal butyrate levels while the IL22 gene was sparsely detected. In addition, PB increased the expression of MHC II protein in the ileum which suggests a gut-protective ability by inducing a robust environment in the ileum capable of efficient

antigen presentation for possible elimination. In agreement with its effect on butyrate, PB increased the abundance of taxa belonging to the SCFA-producing family, *Lachnospiraceae*. These early protective effects of PB in the gut were reflected in the adipose tissue, as PB downregulated iNos gene – a marker of classically activated macrophages. Moreover, PB improved fasting blood glucose and glucose tolerance in the HFS-fed animals. Based on these results, both WG and PB are whole foods with a prebiotic potential capable of mitigating the detrimental outcomes of HFS-feeding in the gut and on adipose inflammation.

Conclusions

Purpose

By using animal models of diet-induced obesity, the purpose of this project is to determine the gut-protective mechanisms of WG and PB when added to a western-style diet and the implication on glucose tolerance and the induction of proinflammatory cytokines in the adipose tissue.

Specific Aim 1: To investigate the gut modulatory potential of WG on the gut microbiome, lamina propria lymphocytes, jejunal antimicrobial peptide expression and adipose tissue inflammation in C57BL6J mice fed a high fat, high sucrose (HFS) diet for 12 weeks

Working Hypothesis 1: WG will prevent aspects of HFS-induced gut dysbiosis and induce AMP genes in the gut, indicating an enhanced capacity to mitigate HF-induced leaky gut. This effect of WG on the gut would be associated with reduced insulin resistance, immune cell infiltration and proinflammatory cytokines in the visceral adipose tissue (VAT).

Based on the results, I reject the null hypothesis (of no effect) and accept the hypothesis stated above.

The Bray-Curtis metrics of β-diversity showed a significant impact of WG on the gut microbiota. Subsequently, supplemental WG in the HFS diet raised the abundance of the beneficial bacteria family, *Lactobacillaceae*, by 4-folds compared to the group fed HFS only. However, WG did not increase fecal SCFAs in the HFS group. WG showed a trend to increase the Treg:Th17 ratio in the small intestine ($P = 0.12$), indicating a potential to induce an anti-inflammatory gut environment.

The pore-forming CLAUDIN 2 protein, associated with a leaky gut, was elevated in the jejunum of HFS-fed mice while WG had no effect. Supplemental WG upregulated Il22 genes in the jejunum by at least 116% ($P \leq 0.035$). The HFS+WG group had a 15-fold increase ($P = 0.0012$) in pSTAT3 compared to the HFS group in the jejunum. Consequently, the mRNA expression of AMPs (Reg3β and Reg3γ) were significantly upregulated in the jejunum by WG supplementation ($P \leq 0.043$) indicating an increased potential to mitigate translocation in a leaky gut environment.

In the VAT, the HFS group had greater NFκBp65 phosphorylation compared to C, while HFS+WG group suppressed this to the level of C ($P = 0.014$). In addition, VAT

Il6 and Lbp genes were downregulated in the HFS+WG group compared to HFS ($P \leq 0.0032$). Macrophage infiltration into the VAT was suppressed, as macrophage-related genes, F4/80, Cd11c, and iNos, were repressed ($P \leq 0.048$) in the WG-supplemented mice.

WG reduced serum concentrations of the pro-inflammatory cytokines, interleukin (IL)-1B, IL-6, interferon-γ, and tumor necrosis factor-α, indicating an improvement in systemic inflammation by supplemental WG. Consequently, supplemental WG significantly improved hyperglycemia, fasting insulin, and HOMA-IR ($P \leq 0.034$) in HFS-fed mice – an effect that was consistent across two studies using differing fat contents (chapters III and V).

In conclusion, this study showed that in C57BL/6J mice fed a HFS diet for 90 days, WG upregulates the Il22 gene, activates the STAT3 pathway, and upregulates antimicrobial peptide genes (Reg3β and Reg3γ) in the jejunum. Accordingly, WG attenuated HFS-induced upregulation of Il6 and Lbp genes, and lessened NFκBp65 phosphorylation in the visceral adipose tissue to the level of C. In addition, supplemental WG improved metabolic parameters in HFS-fed animals, including fasting blood glucose and insulin resistance marker (HOMA-IR). Taken together, the modulatory effects of WG on STAT3 and AMPs in the gut may be vital to reduce the burden of antigen translocation that could initiate adipose tissue inflammation and contribute to diet-induced insulin resistance.

Specific Aim 2: To determine the early protective effects of PB supplementation on the cecal microbiome, antigen presentation marker (MHC II), and antimicrobial

peptide expression, and adipose tissue inflammation in C57BL6J mice fed a high fat, high sucrose (HFS) diet for 30days

Working Hypothesis 2: At the early onset of HFS-induced glucose intolerance, PB will beneficially modulate the gut bacteria, increase SCFAs, upregulate MHC II protein in the gut, and enhance Reg3 transcription. These PB effects in the gut of HFS-fed mice may explain its ability to prevent of glucose intolerance and reduced proinflammatory milieu in the visceral adipose tissue.

Based on the results, I accept the hypothesis that PB will beneficially modulate the gut bacteria, increase SCFAs, upregulate MHC II protein in the gut, and enhance Reg3 transcription. However, I reject the hypothesis that PB's effects in the gut of HFS-fed mice may explain its ability to prevent of glucose intolerance, since the results from the glucose tolerance test was not statistically different between the HFS and HFS+PB groups. Nevertheless, PB showed main effects on fasting blood glucose and the glucose area under the curve that only shows a potential of PB to improve impaired glucose tolerance.

Both HFS and PB impacted the β-diversity of the cecal microbiome. Further analysis of specific taxonomic abundance showed that mice fed a HFS diet had a modest elevation ($P = 0.07$) in the sulphate reducing bacteria (SRB)- *Bilophilia* (f_*Desulfovibrionaceae*) compared to the C group. On the other hand, PB supplementation in both C and HFS diets significantly lowered the abundance of this SRB-genus. PB supplementation in both C and HFS groups elevated the abundance of

taxa within the SCFA-producing bacteria family, *Lachnospiraceae*, in the PB supplemented groups compared to the respective controls by at least 48% ($P \leq 0.01$). Among the assayed SCFAs, butyrate was significantly higher in the PB supplemented groups by at least 50% compared to C and HFS groups ($P \leq 0.001$).

In the distal ileum, total MHC II protein was higher in the PB-supplemented groups compared to C and HFS groups. Further, STAT3 phosphorylation was suppressed in the HFS group while PB supplementation prevented this effect. The antimicrobial peptide genes, Reg3β and Reg3γ, were significantly upregulated in the PB supplemented groups compared to C and HFS groups, suggesting an increased capacity to restrict commensal bacterial to the lumen.

In the VAT, chemokine and macrophage markers were elevated in the HFS groups and PB had no effect. However, supplemental PB significantly reduced iNos gene expression, which is a marker of classically activated (M1) proinflammatory macrophages. However, supplemental PB improved fasting blood glucose and the estimated glucose area under the curve.

In conclusion, PB supplementation induced favorable shifts in the gut that may be central to its potential to improve impaired glucose tolerance and adipose tissue inflammation in diet-induced obesity.

Recommendations for Future Research

A significant limitation of these studies, just as for any whole food study, is the inability to solely attribute the robust effect of WG or PB effects to a single bioactive component (i.e., fiber or tryptophan) since other components may also possess gut-

modulatory potential and through yet uncharacterized mechanisms. Recent understanding show that gut bacterial-derived fiber and tryptophan metabolites can both activate the STAT3 pathway via butyrate and IL22 respectively, and induce antimicrobial peptide expression that aids in restriction of gut bacteria to the mucosa. Analysis of WG and PB in this study and data from the USDA food central database (https://fdc.nal.usda.gov/) show that WG has about 310 mg/100 g tryptophan and 4% fiber, while PB has 98 mg/100g tryptophan and 24% total dietary fiber. Hence, based on the results in this study and current evidence in the literature, it is more likely that WG modulated IL22-STAT3 pathway in the gut due to its rich tryptophan content, while PB modulated the same pathway via butyrate.

Undoubtedly, these studies advance our knowledge of how whole foods, such as WG and PB, may modulate the gut and peripheral inflammation for the improvement of glucose tolerance in obesity. Based on emerging evidence, future projects designed to study the effects of whole foods in the gut may find it important to consider the tryptophan content as much as the fiber content for hypothesis development. While measuring cecal or fecal SCFAs from fiber fermentation is vital, creating an opportunity to evaluate bacterial-derived indole metabolites of tryptophan may further clarify the impact of dietary tryptophan in gut and systemic health. In addition, sensitive measures of intestinal permeability such as the FITC-dextran assay or the use of Ussing chamber may be used in place of the sole measure of intestinal tight junction proteins.

Moreover, since WG and PB prevented the HFS-induced decrease in STAT3 phosphorylation, the direct effect of STAT3 on the outcomes in the gut and adipose may be further investigated using intestinal epithelial cell specific STAT knockout mouse

(STAT3^{IEC-KO}). In conjunction with the measurement of tryptophan metabolites, a future supplemental WG study, or that of any tryptophan-rich food, may take advantage of an IL-22^{KO} mice to determine if the impact of IL22 is needed for STAT3 activation and subsequent benefits observed in studies presented here. An alternative to the IL-22^{KO} mice may be the use of IL-22 receptor antagonists. Importantly, an interesting approach for a future study would be the use gnotobiotic models or broad-spectrum antibiotics to discern if the gut microbiota is required for these beneficial effects of WG or PB observed in the gut and the adipose tissue. Lastly, it may be beneficial to investigate the time-based crosstalk between adipocytes, adipose macrophages, and adipose T-cells to discern the sequence of response to gut-derived signals as it relates to the induction of iNos, Lbp, and NFkB phosphorylation.

Regardless of identified gaps, these studies suggest that the restoration of STAT3 activation in the small intestine is central to the gut-protective abilities of WG and PB albeit through separate mechanisms. Furthermore, they provide valuable foundational insights that should be considered for future studies that aim to identify the benefits of whole foods on gut and peripheral tissues using western diet-induced models of obesity.

REFERENCES

1. Zobel EH, Hansen TW, Rossing P, von Scholten BJJCor. Global changes in food supply and the obesity epidemic. 2016;5:449-55.
2. Ng M, Fleming T, Robinson M, Thomson B, Graetz N, Margono C, Mullany EC, Biryukov S, Abbafati C, Abera SFJTl. Global, regional, and national prevalence of overweight and obesity in children and adults during 1980–2013: a systematic analysis for the Global Burden of Disease Study 2013. 2014;384:766-81.
3. Monteiro R, Azevedo IJMoi. Chronic inflammation in obesity and the metabolic syndrome. 2010;2010.
4. Olefsky JM, Glass CKJArop. Macrophages, inflammation, and insulin resistance. 2010;72:219-46.
5. Cani PD, Amar J, Iglesias MA, Poggi M, Knauf C, Bastelica D, Neyrinck AM, Fava F, Tuohy KM, Chabo CJD. Metabolic endotoxemia initiates obesity and insulin resistance. 2007;56:1761-72.
6. Garidou L, Pomié C, Klopp P, Waget A, Charpentier J, Aloulou M, Giry A, Serino M, Stenman L, Lahtinen SJCm. The gut microbiota regulates intestinal CD4 T cells expressing RORγt and controls metabolic disease. 2015;22:100-12.
7. Cani PD, Bibiloni R, Knauf C, Waget A, Neyrinck AM, Delzenne NM, Burcelin RJD. Changes in gut microbiota control metabolic endotoxemia-induced inflammation in high-fat diet–induced obesity and diabetes in mice. 2008;57:1470-81.
8. Littman DR, Rudensky AYJC. Th17 and regulatory T cells in mediating and restraining inflammation. 2010;140:845-58.
9. Louis P, Hold GL, Flint HJJNrm. The gut microbiota, bacterial metabolites and colorectal cancer. 2014;12:661-72.
10. Ayabe T, Ashida T, Kohgo Y, Kono TJTim. The role of Paneth cells and their antimicrobial peptides in innate host defense. 2004;12:394-8.
11. Hou Q, Ye L, Liu H, Huang L, Yang Q, Turner J, Yu QJCD, Differentiation. Lactobacillus accelerates ISCs regeneration to protect the integrity of intestinal mucosa through activation of STAT3 signaling pathway induced by LPLs secretion of IL-22. 2018;25:1657.
12. Zhao Y, Chen F, Wu W, Sun M, Bilotta AJ, Yao S, Xiao Y, Huang X, Eaves-Pyles TD, Golovko GJMi. GPR43 mediates microbiota metabolite SCFA regulation of antimicrobial peptide expression in intestinal epithelial cells via activation of mTOR and STAT3. 2018;11:752.
13. Wang L, Fouts DE, Stärkel P, Hartmann P, Chen P, Llorente C, DePew J, Moncera K, Ho SB, et al. Intestinal REG3 lectins protect against alcoholic steatohepatitis by

reducing mucosa-associated microbiota and preventing bacterial translocation. 2016;19:227-39.
14. Pomié C, Blasco-Baque V, Klopp P, Nicolas S, Waget A, Loubières P, Azalbert V, Puel A, Lopez F, Dray CJMm. Triggering the adaptive immune system with commensal gut bacteria protects against insulin resistance and dysglycemia. 2016;5:392-403.
15. Takahashi S, Fukuda M, Mitani A, Fujimura T, Iwamura Y, Sato S, Kubo T, Sugita Y, Maeda H, Shinomura TJJopr. Follicular dendritic cell-secreted protein is decreased in experimental periodontitis concurrently with the increase of interleukin-17 expression and the Rankl/O pg mRNA ratio. 2014;49:390-7.
16. Barengolts EJEP. Vitamin D and prebiotics may benefit the intestinal microbacteria and improve glucose homeostasis in prediabetes and type 2 diabetes. 2013;19:497-510.
17. Dehghan P, Gargari BP, Jafar-Abadi MAJN. Oligofructose-enriched inulin improves some inflammatory markers and metabolic endotoxemia in women with type 2 diabetes mellitus: a randomized controlled clinical trial. 2014;30:418-23.
18. Monsan P, Valet P, Remaud-Simeon M, Saulnier-Blache J-S, Burcelin R. Use of prebiotics, preferably glucooligosaccharide, for the prevention of the onset of type II diabetes. Google Patents; 2009.
19. Fuentes-Zaragoza E, Riquelme-Navarrete M, Sánchez-Zapata E, Pérez-Álvarez JJFRI. Resistant starch as functional ingredient: A review. 2010;43:931-42.
20. Carvalho-Wells AL, Helmolz K, Nodet C, Molzer C, Leonard C, McKevith B, Thielecke F, Jackson KG, Tuohy KMJBjon. Determination of the in vivo prebiotic potential of a maize-based whole grain breakfast cereal: a human feeding study. 2010;104:1353-6.
21. Costabile A, Klinder A, Fava F, Napolitano A, Fogliano V, Leonard C, Gibson GR, Tuohy KMJBjon. Whole-grain wheat breakfast cereal has a prebiotic effect on the human gut microbiota: a double-blind, placebo-controlled, crossover study. 2008;99:110-20.
22. Mitsou E, Kougia E, Nomikos T, Yannakoulia M, Mountzouris K, Kyriacou AJA. Effect of banana consumption on faecal microbiota: a randomised, controlled trial. 2011;17:384-7.
23. Ojo B, El-Rassi GD, Payton ME, Perkins-Veazie P, Clarke S, Smith BJ, Lucas EAJTJon. Mango supplementation modulates gut microbial dysbiosis and short-chain fatty acid production independent of body weight reduction in C57BL/6 mice fed a high-fat diet. 2016;146:1483-91.
24. Brandolini A, Hidalgo AJIjofs, nutrition. Wheat germ: not only a by-product. 2012;63:71-4.
25. Matej Brestenský SN, Peter Patráš. Wheat Germs and their Protein Quality for Human Nutrition. Nutri Food Sci Int J. 2019;8:555746.
26. Roager HM, Licht TR. Microbial tryptophan catabolites in health and disease. Nature Communications. 2018;9.
27. Boros LG, Nichelatti M, Shoenfeld YJAotNYAoS. Fermented wheat germ extract (Avemar) in the treatment of cancer and autoimmune diseases. 2005;1051:529-42.
28. MOHAMED DA, ISMAEL AI, IBRAHIM ARJDL-R. Studying the anti-inflammatory and biochemical effects of wheat germ oil. 2005;101:66-72.

29. Alessandri C, Pignatelli P, Loffredo L, Lenti L, Del Ben M, Carnevale R, Perrone A, Ferro D, Angelico F, et al. Alpha-linolenic acid-rich wheat germ oil decreases oxidative stress and CD40 ligand in patients with mild hypercholesterolemia. 2006;26:2577.
30. Haripriya S, Premakumari SJJoLS. Beta sistosterol of wheat germ reduces blood glucose in humans. 2010;2:87-92.
31. Mitchell DC, Lawrence FR, Hartman TJ, Curran JMJJotAda. Consumption of dry beans, peas, and lentils could improve diet quality in the US population. 2009;109:909-13.
32. Messina VJTAjocn. Nutritional and health benefits of dried beans. 2014;100:437S-42S.
33. United States Department of Agriculture ARS, Nutrient Data Laboratory. USDA National nutrient database for standard reference, release 28. 2016.
34. Câmara CR, Urrea CA, Schlegel VJA. Pinto beans (Phaseolus vulgaris L.) as a functional food: Implications on human health. 2013;3:90-111.
35. Finley JW, Burrell JB, Reeves PGJTJon. Pinto bean consumption changes SCFA profiles in fecal fermentations, bacterial populations of the lower bowel, and lipid profiles in blood of humans. 2007;137:2391-8.
36. Stevens GA, Singh GM, Lu Y, Danaei G, Lin JK, Finucane MM, Bahalim AN, McIntire RK, Gutierrez HR, Cowan MJPhm. National, regional, and global trends in adult overweight and obesity prevalences. 2012;10:22.
37. Popkin BM, Adair LS, Ng SWJNr. Global nutrition transition and the pandemic of obesity in developing countries. 2012;70:3-21.
38. Lim SS, Vos T, Flaxman AD, Danaei G, Shibuya K, Adair-Rohani H, AlMazroa MA, Amann M, Anderson HR, Andrews KGJTl. A comparative risk assessment of burden of disease and injury attributable to 67 risk factors and risk factor clusters in 21 regions, 1990–2010: a systematic analysis for the Global Burden of Disease Study 2010. 2012;380:2224-60.
39. Lancet ERFCJT. Separate and combined associations of body-mass index and abdominal adiposity with cardiovascular disease: collaborative analysis of 58 prospective studies. 2011;377:1085-95.
40. Renehan AG, Tyson M, Egger M, Heller RF, Zwahlen MJTL. Body-mass index and incidence of cancer: a systematic review and meta-analysis of prospective observational studies. 2008;371:569-78.
41. Astrup A, Brand-Miller JJTL. Diet composition and obesity. 2012;379:1100.
42. Church TS, Thomas DM, Tudor-Locke C, Katzmarzyk PT, Earnest CP, Rodarte RQ, Martin CK, Blair SN, Bouchard CJPo. Trends over 5 decades in US occupation-related physical activity and their associations with obesity. 2011;6:e19657.
43. Swinburn B, Sacks G, Ravussin EJTAjocn. Increased food energy supply is more than sufficient to explain the US epidemic of obesity. 2009;90:1453-6.
44. Turnbaugh PJ, Ley RE, Mahowald MA, Magrini V, Mardis ER, Gordon JIJn. An obesity-associated gut microbiome with increased capacity for energy harvest. 2006;444:1027.
45. Scheen AJJACB. From obesity to diabetes: why, when and who? 2000;55:9-15.

46. Wild S, Roglic G, Green A, Sicree R, King HJDc. Global prevalence of diabetes: estimates for the year 2000 and projections for 2030. 2004;27:1047-53.
47. Kahn SE, Hull RL, Utzschneider KMJN. Mechanisms linking obesity to insulin resistance and type 2 diabetes. 2006;444:840.
48. Kahn SEJTJoCE, Metabolism. The importance of β-cell failure in the development and progression of type 2 diabetes. 2001;86:4047-58.
49. Scherer PEJD. Adipose tissue: from lipid storage compartment to endocrine organ. 2006;55:1537-45.
50. Shoelson SE, Lee J, Goldfine ABJTJoci. Inflammation and insulin resistance. 2006;116:1793-801.
51. Boden GJD. Role of fatty acids in the pathogenesis of insulin resistance and NIDDM. 1997;46:3-10.
52. Roden M, Price TB, Perseghin G, Petersen KF, Rothman DL, Cline GW, Shulman GIJTJoci. Mechanism of free fatty acid-induced insulin resistance in humans. 1996;97:2859-65.
53. Santomauro A, Boden G, Silva M, Rocha DM, Santos RF, Ursich M, Strassmann PG, Wajchenberg BLJD. Overnight lowering of free fatty acids with Acipimox improves insulin resistance and glucose tolerance in obese diabetic and nondiabetic subjects. 1999;48:1836-41.
54. Randle P, Garland P, Hales C, Newsholme EJTL. The glucose fatty-acid cycle its role in insulin sensitivity and the metabolic disturbances of diabetes mellitus. 1963;281:785-9.
55. Bastard J-P, Jardel C, Bruckert E, Blondy P, Capeau J, Laville M, Vidal H, Hainque BJTJoCE, Metabolism. Elevated levels of interleukin 6 are reduced in serum and subcutaneous adipose tissue of obese women after weight loss. 2000;85:3338-42.
56. Hotamisligil GS, Murray DL, Choy LN, Spiegelman BMJPotNAoS. Tumor necrosis factor alpha inhibits signaling from the insulin receptor. 1994;91:4854-8.
57. Lang CH, Dobrescu C, Bagby GJJE. Tumor necrosis factor impairs insulin action on peripheral glucose disposal and hepatic glucose output. 1992;130:43-52.
58. FEINGOLD KR, Serio MK, ADI S, MOSER AH, GRUNFELD CJE. Tumor necrosis factor stimulates hepatic lipid synthesis and secretion. 1989;124:2336-42.
59. Saghizadeh M, Ong JM, Garvey WT, Henry RR, Kern PAJTJoci. The expression of TNF alpha by human muscle. Relationship to insulin resistance. 1996;97:1111-6.
60. Del Aguila LF, Krishnan RK, Ulbrecht JS, Farrell PA, Correll PH, Lang CH, Zierath JR, Kirwan JPJAJoP-E, Metabolism. Muscle damage impairs insulin stimulation of IRS-1, PI 3-kinase, and Akt-kinase in human skeletal muscle. 2000;279:E206-E12.
61. Corbett JA, Sweetland MA, Wang JL, Lancaster JR, McDaniel MLJPotNAoS. Nitric oxide mediates cytokine-induced inhibition of insulin secretion by human islets of Langerhans. 1993;90:1731-5.
62. Corbett JA, McDaniel MLJJoEM. Intraislet release of interleukin 1 inhibits beta cell function by inducing beta cell expression of inducible nitric oxide synthase. 1995;181:559-68.
63. Dunger A, Cunningham JM, Delaney CA, Lowe JE, Green MH, Bone AJ, Green ICJD. Tumor necrosis factor-α and interferon-γ inhibit insulin secretion and cause

DNA damage in unweaned-rat islets: extent of nitric oxide involvement. 1996;45:183-9.
64. Schroeder BO, Bäckhed FJNm. Signals from the gut microbiota to distant organs in physiology and disease. 2016;22:1079.
65. Huttenhower C, Gevers D, Knight R, Abubucker S, Badger JH, Chinwalla AT, Creasy HH, Earl AM, FitzGerald MG, Fulton RSJn. Structure, function and diversity of the healthy human microbiome. 2012;486:207.
66. Li J, Jia H, Cai X, Zhong H, Feng Q, Sunagawa S, Arumugam M, Kultima JR, Prifti E, Nielsen TJNb. An integrated catalog of reference genes in the human gut microbiome. 2014;32:834.
67. Qin J, Li R, Raes J, Arumugam M, Burgdorf KS, Manichanh C, Nielsen T, Pons N, Levenez F, Yamada TJn. A human gut microbial gene catalogue established by metagenomic sequencing. 2010;464:59.
68. Tamburini S, Shen N, Wu HC, Clemente JCJNm. The microbiome in early life: implications for health outcomes. 2016;22:713.
69. Goodrich JK, Waters JL, Poole AC, Sutter JL, Koren O, Blekhman R, Beaumont M, Van Treuren W, Knight R, Bell JTJC. Human genetics shape the gut microbiome. 2014;159:789-99.
70. Neu J, Rushing JJCip. Cesarean versus vaginal delivery: long-term infant outcomes and the hygiene hypothesis. 2011;38:321-31.
71. Biasucci G, Benenati B, Morelli L, Bessi E, Boehm GnJTJon. Cesarean delivery may affect the early biodiversity of intestinal bacteria. 2008;138:1796S-800S.
72. Duncan SH, Belenguer A, Holtrop G, Johnstone AM, Flint HJ, Lobley GEJAEM. Reduced dietary intake of carbohydrates by obese subjects results in decreased concentrations of butyrate and butyrate-producing bacteria in feces. 2007;73:1073-8.
73. Ley RE, Turnbaugh PJ, Klein S, Gordon JIJn. Microbial ecology: human gut microbes associated with obesity. 2006;444:1022.
74. Dethlefsen L, Huse S, Sogin ML, Relman DAJPb. The pervasive effects of an antibiotic on the human gut microbiota, as revealed by deep 16S rRNA sequencing. 2008;6:e280.
75. Dethlefsen L, Relman DAJPotNAoS. Incomplete recovery and individualized responses of the human distal gut microbiota to repeated antibiotic perturbation. 2011;108:4554-61.
76. David LA, Materna AC, Friedman J, Campos-Baptista MI, Blackburn MC, Perrotta A, Erdman SE, Alm EJJGb. Host lifestyle affects human microbiota on daily timescales. 2014;15:R89.
77. David LA, Maurice CF, Carmody RN, Gootenberg DB, Button JE, Wolfe BE, Ling AV, Devlin AS, Varma Y, Fischbach MAJN. Diet rapidly and reproducibly alters the human gut microbiome. 2014;505:559.
78. Hofstra J, Matamoros S, Van De Pol M, De Wever B, Tanck M, Wendt-Knol H, Deijs M, van der Hoek L, Wolthers K, Molenkamp RJBid. Changes in microbiota during experimental human Rhinovirus infection. 2015;15:336.
79. Medzhitov RJN. Recognition of microorganisms and activation of the immune response. 2007;449:819.

80. Everard A, Belzer C, Geurts L, Ouwerkerk JP, Druart C, Bindels LB, Guiot Y, Derrien M, Muccioli GG, Delzenne NMJPotNAoS. Cross-talk between Akkermansia muciniphila and intestinal epithelium controls diet-induced obesity. 2013;110:9066-71.
81. Hersoug LG, Møller P, Loft SJOR. Gut microbiota-derived lipopolysaccharide uptake and trafficking to adipose tissue: implications for inflammation and obesity. 2016;17:297-312.
82. Ghoshal S, Witta J, Zhong J, De Villiers W, Eckhardt EJJolr. Chylomicrons promote intestinal absorption of lipopolysaccharides. 2009;50:90-7.
83. Erridge C, Attina T, Spickett CM, Webb DJJTAjocn. A high-fat meal induces low-grade endotoxemia: evidence of a novel mechanism of postprandial inflammation. 2007;86:1286-92.
84. Caesar R, Tremaroli V, Kovatcheva-Datchary P, Cani PD, Bäckhed FJCm. Crosstalk between gut microbiota and dietary lipids aggravates WAT inflammation through TLR signaling. 2015;22:658-68.
85. Zheng Y, Valdez PA, Danilenko DM, Hu Y, Sa SM, Gong Q, Abbas AR, Modrusan Z, Ghilardi N, De Sauvage FJJNm. Interleukin-22 mediates early host defense against attaching and effacing bacterial pathogens. 2008;14:282.
86. Maynard CL, Elson CO, Hatton RD, Weaver CTJN. Reciprocal interactions of the intestinal microbiota and immune system. 2012;489:231.
87. Beyaz S, Mana MD, Roper J, Kedrin D, Saadatpour A, Hong S-J, Bauer-Rowe KE, Xifaras ME, Akkad A, Arias EJN. High-fat diet enhances stemness and tumorigenicity of intestinal progenitors. 2016;531:53.
88. Hamilton MK, Boudry G, Lemay DG, Raybould HEJAJoP-G, Physiology L. Changes in intestinal barrier function and gut microbiota in high-fat diet-fed rats are dynamic and region dependent. 2015;308:G840-G51.
89. Blaschitz C, Raffatellu MJJoci. Th17 cytokines and the gut mucosal barrier. 2010;30:196-203.
90. Liu JZ, Pezeshki M, Raffatellu MJC. Th17 cytokines and host-pathogen interactions at the mucosa: dichotomies of help and harm. 2009;48:156-60.
91. Raffatellu M, Santos RL, Verhoeven DE, George MD, Wilson RP, Winter SE, Godinez I, Sankaran S, Paixao TA, Gordon MAJNm. Simian immunodeficiency virus–induced mucosal interleukin-17 deficiency promotes Salmonella dissemination from the gut. 2008;14:421.
92. Slavin JJN. Fiber and prebiotics: mechanisms and health benefits. 2013;5:1417-35.
93. Vieira AT, Teixeira MM, Martins FdSJFii. The role of probiotics and prebiotics in inducing gut immunity. 2013;4:445.
94. Cummings J, Pomare E, Branch W, Naylor C, Macfarlane GJG. Short chain fatty acids in human large intestine, portal, hepatic and venous blood. 1987;28:1221-7.
95. Samuel BS, Shaito A, Motoike T, Rey FE, Backhed F, Manchester JK, Hammer RE, Williams SC, Crowley J, Yanagisawa MJPotNAoS. Effects of the gut microbiota on host adiposity are modulated by the short-chain fatty-acid binding G protein-coupled receptor, Gpr41. 2008;105:16767-72.
96. Rooks MG, Garrett WSJNRI. Gut microbiota, metabolites and host immunity. 2016;16:341-52.

97. Gibson PR, Rosella O, Wilson AJ, Mariadason JM, Rickard K, Byron K, Barkla DHJC. Colonic epithelial cell activation and the paradoxical effects of butyrate. 1999;20:539-44.
98. Wang H-B, Wang P-Y, Wang X, Wan Y-L, Liu Y-CJDd, sciences. Butyrate enhances intestinal epithelial barrier function via up-regulation of tight junction protein Claudin-1 transcription. 2012;57:3126-35.
99. Davie JRJTJon. Inhibition of histone deacetylase activity by butyrate. 2003;133:2485S-93S.
100. Klampfer L, Huang J, Sasazuki T, Shirasawa S, Augenlicht LJMCR. Inhibition of Interferon γ Signaling by the Short Chain Fatty Acid Butyrate11Montefiore Medical Center New Research Initiative Award to LK and the American Cancer Society Institutional Research Grant to LK (ACS IRG# 98-274-01), UO1 CA88104 (to LA), and P30-13330 from NCI. 2003;1:855-62.
101. Lührs H, Gerke T, Müller J, Melcher R, Schauber J, Boxberger F, Scheppach W, Menzel TJSjog. Butyrate inhibits NF-κB activation in lamina propria macrophages of patients with ulcerative colitis. 2002;37:458-66.
102. Schwab M, Reynders V, Ulrich S, Zahn N, Stein J, Schröder OJA. PPARγ is a key target of butyrate-induced caspase-3 activation in the colorectal cancer cell line Caco-2. 2006;11:1801-11.
103. Maslowski KM, Vieira AT, Ng A, Kranich J, Sierro F, Yu D, Schilter HC, Rolph MS, Mackay F, Artis DJN. Regulation of inflammatory responses by gut microbiota and chemoattractant receptor GPR43. 2009;461:1282.
104. Smith PM, Howitt MR, Panikov N, Michaud M, Gallini CA, Bohlooly-Y M, Glickman JN, Garrett WSJS. The microbial metabolites, short-chain fatty acids, regulate colonic Treg cell homeostasis. 2013;341:569-73.
105. Singh N, Gurav A, Sivaprakasam S, Brady E, Padia R, Shi H, Thangaraju M, Prasad PD, Manicassamy S, Munn DHJI. Activation of Gpr109a, receptor for niacin and the commensal metabolite butyrate, suppresses colonic inflammation and carcinogenesis. 2014;40:128-39.
106. Groschwitz KR, Hogan SPJJoa, immunology c. Intestinal barrier function: molecular regulation and disease pathogenesis. 2009;124:3-20.
107. Konrad D, Wueest SJP. The gut-adipose-liver axis in the metabolic syndrome. 2014;29:304-13.
108. Amar J, Chabo C, Waget A, Klopp P, Vachoux C, Bermúdez-Humarán LG, Smirnova N, Bergé M, Sulpice T, Lahtinen SJEmm. Intestinal mucosal adherence and translocation of commensal bacteria at the early onset of type 2 diabetes: molecular mechanisms and probiotic treatment. 2011;3:559-72.
109. Lam YY, Ha CW, Campbell CR, Mitchell AJ, Dinudom A, Oscarsson J, Cook DI, Hunt NH, Caterson ID, Holmes AJJPo. Increased gut permeability and microbiota change associate with mesenteric fat inflammation and metabolic dysfunction in diet-induced obese mice. 2012;7:e34233.
110. Drewe J, Beglinger C, Fricker GJEjoci. Effect of ischemia on intestinal permeability of lipopolysaccharides. 2001;31:138-44.
111. Deitch EAJCoicc. Role of the gut lymphatic system in multiple organ failure. 2001;7:92-8.

112. Deitch EAJS. Bacterial translocation or lymphatic drainage of toxic products from the gut: what is important in human beings? 2002;131:241-4.
113. Manco M, Putignani L, Bottazzo GFJEr. Gut microbiota, lipopolysaccharides, and innate immunity in the pathogenesis of obesity and cardiovascular risk. 2010;31:817-44.
114. Vreugdenhil AC, Rousseau CH, Hartung T, Greve JWM, van't Veer C, Buurman WAJTJoI. Lipopolysaccharide (LPS)-binding protein mediates LPS detoxification by chylomicrons. 2003;170:1399-405.
115. Wright SD, Ramos RA, Tobias PS, Ulevitch RJ, Mathison JCJS. CD14, a receptor for complexes of lipopolysaccharide (LPS) and LPS binding protein. 1990;249:1431-3.
116. Moreno-Navarrete J, Ortega F, Serino M, Luche E, Waget A, Pardo G, Salvador J, Ricart W, Frühbeck G, Burcelin RJIjoo. Circulating lipopolysaccharide-binding protein (LBP) as a marker of obesity-related insulin resistance. 2012;36:1442.
117. Macpherson AJ, Uhr TJS. Induction of protective IgA by intestinal dendritic cells carrying commensal bacteria. 2004;303:1662-5.
118. Sansonetti PJ, Di Santo JPJI. Debugging how bacteria manipulate the immune response. 2007;26:149-61.
119. Peyrin-Biroulet L, Gonzalez F, Dubuquoy L, Rousseaux C, Dubuquoy C, Decourcelle C, Saudemont A, Tachon M, Béclin E, Odou M-FJG. Mesenteric fat as a source of C reactive protein and as a target for bacterial translocation in Crohn's disease. 2012;61:78-85.
120. Luche E, Cousin B, Garidou L, Serino M, Waget A, Barreau C, André M, Valet P, Courtney M, Casteilla LJMm. Metabolic endotoxemia directly increases the proliferation of adipocyte precursors at the onset of metabolic diseases through a CD14-dependent mechanism. 2013;2:281-91.
121. Xu H, Barnes GT, Yang Q, Tan G, Yang D, Chou CJ, Sole J, Nichols A, Ross JS, Tartaglia LAJTJoci. Chronic inflammation in fat plays a crucial role in the development of obesity-related insulin resistance. 2003;112:1821-30.
122. Ma Y, Liu H, Tu-Rapp H, Thiesen H-J, Ibrahim SM, Cole SM, Pope RMJNi. Fas ligation on macrophages enhances IL-1R1–Toll-like receptor 4 signaling and promotes chronic inflammation. 2004;5:380.
123. Ramana KV, Srivastava SKJC. Mediation of aldose reductase in lipopolysaccharide-induced inflammatory signals in mouse peritoneal macrophages. 2006;36:115-22.
124. Italiani P, Boraschi DJFii. From monocytes to M1/M2 macrophages: phenotypical vs. functional differentiation. 2014;5:514.
125. Orecchioni M, Ghosheh Y, Akula Bala P, Ley KJFii. Macrophage polarization: different gene signatures in M1 (LPS+) versus classically and M2 (LPS-) versus alternatively activated macrophages. 2019;10:1084.
126. Bäckhed F, Manchester JK, Semenkovich CF, Gordon JIJPotNAoS. Mechanisms underlying the resistance to diet-induced obesity in germ-free mice. 2007;104:979-84.
127. Rabot S, Membrez M, Bruneau A, Gérard P, Harach T, Moser M, Raymond F, Mansourian R, Chou CJJTFJ. Germ-free C57BL/6J mice are resistant to high-fat-

diet-induced insulin resistance and have altered cholesterol metabolism. 2010;24:4948-59.
128. Tran H, Bretin A, Adeshirlarijaney A, San Yeoh B, Vijay-Kumar M, Zou J, Denning TL, Chassaing B, Gewirtz ATJC, et al. "Western-diet"-induced adipose inflammation requires a complex gut microbiota. 2019.
129. Ihle JNJCoicb. The Stat family in cytokine signaling. 2001;13:211-7.
130. Takeda K, Noguchi K, Shi W, Tanaka T, Matsumoto M, Yoshida N, Kishimoto T, Akira SJPotNAoS. Targeted disruption of the mouse Stat3 gene leads to early embryonic lethality. 1997;94:3801-4.
131. Neufert C, Pickert G, Zheng Y, Wittkopf N, Warntjen M, Nikolae A, Ouyang W, Neurath MF, Becker CJCC. Activation of epithelial STAT3 regulates intestinal homeostasis. 2010;9:652-5.
132. Bollrath J, Phesse TJ, von Burstin VA, Putoczki T, Bennecke M, Bateman T, Nebelsiek T, Lundgren-May T, Canli Ö, Schwitalla SJCc. gp130-mediated Stat3 activation in enterocytes regulates cell survival and cell-cycle progression during colitis-associated tumorigenesis. 2009;15:91-102.
133. Grivennikov S, Karin E, Terzic J, Mucida D, Yu G-Y, Vallabhapurapu S, Scheller J, Rose-John S, Cheroutre H, Eckmann LJCc. IL-6 and Stat3 are required for survival of intestinal epithelial cells and development of colitis-associated cancer. 2009;15:103-13.
134. Pickert G, Neufert C, Leppkes M, Zheng Y, Wittkopf N, Warntjen M, Lehr H-A, Hirth S, Weigmann B, Wirtz SJJoEM. STAT3 links IL-22 signaling in intestinal epithelial cells to mucosal wound healing. 2009;206:1465-72.
135. Bachmann M, Meissner C, Pfeilschifter J, Mühl HJB. Cooperation between the bacterial-derived short-chain fatty acid butyrate and interleukin-22 detected in human Caco2 colon epithelial/carcinoma cells. 2017;43:283-92.
136. Teng Y, Ren Y, Sayed M, Hu X, Lei C, Kumar A, Hutchins E, Mu J, Deng Z, et al. Plant-derived exosomal microRNAs shape the gut microbiota. 2018;24:637-52. e8.
137. Eisenmenger M, Dunford NT, Eller F, Taylor S, Martinez JJJotAOCS. Pilot-scale supercritical carbon dioxide extraction and fractionation of wheat germ oil. 2006;83:863-8.
138. U.S. Department of Agriculture ARS. Agricultural Research Service. FoodData Central. 2019. https://fdc.nal.usda.gov/.
139. Zhang J-y, Xiao X, Dong Y, Wu J, Yao F, Zhou X-hJJoa, chemistry f. Effect of fermented wheat germ extract with lactobacillus plantarum dy-1 on HT-29 cell proliferation and apoptosis. 2015;63:2449-57.
140. Anwar M, Mohamed NJJoRR, Sciences A. Amelioration of liver and kidney functions disorders induced by sodium nitrate in rats using wheat germ oil. 2015;8:77-83.
141. Moreira-Rosário A, Marques C, Pinheiro H, Norberto S, Sintra D, Teixeira JA, Calhau C, Azevedo LFJEjon. Daily intake of wheat germ-enriched bread may promote a healthy gut bacterial microbiota: a randomised controlled trial. 2019:1-11.
142. Messina MJJTAjocn. Legumes and soybeans: overview of their nutritional profiles and health effects. 1999;70:439s-50s.

143. Marathe SA, Rajalakshmi V, Jamdar SN, Sharma AJF, Toxicology C. Comparative study on antioxidant activity of different varieties of commonly consumed legumes in India. 2011;49:2005-12.
144. Thorne MJ, Thompson L, Jenkins DJTAJoCN. Factors affecting starch digestibility and the glycemic response with special reference to legumes. 1983;38:481-8.
145. Murphy MM, Douglass JS, Birkett AJJotADA. Resistant starch intakes in the United States. 2008;108:67-78.
146. Galisteo M, Duarte J, Zarzuelo AJTJonb. Effects of dietary fibers on disturbances clustered in the metabolic syndrome. 2008;19:71-84.
147. Henningsson ÅM, Margareta E, Nyman G, Björck IMJBJoN. Content of short-chain fatty acids in the hindgut of rats fed processed bean (Phaseolus vulgaris) flours varying in distribution and content of indigestible carbohydrates. 2001;86:379-89.
148. Le Leu RK, Brown IL, Hu Y, Morita T, Esterman A, Young GPJC. Effect of dietary resistant starch and protein on colonic fermentation and intestinal tumourigenesis in rats. 2007;28:240-5.
149. Jenkins D, Wolever T, Taylor RH, Barker HM, Fielden HJBMJ. Exceptionally low blood glucose response to dried beans: comparison with other carbohydrate foods. 1980;281:578-80.
150. Thompson SV, Winham DM, Hutchins AMJNj. Bean and rice meals reduce postprandial glycemic response in adults with type 2 diabetes: a cross-over study. 2012;11:23.
151. Jenkins DJ, Kendall CW, Augustin LS, Mitchell S, Sahye-Pudaruth S, Mejia SB, Chiavaroli L, Mirrahimi A, Ireland C, Bashyam BJAoim. Effect of legumes as part of a low glycemic index diet on glycemic control and cardiovascular risk factors in type 2 diabetes mellitus: a randomized controlled trial. 2012;172:1653-60.
152. Villegas R, Gao Y-T, Yang G, Li H-L, Elasy TA, Zheng W, Shu XOJTAjocn. Legume and soy food intake and the incidence of type 2 diabetes in the Shanghai Women's Health Study. 2008;87:162-7.
153. Winham DM, Hutchins AM, Johnston CSJJotACoN. Pinto bean consumption reduces biomarkers for heart disease risk. 2007;26:243-9.
154. Shutler SM, Bircher GM, Tredger JA, Morgan LM, Walker AF, Low AJBJoN. The effect of daily baked bean (Phaseolus vulgaris) consumption on the plasma lipid levels of young, normo-cholesterolaemic men. 1989;61:257-65.
155. Anderson JW, Gustafson NJ, Spencer DB, Tietyen J, Bryant CAJTAjocn. Serum lipid response of hypercholesterolemic men to single and divided doses of canned beans. 1990;51:1013-9.
156. Oseguera-Toledo ME, de Mejia EG, Dia VP, Amaya-Llano SLJFC. Common bean (Phaseolus vulgaris L.) hydrolysates inhibit inflammation in LPS-induced macrophages through suppression of NF-κB pathways. 2011;127:1175-85.
157. Oomah BD, Corbé A, Balasubramanian PJJoa, chemistry f. Antioxidant and anti-inflammatory activities of bean (Phaseolus vulgaris L.) hulls. 2010;58:8225-30.

APPENDICES

Oklahoma State University Institutional Animal Care and Use Committee (IACUC)

Protocol Expires: 1/24/2020

Date : Tuesday, September 19, 2017 Animal Care and Use Protocol (ACUP) – HS-16-2

Proposal Title: The Prebiotic Effect of Dry Beans (Phaseolus vulgaris) in Modulating the Crosstalk between the Gut Microbiome and Immune Cells at the Onset of Insulin Resistance in C57BL6/J Mice Fed a High Fat Diet

Principal Investigator:

Edralin Lucas
Nutritional Sciences
301 HS
Campus

Reviewed and Processed as: Special Review **Modification**
Approval Status Recommended by Reviewer(s): Approved

The ACUP modification is approved as written including a change in bean preparation and an increase of 48 mice.

Signatures

Dr. Ronald Van Den Bussche, IACUC Chair

Approvals are valid for three calendar years, after which time a request for renewal must be submitted. Any modifications to the research project, course, or testing procedures must be submitted for review and approval by the IACUC, prior to initiating any changes. Modifications do not affect the original approval period. Modification approvals are valid for the duration of the protocol approval (see protocol expiration date). Approved projects are subject to monitoring by the IACUC. OSU is a USDA registered research facility and maintains an Animal Welfare Assurance document with the Public Health Service Office of Laboratory Animal Welfare, Assurance number AA3722-01.

Oklahoma State University
Institutional Animal Care and Use Committee (IACUC)

Protocol expires: 4/28/2018

Date: Thursday, January 21, 2016 Animal Care and Use Protocol (ACUP) HS-15-3

Proposal: Effect of Wheat Germ Oil (WGO) from Oklahoma Red Winter Wheat on Inflammation, Gut Integrity and Microbial Population in Obese Mice

Principal
Investigator:

Edralin Lucas
Nutritional Sciences
301 HS
Campus

Reviewed and
Processed as: Special Review **Modification**

Approval Status Recommended by Reviewer(s): Approved

The modification request for a change in animal disposition is approved. You are approved to transfer a second mouse from this protocol to ACUP VM-15-12 to be used as described.

Signatures

Thursday, January 21, 2016
Dr. Karen McBee, IACUC Chair Date

cc: Department Head, Nutritional Sciences
LAR

Approvals are valid for three calendar years, after which time a request for renewal must be submitted. Any modifications to the research project, course, or testing procedures must be submitted for review and approval by the IACUC, prior to initiating any changes. Modifications do not affect the original approval period. Modification approvals are valid for the duration of the protocol approval (see protocol expiration date). Approved projects are subject to monitoring by the IACUC. OSU is a USDA registered research facility and maintains an Animal Welfare Assurance document with the Public Health Service Office of Laboratory Animal Welfare, Assurance number AA3722-01.

VITA

Babajide Abidemi Ojo

Candidate for the Degree of

Doctor of Philosophy

Dissertation: THE EFFECT OF WHOLE FOODS ON THE GUT-ADIPOSE AXIS IN MODELS OF DIET-INDUCED OBESITY: THE CASE OF WHEAT GERM AND PINTO BEANS

Major Field: Nutritional Sciences

Biographical:

Education:
Completed the requirements for the Doctor of Philosophy in Nutritional Sciences at Oklahoma State University, Stillwater, Oklahoma in December, 2019.

Completed the requirements for the Master of Science in Nutritional Sciences at Oklahoma State University, Stillwater, Oklahoma in July, 2015.

Completed the requirements for the Bachelor of Science in Biochemistry at Ekiti State University, Ado Ekiti, Ekiti State, Nigeria in August, 2011.

Experience:
Graduate Research Associate—Dept. of Nutritional Sciences, *Oklahoma State University, Stillwater, OK* (Fall 2014 - Fall 2019)

Graduate Teaching Associate—Dept. of Nutritional Sciences, *Oklahoma State University, Stillwater, OK* (Fall 2015 – Spring 2019)

Biology Instructor —Immaculate Group of Schools, Oba-Ile, Ondo State, Nigeria, (Nov 2011 – Oct 2013).

Professional Memberships:
American Society of Nutrition
Society of Experimental Biology and Medicine